



12-2017

## **Biomass processing using ionic liquids: Effects of 3-methylimidazolium cations and carboxylate anions**

Preenaa Moyer

*University of Tennessee*, [pvenugop@vols.utk.edu](mailto:pvenugop@vols.utk.edu)

Follow this and additional works at: [https://trace.tennessee.edu/utk\\_gradthes](https://trace.tennessee.edu/utk_gradthes)

---

### **Recommended Citation**

Moyer, Preenaa, "Biomass processing using ionic liquids: Effects of 3-methylimidazolium cations and carboxylate anions. " Master's Thesis, University of Tennessee, 2017.  
[https://trace.tennessee.edu/utk\\_gradthes/5007](https://trace.tennessee.edu/utk_gradthes/5007)

This Thesis is brought to you for free and open access by the Graduate School at TRACE: Tennessee Research and Creative Exchange. It has been accepted for inclusion in Masters Theses by an authorized administrator of TRACE: Tennessee Research and Creative Exchange. For more information, please contact [trace@utk.edu](mailto:trace@utk.edu).

To the Graduate Council:

I am submitting herewith a thesis written by Preenaa Moyer entitled "Biomass processing using ionic liquids: Effects of 3-methylimidazolium cations and carboxylate anions." I have examined the final electronic copy of this thesis for form and content and recommend that it be accepted in partial fulfillment of the requirements for the degree of Master of Science, with a major in Biosystems Engineering.

Nicole Labbe, Major Professor

We have read this thesis and recommend its acceptance:

Nourredine H. Abdoumoumine, Danielle J. Carrier, Stephen C. Chmely

Accepted for the Council:

Dixie L. Thompson

Vice Provost and Dean of the Graduate School

(Original signatures are on file with official student records.)

**Biomass processing using ionic liquids:  
Effects of 3-methylimidazolium cations and carboxylate  
anions**

**A Thesis Presented for the  
Master of Science  
Degree**

**The University of Tennessee, Knoxville**

**Preenaa Moyer**

**December 2017**

Copyright © 2017 by Preenaa Moyer

All rights reserved.

## **DEDICATION**

To my parents  
I wouldn't be here without you.

To my amazing husband, Seth  
I wouldn't have made it without your love, support, encouragement, and monthly  
1200-mile travel.

## ACKNOWLEDGMENTS

I would like to sincerely thank my major advisers, Dr. Nicole (Niki) Labbé and Dr. Nourredine (Nour) Abdoulmoumine for giving me the opportunity to work with them. Niki, you have always recognized my abilities and shown confidence in my work. Thank you for your knowledge, optimism, and continual support. Nour, thank you for your valuable insight and constant assistance with many aspects of my research. Drs. Stephen Chmely and Julie Carrier, thanks to the both of you for serving as my committee members and providing valuable feedback and perspective based on your expertise.

I am also grateful to my co-workers, Dr. Omid Hosseinaei, Dr. David Harper, Dr. Jing Wang, Ms. Anna Kim, Ms. Valerie García-Negrón, and Mr. Chris Helton for addressing all my questions and doubts. And thank you to all the staff of the Biosystems Engineering and Soil Science department as well as the Center for Renewable Carbon.

## ABSTRACT

As the global transportation and industrial sectors continue to grow, fuels, chemicals, and products derived from lignocellulosic biomass have become a key alternative to petroleum-based products. Lignocellulosic biomass is composed of lignin, cellulose, and hemicellulose linked together in a rigid structure. This spatial arrangement contributes to its resistance to degradation and requires pretreatment and/or separation before being processed to produce valuable chemicals and fuels. Biomass pretreatment has mainly been optimized to convert carbohydrates into monosugars. However, better sustainability is attained when the entire feedstock is utilized to produce fuel and value-added chemicals and products. To achieve this goal, an integrated biorefinery will require a highly selective and economically viable fractionation process. Although traditionally used for pretreatment, recent studies have found ionic liquids to be ideal solvents for biomass dissolution, “activation”, and fractionation to produce various end products for biorefinery and industrial applications.

Previous works have demonstrated that the IL 1-ethyl-3-methylimidazolium acetate ([EMIM]Acetate) is ideal for the above processes to produce sugars as well as lignin-based products. However, our study shows that three other ILs with 3-methylimidazolium cations and carboxylate anions (1-ethyl-3-methylimidazolium formate ([EMIM]Formate), 1-allyl-3-methylimidazolium formate ([AMIM]Formate), and 1-allyl-3-methylimidazolium acetate ([AMIM]Acetate)) are effective for biomass dissolution, with [AMIM]Formate having a 40% increase in biomass solubility compared to [EMIM]Acetate. Both [AMIM]Formate and [EMIM]Acetate are further evaluated for their activation and fractionation capability by studying crystallinity changes and enzymatic conversion rates of cellulose and hemicellulose into soluble sugars. Our findings show that although [AMIM]Formate is better at biomass dissolution, [EMIM]Acetate is better for biomass activation and

fractionation. Following activation using [AMIM]Formate, biomass retains its most of its crystallinity and acetyl groups, whereas activation using [EMIM]Acetate significantly reduces crystallinity and acetyl groups, leading to higher enzymatic conversion of cellulose and hemicellulose. Future studies should investigate the potential for *in situ* saccharification in ILs using commercial cellulases and hemicellulases, as our preliminary data show that enzymes remain active in these two ILs. Ultimately, this research will provide technological breakthroughs needed to develop a robust means of biomass fractionation and subsequent conversion into high value organics and biofuels.



## PREFACE

This thesis is comprised of a multipart paper with four chapters: an introduction, two research manuscripts, and an overall conclusion.

Chapter I will provide an overview of the recalcitrant nature of lignocellulosic biomass and several methods to overcome it using various pretreatment and fractionation methods.

Chapter II focuses on lignocellulosic biomass dissolution in four ionic liquids, and how the cation and anion of an IL play a role in dissolving each biomass component at different capacities. A structure-property relationship is established whereby the biomass dissolution is explained through viscosity measurements, Kamlet-Taft solvation parameters, and molecular dynamics simulations (with the assistance of researchers from Oak Ridge National Laboratory). Chapter II has been submitted to Physical Chemistry Chemical Physics.

Chapter III is a follow-up to the results obtained in Chapter II in terms of comparing the IL with highest biomass solubility to a commonly used reference IL, [EMIM]Acetate, for its ability to activate and fractionate lignocellulosic biomass. Data were collected to study parameters known to influence biomass recalcitrance including the biomass acetyl content, cellulose crystallinity, enzymatic conversion of cellulose and hemicellulose, as well as anatomical changes by scanning electron microscopy (SEM) after ionic liquid activation. This chapter is being prepared for submission to a peer-reviewed journal.

Finally, Chapter IV presents some concluding remarks of this work and recommendations related to the outcomes of selecting an ideal ionic liquid as well as some future work that are already underway.

# TABLE OF CONTENTS

Chapter I Introduction .....	1
Motivation .....	2
Lignocellulosic biomass .....	2
Biomass conversion processes .....	5
Ball and compression milling .....	6
Acid pretreatment.....	6
Liquid hot water / Autohydrolysis .....	7
Uncatalyzed steam explosion .....	10
Wet oxidation .....	10
Alkali treatment .....	11
Ammonia fiber expansion (AFEX).....	12
Organosolv .....	13
Gamma valerolactone (GVL) extraction.....	14
Tetrahydrofuran (THF) extraction.....	17
Summary .....	17
Ionic liquids.....	20
Brief history .....	20
Ionic liquid pretreatment.....	21
Ionic liquid activation and regeneration.....	22
Biomass fractionation.....	22
Biomass dissolution in ionic liquid.....	23

Summary .....	23
Chapter II Relationship between lignocellulosic biomass dissolution and physicochemical properties of ionic liquids composed of 3-methylimidazolium cations and carboxylate anions.....	25
Abstract .....	26
Introduction.....	27
Materials and methods .....	30
Biomass and ionic liquids.....	30
Biomass characterization.....	31
Solubility of hybrid poplar in ionic liquids.....	32
Thermal analysis of ionic liquids .....	32
Rheological property measurements of ionic liquids .....	33
Kamlet-Taft measurements.....	33
Simulation details.....	34
Results and discussion.....	35
Conclusions.....	46
Acknowledgments .....	46
Appendix .....	48
Chapter III Lignocellulosic biomass activation with ionic liquids comprising 3-methylimidazolium cations and carboxylate anions .....	49
Abstract .....	50
Introduction.....	51
Materials and methods .....	55
Anatomical characterization.....	58

Results and discussion .....	59
Conclusion.....	74
Acknowledgments .....	75
Chapter IV Conclusions and future work.....	76
Overall conclusions .....	77
Future work.....	81
In situ saccharification of activated biomass .....	81
Designing an apparatus setup to enable higher biomass loading.....	82
Understanding the role of acetate anion as during activation .....	83
Analyzing the structure and interactions of ILs using small-angle neutron scattering (SANS).....	84
Understanding the potential for [AMIM]Formate to spin fibers .....	84
Analyzing [EMIM]Formate and [AMIM]Acetate for biomass activation.....	85
References .....	86
Vita.....	104

## LIST OF TABLES

Table 1. Lignin content changes in hardwood during LHW. Reproduced from Ko et al., 2015. <sup>37</sup> .....	9
Table 2. Summary of the effects of pretreatment and fractionation on the structure of lignocellulosic biomass. ....	19
Table 3. Chemical composition of hybrid poplar. ....	31
Table 4. Hybrid poplar solubility in ionic liquids measured at 80 °C. ....	36
Table 5. Decomposition temperatures (Td) and viscosity of ILs (at 80 °C). ....	41
Table 6. Kamlet-Taft parameters for each ionic liquid. ....	42
Table 7. Calculated lignin-IL and hemicellulose-IL virial coefficients. ....	45
Table 8. Mass recovery of hybrid poplar (%) by ionic liquid type. ....	59
Table 9. Chemical composition of regenerated HP after IL activation at 10 wt.% loading. ....	66
Table 10. Comparison of index of crystallinity (Crl) measured through XRD for [EMIM]Acetate and [AMIM]Formate-activated samples. ....	68
Table 11. Comparison of physical and chemical properties for [EMIM]Acetate and [AMIM]Formate. ....	80

## LIST OF FIGURES

Figure 1. Comparison of relative reduction of GHG emissions based on different feedstocks. <sup>3b, 9</sup> .....	4
Figure 2. Structural representation of lignocellulosic biomass components. <sup>5</sup> .....	4
Figure 3. Structure of gamma valerolactone. ....	14
Figure 4. Products derived from lignocellulosic biomass using the GVL pathway. Reproduced from Alonso et al., 2013. <sup>70</sup> .....	16
Figure 5. Chemical structure of the ionic liquid cation (left) and anion (right). ....	35
Figure 6. Ionic liquids used in this experiment. Top: [EMIM]Acetate (left), [EMIM]Formate (right). Bottom: [AMIM]Acetate (left), [AMIM]Formate (right). ....	36
Figure 7. TGA thermographs for ionic liquids measured at a heating rate of 10 °C/min. ....	39
Figure 8. DTG curves for all four ionic liquids. The global maxima of each curve shows $T_d$ . ....	39
Figure 9. Thermal stability of ionic liquids over a 7-day period. Standard deviations were measured but not shown in the graph. ....	40
Figure 10. Radial distribution functions between the center of mass of ions and plant polymers. (a) solute-anion RDF for lignin and (b) hemicellulose. And the figures on the right-side show solute-cation RDF for (c) lignin and (d) hemicellulose. ....	45
Figure 11. (a) Temperature-dependent viscosity of [EMIM]Acetate. (b) Temperature-dependent viscosity of [EMIM]Formate, [AMIM]Formate, and [AMIM]Acetate (Bottom). ....	48

Figure 12. Principal component analysis (PCA) on [EMIM]Acetate-activated samples for 3, 24, 48, and 72-hour activation times. The scores plot is shown on the left (a), and the loadings plot for PC 1 on the right (b). .....62

Figure 13. Principal component analysis (PCA) on [AMIM]Formate-activated samples for 3, 24, 48, and 72-hour activation times. The scores plot is shown on the left (a), and the loadings plot for PC 1 on the right (b). .....63

Figure 14. (a) Principal component analysis (PCA) scores plot of IL-activated hybrid poplar compared to untreated HP (control). (b) PCA loadings plot for PC 1.....65

Figure 15. X-Ray diffraction (XRD) patterns for IL-activated sample at 10 wt.% biomass loading. Index of crystallinity for cellulose was calculated using Eq.17. ....67

Figure 16. (a) SEM micrographs of control (untreated HP), (b) [EMIM]Acetate-activated HP, and (c) [AMIM]Formate-activated HP. Images were taken at 400x magnification.....71

Figure 17. Mechanism for deacetylation of biomass using ionic liquids. R represents the H or CH<sub>3</sub> attached to the formate or acetate anion. R<sub>1</sub> and R<sub>2</sub> represent the carbon chain on the biomass structure. ....72

Figure 18. Kinetics of enzymatic saccharification on cellulose (a) and hemicellulose (b) of 72-hour activated biomass at a 10 wt.% biomass loading. The conversion was calculated based on the chemical composition of raw hybrid poplar.....73

Figure 19. Overall process scheme for lignocellulosic biomass processing.....79

Figure 20. Activity of CTec 3 cellulases (a) and HTec 3 hemicellulases (b) in the presence of 0, 5, 10, and 20% IL. ....83

# CHAPTER I

## INTRODUCTION



## Motivation

Chemicals and transportation fuels that derive from fossil fuels, are not renewable or sustainable. Concerns over long-term economics, job security, and rural development have motivated research in renewable fuels as an alternative to fossil fuels.<sup>1</sup> In analyzing sustainable energy routes, lignocellulosic biomass has been identified as the most suitable feedstock; an abundant, non-food material that can produce fuels and chemicals.<sup>2</sup> In 2011, the International Energy Agency stated that biomass-derived fuels are expected to contribute to at least 27% of the global share of total transportation fuels by 2050 and the projected use of biofuels could lead to a reduction of 2.1 gigatons of CO<sub>2</sub> emissions per year. In accordance to this, research shows that biofuels from lignocellulosic crops generally have a higher greenhouse gas (GHG) efficiency than rotational arable crops due to lower input requirements and higher energy yield per hectare (Figure 1).<sup>3</sup>

## Lignocellulosic biomass

Lignocellulosic biomass is mainly composed of cellulose (30-45%), hemicellulose (20-30%), and lignin (5-25%).<sup>4</sup> Cellulose is the main component of the plant cell wall, in which it is a highly stable linear homopolymer, unlike starch molecules that branch and coil. Cellulose comprises glucose monomer units which are linked by  $\beta$  (1 $\rightarrow$ 4) glycosidic bonds. When two  $\beta$ -glucose are linked by  $\beta$  (1 $\rightarrow$ 4), a disaccharide known as cellobiose is formed.<sup>5</sup>

Hemicellulose differs from cellulose as a diverse class of polysaccharides that include xylan, glucuronoxylan, arabinoxylan, glucomannan, and xyloglucan. While cellulose has high crystallinity, and is resistant to degradation, hemicellulose has a random, amorphous structure that lacks strength. Hemicellulose has a high susceptibility to chemical and biological hydrolysis using dilute acid, bases, and hemicellulases.<sup>6</sup>

Lignin is an amorphous polymer that binds hemicellulose and cellulose through ester linkages and hydrogen bonds, respectively. Lignin forms the important structural materials for the support tissues in plants. The principal lignol monomers of lignin are *p*-coumaryl, coniferyl, and sinapyl alcohol.<sup>7</sup> These monomers form cross-linked phenylpropanoid units: *p*-hydroxyphenyl (H), guaiacyl (G), and syringyl (S). Softwood mainly consists of lignin that is made up of G-type subunits with a small amount of S or none at all, whereas hardwood consists of a mixture of both G and S. The overall spatial arrangements of cellulose, hemicellulose, and lignin in lignocellulosic biomass are shown in Figure 2.

The predominant polysaccharides, namely cellulose and hemicellulose, can be hydrolyzed into simple sugars using enzymes or chemicals. The resultant sugars are then converted to valuable fuels and chemicals such as bioethanol, carboxylic acids, or methane by fermentation.<sup>8</sup> However, the hydrogen bonds and covalent cross-linkages between polysaccharides and lignin form a rigid structure and build resistance against biomass degradation.<sup>6</sup> This phenomenon is also known as biomass recalcitrance. Making cellulose and hemicellulose more accessible for enzymatic hydrolysis requires pretreatment to alter the structure of lignocellulosic biomass and reduce biomass recalcitrance.<sup>1</sup>

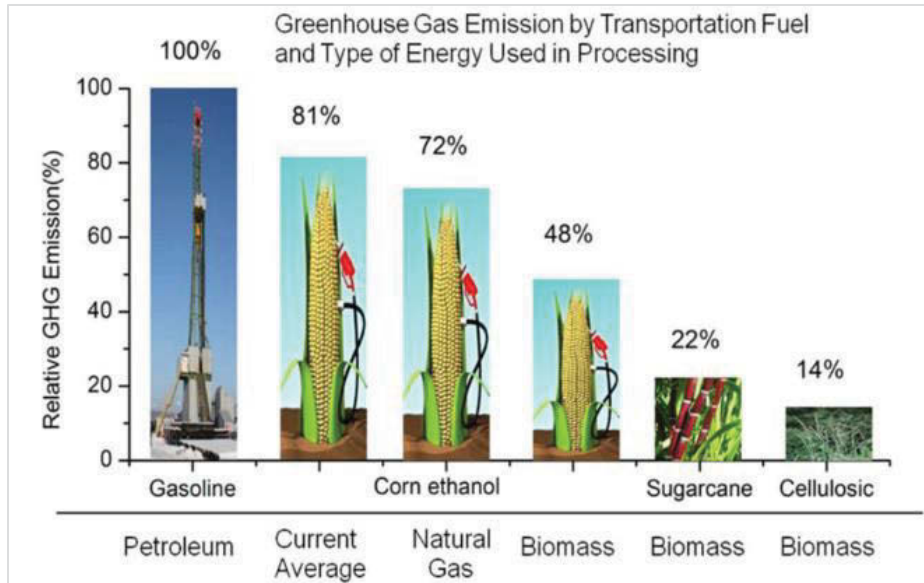


**Figure 1.** Comparison of relative reduction of GHG emissions based on different feedstocks.<sup>3b, 9</sup>

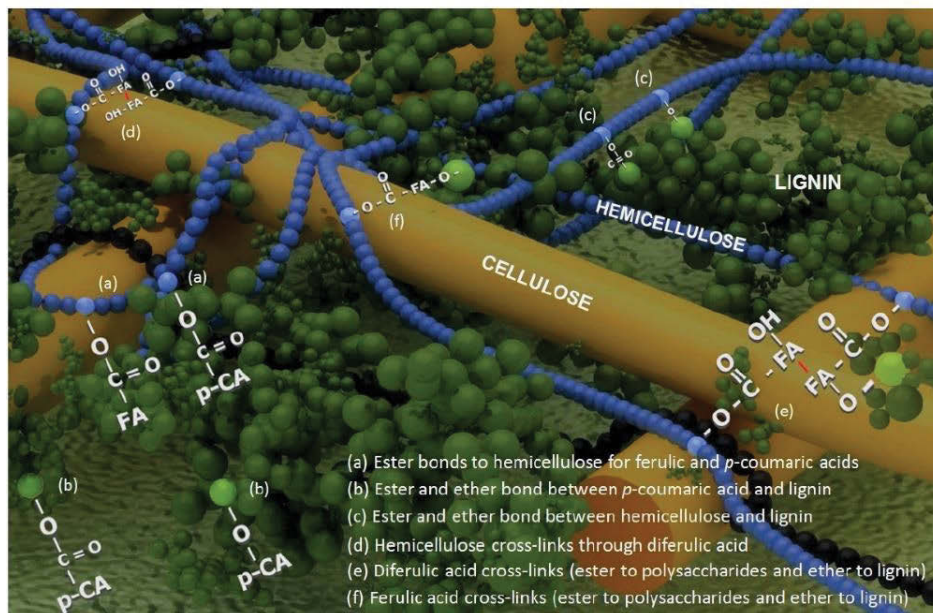


**Figure 2.** Structural representation of lignocellulosic biomass components.<sup>5</sup>

## Biomass conversion processes

To compete with existing fossil fuel industries, various novel technologies and diverse biomass feedstocks need to be used for a successful integrated biorefinery. As stated by the Office of Energy Efficiency and Renewable Energy (EERE), the development of bioindustries in the US requires a vital step of establishing integrated biorefineries that efficiently convert various biomass feedstocks into commercially viable biofuels and bioproducts.<sup>10</sup> Essentially, integrated biorefineries need to produce a range of products similar to conventional refineries for the optimization of feedstocks and production economics.

Biomass pretreatment has been carried out for decades to mainly produce sugars that can be converted into platform building blocks for fuels and chemicals. However, biomass fractionation has been more prevalent recently due its valorization, to recover pure streams of lignin, hemicellulose, and cellulose with minimal degradation. It is essential to valorize various intermediate chemicals to counterbalance production logistics, therefore making the business model attractive for investors.<sup>11</sup>

The separation process of lignocellulosic biomass requires either a biochemical, thermochemical, or physical method of pretreatment and/or fractionation. Biomass pretreatment involves removing or disrupting the impending layers of biomass, namely lignin and hemicellulose, for easy-access of cellulose during chemical or enzymatic hydrolysis.<sup>12</sup> Biomass fractionation separates lignocellulosic biomass into its primary components, namely cellulose, hemicellulose, and lignin with high purity and yield and minimal degradation.

Scientists have attempted to use many different methods, such as ball milling, compression milling, acid wash, alkali treatment, autohydrolysis, wet oxidation, steam explosion, ammonia fiber expansion (AFEX), *gamma*-valerolactone, organosolv, and ionic liquids to recover cellulose, and in the case of fractionation, to obtain streams of cellulose, lignin, and hemicellulose. The

following processes describe the currently available pretreatment and fractionation methods.

### ***Ball and compression milling***

Ball milling and compression milling are physical pretreatment methods that subject biomass to shear force and subsequent size reduction.<sup>13</sup> Biomass size reduction is similar to wood fiber production and involves two steps.<sup>14</sup> The first step is a mechanical size reduction through wood chipping, and the second step is a further size reduction from wood chips to wood fiber bundles or particles through grinding and milling.<sup>15</sup> Vibratory ball milling of cellulose decreases the particle size of biomass to about 10 mm and converts crystalline cellulose to amorphous cellulose. The fragmentation of lignin polymers occurs via cleavage of  $\beta$ -ether bonds.<sup>16</sup> Typically, an additional method of delignification i.e., lignin removal is required to produce higher sugar yields during enzymatic hydrolysis.

Often times, ball milling is a precursor to another method of pretreatment in order to improve glucose and xylose yields.<sup>17</sup> Although ball and compression milling increase the contact surface area of reactants, these methods are energy and time-intensive, therefore other pretreatment steps are often considered in addition to these.

### ***Acid pretreatment***

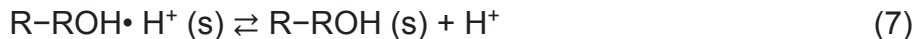
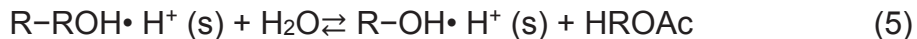
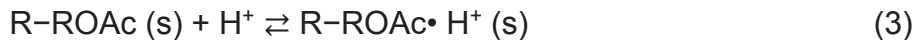
Acid pretreatment or hydrolysis involves dilute/concentrated sulfuric, phosphoric, or hydrochloric acid at high temperatures to remove hemicellulose from biomass. The National Renewable Energy Laboratory (NREL) favors acid pretreatment mainly due to the high recovery of hemicellulose, at about 80-90%.<sup>18</sup> Following hydrolysis of hemicellulose, the lignin fraction is disrupted, increasing cellulose access to enzymes.<sup>19</sup> Dilute acid (DA) pretreatment produces high sugar (glucan and xylan) yields when applied to hardwoods such as poplar.<sup>20</sup> As for concentrated acid pretreatment, Du et al. reports that an 85% phosphoric acid

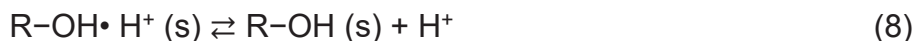
pretreatment is more effective for reducing cellulose crystallinity of loblolly pine compared to sulfuric acid or ionic liquids.<sup>21</sup>

In addition to being used on its own, acid wash has been coupled with other pretreatment methods such as alkaline treatment, microwave irradiation, and steam explosion.<sup>22, 23, 24</sup> However, due to its corrosive nature, high-grade alloy reactor is required for the pretreatment as well as a neutralization step prior to biological steps involving enzymes.

### ***Liquid hot water / Autohydrolysis***

Liquid Hot Water (LHW) treatment, also known as autohydrolysis, is a hydrothermal treatment of biomass to solubilize hemicellulose and allow better accessibility of cellulose and lignin.<sup>25</sup> During LHW treatment, pressure is applied at elevated temperatures (120-240 °C) to maintain water in the liquid state.<sup>7, 26</sup> At increased temperature and pressure, alteration of the lignocellulosic biomass structure is promoted without the employment of catalysts or solvents other than water. The use of high temperatures dissolves acetyl groups from the hemicellulose, “automatically”, releases hydronium ions (from water, acetic, formic, phenolic and uronic acids), and accelerates hydrolysis reactions.<sup>27</sup> This phenomenon is called auto-hydrolysis with the following reaction steps:





LHW has been used extensively for biomass pretreatment due to the minimal degradation of sugars, low production of inhibitors, and absence of toxic solvents, thus making it a “green technology”.<sup>28</sup> Hemicellulose is the main component removed in this method, with a small portion of the lignin also dissolved at temperatures of 160 °C or higher, depending on the type of feedstock.<sup>7, 29</sup> The removal of hemicellulose from the lignocellulosic component allows for saccharification of cellulose, leaving behind lignin as a solid.

However, studies show that LHW affects lignin by decreasing  $\beta$ -O-4 linkages, increasing phenolic hydroxyl groups, decreasing aliphatic hydroxyl groups, and depleting acetyl groups.<sup>30</sup> The use of mild temperatures, controlled pH levels, and several trial and error runs are essential to optimize LHW. This ensures maximum removal of hemicellulose and avoids excessive depolymerization of cellulose and degradation of lignin.<sup>1, 12c, 26a, 31</sup> The amount of degradation and lignin removal also highly depend on the “severity factor”.<sup>32</sup> As proposed by Overend and Chornet, the reaction severity or severity factor of LHW pretreatment,  $S_0$ , can be calculated as a function of reaction time and reactor temperature using the Equation 9. Severe pretreatment conditions can result in accumulation of organic acids, resulting in an acidic environment that promotes degradation of monomeric sugars into inhibitory compounds (e.g., furfural, hydroxymethyl furfural (HMF), formic acid, and levulinic acid).<sup>33</sup>

$$S_0 = \log \left\{ \exp \left[ \frac{T-100}{14.75} \right] * t \right\} \quad (9)$$

A small amount of lignin is hydrolyzed at LHW temperature ranges of 120-160 °C, as acid soluble lignin (ASL).<sup>34,35</sup> The remaining lignin is present in the solid fraction and identified as acid insoluble lignin.<sup>4b</sup> AIL and ASL account for total lignin quantification via the Klason lignin method, using 72% sulfuric acid for hydrolysis and subsequent boiling in 4% sulfuric acid to separate lignin through

dissolution of carbohydrates.<sup>36</sup> With increasing pretreatment severity, the pH of hydrolysate (liquid fraction of LHW) decreases and this in turn increases the lignin content in hydrolysates, or ASL. To ensure high lignin recovery, it is essential to minimize ASL and maximize AIL by understanding the effect of severity factor on biomass. Table 1 shows the changes in lignin during LHW pretreatment of hardwood (adapted from the work of Ladisch and collaborators).<sup>37</sup>

Over the years, several methods have been applied to increase the efficiency of LHW to study fluid velocity, particle size, residence time, as well as a coupled pretreatment method. Flow-through LHW systems have shown higher removal of xylan and lignin compared to batch systems, when flow is increased and particle size decreased.<sup>25, 38</sup> However, the system requires optimization to avoid excessive water consumption and large energy costs for downstream processing.

**Table 1.** Lignin content changes in hardwood during LHW. Reproduced from Ko et al., 2015.<sup>37</sup>

Sample	Severity factor	Temp (°C)	AIL <sup>a</sup> (%)	ASL <sup>b</sup> (%)	AIL/ASL ratio	Total lignin <sup>c</sup> (%)	Lignin recovery <sup>d</sup> (%)
Untreated	N/A	N/A	28.1	3.8	7.4	31.8	N/A
Changes during LHW treatment	8.25 ↓ 12.51	180 ↓ 220	25.5 ↓ 37.6	3.9 ↑ 2.7	6.5 ↓ 13.9	29.3 ↓ 40.3	86.5 ↓ 90.1

<sup>a</sup> Acid insoluble Kraft lignin

<sup>b</sup> Acid soluble Kraft lignin

<sup>c</sup> Total lignin (%) = {AIL (g)/ total biomass (g) \*100%} + ASL (%)

<sup>d</sup> Lignin recovery (%) = [Lignin recovered after pretreatment (g)/Initial amount of lignin (g)]\*100%.



### ***Uncatalyzed steam explosion***

Uncatalyzed steam explosion is mainly used as a commercial method to hydrolyze hemicellulose for the manufacturing of fiber boards.<sup>1, 39</sup> The steam explosion is carried out in a large vessel, in which high pressured steam is applied for a few minutes without the use of toxic solvents.<sup>40</sup> The explosion causes the structure of lignocellulosic biomass to break and defibrate. After a specified residence time, steam is rapidly vented from the vessel and the pretreated biomass is discharged into a large cooling tank.

During the steam addition process, hemicellulose is hydrolyzed by acetic acid, which is produced by deacetylation. Similar to LHW treatment, changes in lignocellulosic biomass by steam explosion are initiated by the removal of hemicellulose, enhancing the enzymatic digestibility of cellulose.<sup>33</sup> However, one of the main drawbacks of steam explosion is the production of inhibitory compounds after the explosion steps which can hinder hydrolysis and fermentation steps of the products. Besides that, furan derivatives such as furaldehyde and 5-hydroxymethyl-2-furaldehyde, and phenolic compounds (from lignin depolymerization) also act as inhibitors.<sup>41</sup> An extensive washing step is required to remove these inhibitors. However, the water removes soluble sugars and reduces saccharification rates in the liquid fraction of the pretreated biomass.

### ***Wet oxidation***

Wet oxidation involves combining air or oxygen with water at elevated temperature and pressure, to therefore oxidize organic matter. It is crucial to apply a high temperature to this process to avoid hydrolysis of biomass instead (occurs at low temperatures).<sup>42</sup> The wet oxidation process breaks down hemicellulose, and solubilizes lignin into carbon dioxide, water, and carboxylic acids, namely succinic acid, glycolic acid, formic acid, and acetic acid.<sup>43</sup> Wet oxidation has been known as an industrial process to treat wastes with high organic matter, by oxidizing the suspended wastes at high temperatures (180-200 °C).<sup>8</sup>

This process has been long used for treating waste and carrying out subsequent fermentation.<sup>44</sup> Pretreatment of rice straw to produce ethanol was studied by Banerjee et al., and they found that the optimum pretreatment conditions were 185 °C, 0.5 MPa for 15 minutes, which yielded 67% w/w cellulose, and over 70% hemicellulose and lignin solubilization.<sup>45</sup> Similarly, Szijarto et al. studied wet oxidation to enhance digestibility of cellulose, and found that this method has an increased effectiveness of three times when compared to an untreated biomass control.<sup>46</sup> Recently, Banerjee et al. investigated the use of Alkaline Peroxide-Assisted Wet Air Oxidation (APAWAO) and found that within 24 hours there was a 13-fold increase in glucose yields in rice husk, compared to an untreated rice husk.<sup>47</sup>

Although wet oxidation is considered a suitable pretreatment process for biomass with high lignin content, there are several drawbacks. The use of high temperature, pressure and oxidizing agents lead to high energy costs and safety hazards. Additionally, Martin et al. found that the many byproducts were obtained from wet oxidation, such as succinic acid, glycolic acid, formic acid, acetic acid and phenolics, which would all have inhibitory effects on further downstream processing.<sup>48</sup>

### ***Alkali treatment***

Alkali treatment or lime pretreatment utilizes lower temperatures and pressures compared to other existing methods.<sup>1</sup> Some of the common agents used for alkali treatment are sodium, potassium, calcium, and ammonium hydroxide. Although sodium hydroxide has been studied the most, calcium hydroxide (slake lime) has shown to be the most effective and cheapest alkaline agent. In addition to being cost-effective, lime can also be recovered via a neutralization step.<sup>49</sup>

The process of using calcium hydroxide or lime pretreatment involves slurring lime with water, spraying it onto biomass, and storing it for a specific period (depending on the operating temperature). As a pretreatment method, lime

delignifies biomass and deacetylates hemicellulose, leaving behind highly crystalline cellulose. Kong et al. reported that alkali agents remove acetyl groups in hemicellulose, therefore enhancing carbohydrate digestibility during enzymatic hydrolysis.<sup>50</sup> Similarly, reports show that enzymatic activity increases when lignin is removed, resulting in a decrease in nonproductive adsorption sites.<sup>51</sup> Dilute NaOH has also been found to pretreat biomass in a similar way as lime.<sup>52</sup>

Recently, technological advances have been used to develop a microwave-assisted alkaline pretreatment. Hu et al. showed that radio-frequency based heating resulted in higher sugar yields during enzymatic hydrolysis when compared to conventional heating.<sup>53</sup>

### ***Ammonia fiber expansion (AFEX)***

Ammonia fiber expansion (AFEX), formerly known as ammonia freeze/ fiber explosion, is an effective pretreatment method for herbaceous and agricultural residues.<sup>1, 54</sup> In a flow-through system, aqueous ammonia is added into a high temperature biomass-packed column reactor, at specified residence time and fluid velocity. Under these conditions, aqueous ammonia reacts with lignin in the biomass causing depolymerization of the lignin-carbohydrate complex (LCC). The combined effect of ammonia under high pressure results in swelling of biomass, disruption of its architecture, and subsequent hydrolysis and decrystallization of cellulose, respectively.<sup>55</sup> Yoon et al. and Iyer et al. have reported large delignification in hardwood under 160-180 °C at a residence time of 14 minutes. However, lignin removal in a softwood substrate was less efficient.<sup>56</sup> Pretreatment with AFEX and ammonia itself, has proven to be an efficient method for biomass with low lignin content. Among various alkaline pretreatment methods currently used, AFEX claims to have the highest yield of reducing sugars (80–90 %).<sup>57</sup>

There has been much debate on AFEX as a biomass fractionation method as opposed to a pretreatment method. Since removal of lignin is achieved by disrupting LCC, the remaining biomass components can be hydrolyzed using

enzymes. Kim et al. reports a 90% enzymatic digestibility of ammonia-treated corn stover.<sup>58</sup> While removing lignin, the AFEX process simultaneously removes some hemicellulose and reduces cellulose crystallinity. Therefore, the micro- and macro-accessibility of cellulases are affected, whereby ammonia causes cellulose to undergo phase change from cellulose I to cellulose III. Although lignin is not obtained in its native structure, lignin recovery is still achieved, along with cellulose.

Despite its claim of being an effective pretreatment and fractionation process, the use of ammonia and its recovery have a substantial cost. Although recycling ammonia during pretreatment has shown to decrease the operating cost, it is a tedious process regardless.<sup>58b</sup> Another significant concern while using ammonia is the environmental effects that come from ammonia usage.<sup>12c</sup> Safety measures and emergency response systems need to be in place to prevent any leakage into the environment. However this adds to the cost of the process.<sup>55</sup>

### ***Organosolv***

The organosolv process uses a mixture of organic solvents with an acid catalyst at high temperatures to cleave hemicellulose and cellulose linkages. Solvents that are normally applied include ethanol, methanol, acetone, and methyl isobutyl ketone (MIBK).<sup>59</sup> Typical operating temperatures used can be up to 200 °C, but lower temperatures have been used with the presence of a catalyst.<sup>60</sup>

The organosolv extraction process hydrolyzes not only the internal bonds in lignin, but also between lignin and hemicellulose. Hydrolysis of the glycosidic bonds in hemicelluloses also occurs. When catalysts are present, an acid-catalyzed degradation occurs, where monosaccharides degrade into furfural and 5-hydroxymethyl furfural followed by condensation reactions between lignin and these reactive aldehydes.<sup>61</sup> Following the removal of lignin, the remaining cellulose fraction can be used for enzymatic saccharification.<sup>62</sup>

Organosolv has been extensively used for extraction of high-quality and high yield lignin. It is claimed to be a biomass fractionation process as opposed to

pretreatment, because once the lignin is removed from the biomass, the cellulose fibers become accessible to cellulolytic enzymes which leads to conversion of cellulose into sugars. However, the hemicellulose fraction is difficult to recover through this process as it forms a black liquor during removal of lignin. Bozell et al. recommends an ion exchange chromatography to recover hemicellulose, but this step has not been optimized and no work has been reported on it so far.<sup>63</sup>

The main drawback of the process is that the solvents and catalysts employed are expensive. Nevertheless, qualitative recovery of the solvent can considerably reduce the operational cost.<sup>64</sup> Another important aspect involving cost is the need for implementation of safety measures due to the high flammability of organic solvents. As for the enzymatic hydrolysis step, washing steps need to follow due to organic solvents being inhibitors of enzymatic activity.<sup>1, 65</sup>

### ***Gamma valerolactone (GVL) extraction***

In early 2014, researchers at UW-Madison discovered a method to deconstruct lignocellulosic biomass and produce sugars using a solvent known as gamma valerolactone or GVL. GVL is a cyclic atom with 5 carbons (valero-), which consists of 5 atoms (four carbons and one oxygen) in the ring ( $\gamma$ -lactone) (Figure 3). The solvent is colorless and stable at atmospheric conditions, with a sweet herbaceous odor.<sup>66</sup> In addition to that, GVL is inexpensive, recyclable and can be produced from biomass.

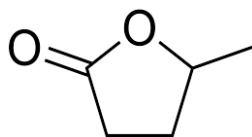


**Figure 3.** Structure of gamma valerolactone.

The proposed solvent was first studied by Horvath et al. as a promising renewable solvent for the production of energy and carbon-based products.<sup>66</sup> As a solvent for lignocellulosic biomass processing, biomass is allowed to react with GVL and water under the presence of an acid catalyst and moderate temperatures. As a result, water-insoluble carbohydrates are converted to water-soluble carbohydrates. The desired products are separated into an aqueous layer and can be recovered, while the GVL solvent forms another layer and is recycled.<sup>67</sup>

Typically following biomass pretreatment, cellulose is converted into glucose through enzymatic hydrolysis, and further converted into platform chemicals such as levulinic acid (LA), 5-hydroxymethylfurfural (HMF), and liquid fuels.<sup>68</sup> The Department of Energy, as well as Bozell and Petersen<sup>69</sup> confirmed that LA is a promising building block for production of fuels, and can be produced from cellulose and hemicellulose. The conversion into chemicals can also be achieved through single step methods like pyrolysis. However, pyrolysis relies on high temperatures to deconstruct lignocellulosic biomass and require additional steps for downstream separations.<sup>70</sup> GVL was recently reported as an effective solvent to directly produce high value platform molecules from cellulose and hemicellulose. Alonso et al. successfully processed cellulose and hemicellulose from corn stover by eliminating the fractionation step and simultaneously producing organic compounds using GVL (Figure 4).<sup>70</sup>

In addition to production of chemicals, lignin can also be extracted through GVL/ H<sub>2</sub>O mixtures.<sup>71</sup> Tabasso et al. studied the fractionation of post-harvested tomato plants in a microwave reactor by using GVL and H<sub>2</sub>O at 170 °C for 2 hours.<sup>72</sup> In their study, the cellulose fraction was rapidly converted to LA in a biphasic system, whereas the lignin was extracted via precipitation. Following fractionation, the addition of NaCl favors the separation of GVL into an organic layer, along with LA, lignin and some lignin-like condensation products. A more recent advance in biomass fractionation through GVL was presented when researchers reported that lignin can not only be isolated, but also upgraded via a

Ru/C catalyst.<sup>73</sup> Following the dilution and precipitation step of lignin after GVL treatment, the extracted lignin was determined to be similar to the native lignin, based on a heteronuclear single quantum coherence nuclear magnetic resonance (HSQC NMR) spectroscopy study. Relative to cellulase-digested enzymatic lignin, GVL lignin was reported to be cleaner; relatively free of carbohydrates with little degradation resulting in some molecular weight reduction.<sup>74</sup>

One of the many appealing features of GVL compared to other available methods is the residence time efficiency. At a reaction time of 30 minutes, GVL still produces high yields of native-like lignin, i.e., objectively free of carbohydrates and little degradation of lignin structure.

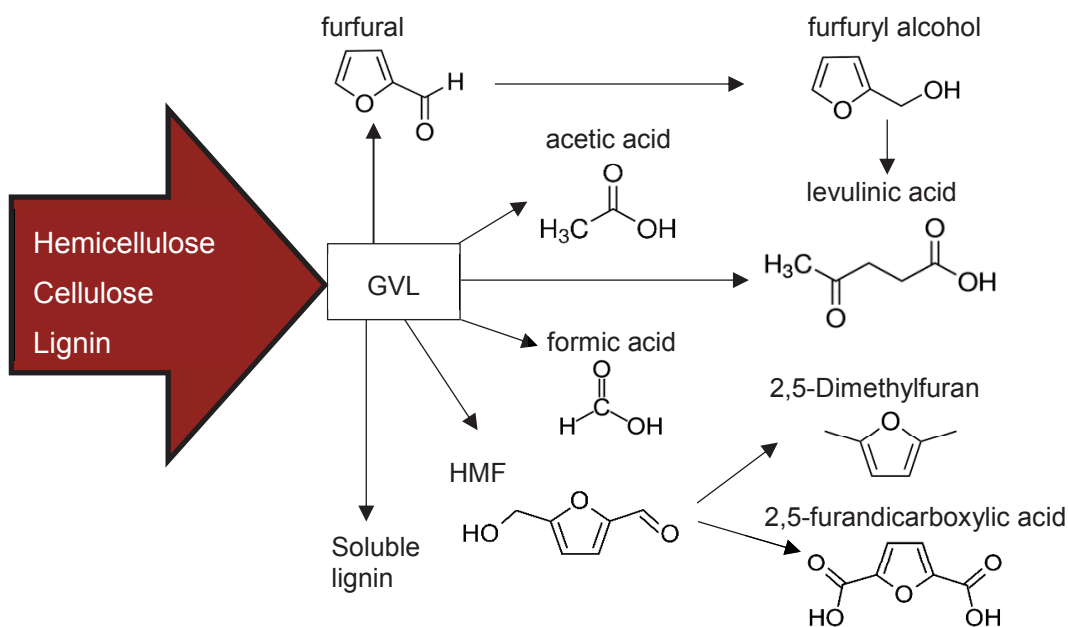


**Figure 4.** Products derived from lignocellulosic biomass using the GVL pathway.

Reproduced from Alonso et al., 2013.<sup>70</sup>

### ***Tetrahydrofuran (THF) extraction***

Tetrahydrofuran is another traditional, organic solvent that has been used more recently for biomass fractionation. Leitner's group calls this process an OrganoCat process, in which hemicellulose, cellulose pulp, and lignin are separated in a single-step process.<sup>75</sup> Hemicellulose is first depolymerized, therefore liberating the two other major components. One of the pioneer works that introduced this method is the use of 2-methyltetrahydrofuran (2-MTHF) and oxalic acid to separate lignin from cellulose pulp and soluble sugars by *in situ* extraction.<sup>76</sup>

One of the most recent reports of purity using this method is ~70 wt.% for cellulose from corn stover, whereas the yields are 83 wt.% for cellulose, 79.6 wt.% hemicellulose (through production of lactic acid and xylose), and about 60-70% lignin.<sup>77</sup> However, much like many other pretreatment and fractionation methods listed above, THF is associated with several safety and sustainability issues. Although relatively non-toxic, THF can penetrate the skin through latex gloves and cause rapid dehydration. Additionally, it is highly flammable and forms highly explosive peroxides when in contact with air.<sup>78</sup> The dangers associated with this solvent affect its sustainability due to the need for costly disposal and handling methods.

## **Summary**

A summary of the effects of pretreatment and fractionation methods on the structure of biomass is shown in Table 2 below.

Unlike the other pretreatment methods described above, organosolv, GVL, tetrahydrofuran (THF), and AFEX have also been used for biomass fractionation. Similarly, ionic liquids, which will be introduced in the next section, have been a remarkable pathway for both pretreatment and fractionation.



A major difference between ILs and two of the methods mentioned above (organosolv and AFEX) is that the latter use highly toxic solvents and hazardous process conditions to completely decrystallize cellulose and hydrolyze hemicellulose at high biomass loadings and short residence times.<sup>13a, 79</sup> The organosolv method uses flammable organic solvents and has a high risk of combustion and explosion due to high operating temperatures. Besides that, organic solvents are expensive and therefore need to be recovered for cost-effectiveness. Similarly, AFEX is not only a tedious fractionation process, but also creates safety concerns like the organosolv process. The ammonia-treated substrate contains traces of lignin that can only be removed through extensive water washing. Additionally, AFEX is not suitable for all biomass types and less effective when lignin content increases.

On the other hand, the two most recently used organic solvents (GVL and THF) for biomass fractionation use processes that are similar to ionic liquids. However, GVL and THF are more traditional organic solvents while ionic liquids are known as “modern” solvents for biomass processing. Since then, a significant amount of research has been done on a more effective and safer fractionation process through these solvents, and this thesis will only focus on ionic liquids.

**Table 2.** Summary of the effects of pretreatment and fractionation on the structure of lignocellulosic biomass.

	Decrystallize cellulose	Removes hemicellulose	Removes lignin	Alters lignin structure	Alters hemicellulose	Increase accessible area
Ball milling and compression milling	•					•
Acid wash		•		•		•
Alkali treatment	•	•	•	•		•
Hydrothermal treatment		•	•	•		
Wet oxidation		•	•	•		
AFEX	•		•	•		•
Organosolv	•	•	•	•	•	
GVL	•	•	•	•	•	
THF	•	•	•	•	•	
Ionic liquids	•	•	•			•

## Ionic liquids

### ***Brief history***

Although the discovery of the “first” ionic liquid (IL) is often disputed, the development of an imidazolium-based IL was reported more than half a century ago when 1-ethyl-3-methylimidazolium ([EMIM])Chloride was mixed with  $\text{AlCl}_3$  to form a series of equilibria between the following ILs:  $[\text{EMIM}]\text{AlCl}_4$ ,  $[\text{EMIM}]\text{Al}_2\text{Cl}_7$ , and  $[\text{EMIM}]\text{Al}_3\text{Cl}_{10}$ .<sup>80</sup> Since then, ILs have been used in various fields of science as catalysts, pharmaceutical drugs, and electrolyte media for batteries and nuclear fuel, to cite a few.<sup>81</sup>

While common liquids such as water and gasoline constitute neutral molecules, ILs consist of ions and short-lived ion pairs with high ionic conductivity and wide electrochemical range, and better dissolving capacity for most biopolymers.<sup>82</sup> Ionic liquids are advantageous for biomass pretreatment and fractionation due to the low requirement of equipment and energy cost, their ability to be recovered, and the absence of inhibitory compounds.<sup>4a, 83</sup> Besides that, ILs are also environmentally-safe, with minimal emissions and low toxin production, compared to other solvents.<sup>83</sup> They are considered as “green” solvents.

To date, three classes of ILs are used in biomass processing, namely aromatic ILs, molten salt hydrates (MSH), and deep eutectic solvents.<sup>84</sup> Despite being grouped separately, these ILs share similar chemical properties that are unique and favorable for a viable biomass pretreatment or fractionation process. In addition to having negligible vapor pressure, high thermal stability, solvent miscibility, and various tunable properties<sup>82, 85</sup>, ILs are one of the few solvents that are capable of solubilizing biopolymers such as cellulose, lignin, and to some extent, whole biomass.<sup>86</sup> For the purpose of this document, only imidazolium-based ILs will be discussed.

Before rising to fame as solvents for biomass processing, ionic liquids were known as cellulose solvents to dissolve cellulose for extrusion of thin fibers or rods. Swatloski et al. (Rogers and group) were pioneers in showing that the IL 1-butyl-3-methylimidazolium ([BMIM])Chloride is able to dissolve up to 25 wt.% of cellulose.<sup>87</sup> Since then, researchers have investigated many other ILs that can efficiently dissolve cellulose. Several common ones are 1-allyl-3-methylimidazolium ([AMIM])Chloride; dissolving 14.5 wt.% at 80 °C and 1-ethyl-3-methylimidazolium ([EMIM])Acetate dissolving up to 16 wt.% at 90 °C.<sup>88</sup> Besides cellulose, lignin has also been shown to dissolve in ILs. Pu et al. showed that the ILs 1,3-dimethylimidazolium ([MMIM])Methylsulfate, 1-hexyl-3-methylimidazolium ([HMIM]) trifluoromethanesulfonate, and 1-butyl-3-methylimidazolium ([BMIM]) Methylsulfate can dissolve up to 20 wt.% of lignin from kraft pine.<sup>89</sup>

Since ILs are able to dissolve biopolymers so efficiently, researchers found several ways to use them for biomass processing, namely pretreatment, activation, fractionation, and dissolution. These processes are described below.

### ***Ionic liquid pretreatment***

Ionic liquids pretreatment involves the use of high temperatures to disrupt and remove the lignin and hemicellulose fractions, to allow cellulose to solubilize in ILs. Then, upon addition of an anti-solvent, biomass is precipitated through a solute-displacement mechanism, and further hydrolyzed by cellulases and hemicellulases.

Researchers at the Joint BioEnergy Institute (JBEI) have tested many different ILs for pretreatment of lignocellulosic biomass, and have mainly focused on [EMIM]Acetate in the recent years.<sup>79, 90</sup> Although a high yield of sugars are released from cellulose, a pretreatment approach is inefficient in the sense that only the cellulose fraction of lignocellulosic biomass is recovered, leaving behind lignin and hemicellulose that have been depolymerized. Even if the lignin and hemicellulose are processed, the starting yields of these fractions would be much

lower than it originally used to be.<sup>79, 91</sup> Since then, IL activation has replaced pretreatment in order to extract all the lignocellulosic components with minimal degradation.

### ***Ionic liquid activation and regeneration***

Ionic liquid activation involves a similar pathway to IL pretreatment, but is a better approach using milder process conditions such as low temperatures and less time.<sup>92</sup> During activation, the fractions of biomass are gently loosened by cleaving the acetyl groups on the hemicellulose with minimal impact to the lignin. Following activation, biomass is regenerated through the addition of an anti-solvent similar to IL pretreatment.

However, in the case of IL activation, it is important to note that the regeneration step allows for the whole biomass to be recovered, whereby the carbon content is preserved and the chemical composition, yield is similar to native biomass. After recovery, the whole biomass can be further processed to produce sugars and lignin (as intermediates), as opposed to having losing some of the hemicellulose and lignin yields during pretreatment.

### ***Biomass fractionation***

Biomass fractionation through an ionic liquid process allows for recovery of products with high yield and high purity. Following IL activation, biomass regeneration allows for the loosened and deacetylated structure to undergo enzymatic saccharification to convert the cellulose and hemicellulose fractions, leaving a solid fraction of lignin with high purity. Due to recent needs for biomass valorization, ionic liquids have become an attractive fractionation solvent mainly due to its non-toxicity and non-hazardous process conditions.

To date, researchers have yet to identify an IL that can effectively fractionate biomass without an additional pretreatment step. Jiang et al. and Singh's group (JBEI) showed that a combined dilute-acid pretreatment and IL

“activation” produces better cellulose conversion due to the removal of hemicellulose.<sup>93</sup> A coupled autohydrolysis-IL fractionation have also been used by first treating the feedstock at temperatures of 160-220 °C, and subsequent IL activation/pretreatment.<sup>94</sup> In our group, Wang et al. showed that an autohydrolysis-IL fractionation only requires a 3 hour activation time for complete conversion of cellulose after autohydrolysis of 160 °C for 60 minutes.<sup>95</sup>

### ***Biomass dissolution in ionic liquid***

Biomass dissolution in ionic liquids have been explored since Rogers’ group first dissolved cellulose in ILs. However, many researchers report that several IL properties are a barrier to complete dissolution of ILs. Dissolving whole biomass in ILs allows for direct product development through extrusion of films and fibers, which can be used in the textile and packaging industries. The challenge however lies in identifying an IL with good dissolution properties without requiring a hemicellulose extraction step in order to reach a suitable viscosity for extrusion.<sup>96</sup>

Viscosity has been one of the most commonly addressed topics when using ionic liquids. Ionic liquids have a considerably higher viscosity than most solvents used for pretreatment and fractionation of biomass.<sup>97</sup> Therefore, the physicochemical properties of ILs require close analysis in order to identify ILs that are suitable for either dissolution, activation, or fractionation. These physicochemical properties and respective changes in biomass structure are studied closely in the following sections.

## **Summary**

During IL pretreatment, activation, fractionation, or dissolution, one of the most important aspects to consider is the nature of ILs. Despite extensive trial-and-error research in finding a suitable IL for these applications, a rational screening process is required of ILs to consider viscosity, density, thermal stability,

polarity, hygroscopicity, to name a few. Some of these will be addressed in Chapter II and III of this thesis.

## **CHAPTER II**

# **RELATIONSHIP BETWEEN LIGNOCELLULOSIC BIOMASS DISSOLUTION AND PHYSICOCHEMICAL PROPERTIES OF IONIC LIQUIDS COMPOSED OF 3-METHYLIMIDAZOLIUM CATIONS AND CARBOXYLATE ANIONS**



*A version of this chapter has been submitted to Physical Chemistry Chemical Physics as a peer-reviewed article.*

Preenaa Moyer, Micholas Dean Smith, Nourredine Abdoulmoumine, Stephen C. Chmely, Jeremy C. Smith, Loukas Petridis, and Nicole Labbé. (2017). Relationship between lignocellulosic biomass dissolution and physicochemical properties of ionic liquids composed of 3-methylimidazolium cations and carboxylate anions. *Physical Chemistry Chemical Physics*.

Preenaa Moyer performed the experiments, conducted data analysis, and wrote the first draft of the manuscript. Dr. Micholas Dean Smith and Dr. Loukas Petridis performed molecular dynamics simulations, provided data interpretation, and co-wrote the manuscript. Dr. Nourredine Abdoulmoumine, Dr. Stephen C. Chmely, and Dr. Jeremy C. Smith assisted with some data interpretation and edited the manuscript. Dr. Nicole Labbé oversaw the experimental design, assisted with data analysis, and edited the manuscript.

## **Abstract**

The ionic liquid (IL) 1-ethyl-3-methylimidazolium acetate ([EMIM]Acetate) has been widely used for biomass processing, i.e. to pretreat, activate, or fractionate lignocellulosic biomass to produce soluble sugars and lignin. However, this IL does not achieve high biomass solubility, therefore minimizing the efficiency of biomass processing. In this study, [EMIM]Acetate and three other ILs composed of different 3-methylimidazolium cations and carboxylate anions ([EMIM]Formate, 1-allyl-3-methylimidazolium ([AMIM]) formate, and [AMIM]Acetate) were analyzed to relate their physicochemical properties to their biomass solubility performance. While all four ILs are able to dissolve hybrid poplar under fairly mild process conditions (80 °C and 100 RPM stirring), [AMIM]Formate and [AMIM]Acetate have particularly increased biomass solubility of 40 and 32%, respectively, relative to [EMIM]Acetate. Molecular dynamics simulations suggest that strong interactions

between IL and specific plant biopolymers may contribute to this enhanced solubilization, as the calculated second virial coefficients between ILs and hemicellulose are most favorable for [AMIM]Formate, matching the trend of the experimental solubility measurements. The simulations also reveal that the interactions between the ILs and hemicellulose are an important factor in determining the overall biomass solubility, whereas lignin-IL interactions were not found to vary significantly, consistent with literature. The combined experimental and simulation studies identify [AMIM]Formate as an efficient biomass solvent and explain its efficacy, suggesting a new approach to rationally select ionic liquid solvents for lignocellulosic deconstruction.

## Introduction

Ionic liquids have been used for biomass pretreatment and fractionation as a means of obtaining products from lignin, cellulose, and hemicellulose.<sup>1, 98</sup> Three classes of ILs are used in biomass processing, namely aromatic ILs, molten salt hydrates, and deep eutectic solvents.<sup>84, 99</sup> Despite this separate classification, all ILs essentially consist of ion pairs, and the possible combinations of cations and anions are endless. As “designer” solvents, ILs can have many desirable properties, such as a wide electrochemical range, low vapor pressure, and high thermal stability.<sup>100</sup> These and other unique properties of ILs that are important in industrial applications, such as viscosity, polarity, hygroscopicity, and solvation, are widely tunable by selecting specific cations and anions. For efficient biomass dissolution, specific cationic-anionic combinations are required of an IL. The anions need to have strong hydrogen bond acceptability to form hydrogen bonds with components of biomass, whereas IL cations need to possess strong acidic protons and short side chains to reduce steric hindrance between the IL and biomass during dissolution.<sup>101</sup>

Dissolution or solubilization of lignocellulosic biomass in an IL improves the accessibility of carbohydrates for conversion into mono sugars.<sup>102</sup> Numerous studies have focused on dissolving plant biopolymers, i.e., cellulose, hemicellulose, and lignin in ILs to demonstrate the potential for ILs to pretreat, “activate” or precipitate and recover certain lignocellulosic components.<sup>92, 103</sup> During IL pretreatment, high severity is mostly employed to disrupt the whole lignocellulosic structure, facilitating easy access to cellulose, which is then converted into simple sugars. Subsequently, these sugars are fermented into chemicals and fuels. In contrast, an IL fractionation process uses an approach known as “activation”, with mild operating conditions to deacetylate the biomass structure, reduce the recalcitrance of biomass while minimizing degradation, such that the main linkages in biomass are preserved, therefore allowing for fabrication of products such as high quality films and fibers.<sup>96</sup>

In particular, the IL 1-ethyl-3-methylimidazolium ([EMIM]) acetate has been popular for the above applications<sup>90, 92a, 103b, 104</sup> as it is composed of an unsaturated heterocyclic cation with an ethyl chain, coupled with a basic acetate anion. This particular ion combination is believed to efficiently process biomass across wide temperature ranges, time scales, and stirring conditions for pretreatment to produce sugars, and also for fractionation to recover sugars and lignin.<sup>98a</sup> Unlike IL pretreatment however, IL activation requires screening for ionic liquids that have a high capacity for dissolving biomass under low severity. This screening process has identified several limitations of using [EMIM]Acetate, such as high viscosity<sup>92b</sup>, insolubility of xylan, and subsequently, low solubility of the whole biomass.<sup>98a</sup> These setbacks have encouraged efforts to identify other ionic liquids that perform better than [EMIM]Acetate.<sup>105</sup>

A thorough understanding of the physicochemical properties of [EMIM]Acetate and other ILs can help explain the relative efficiencies in solubilizing cellulose, lignin, and whole biomass.<sup>98b, 106</sup> One of the important physical properties of pretreatment solvents that influences solubility of biomass is

viscosity, with lower viscosity facilitating biomass dissolution.<sup>107</sup> In general, all ILs are highly viscous. While solvents such as methyl isobutyl ketone (MIBK) and ethanol (used in Organosolv fractionation) have viscosity of 0.58 mPa-s and 1.13 mPa-s, respectively at room temperature, ILs have viscosity about 2 or 3 orders of magnitude higher.<sup>97</sup> Additionally, swelling of the lignocellulose occurs during a biomass dissolution process, causing increased viscosity in the IL environment, limiting subsequent solubilization.<sup>108</sup> As a temperature-dependent property, lower viscosities are observed at higher temperatures. For instance, the viscosity of 1-butyl-3-methylimidazolium ([BMIM]) acetate decreases from 646 to 6 mPa-s upon heating from 20 to 100 °C.<sup>108a, 109</sup> However, viscosity can be altered completely due to its dependence on the cations and anions used. Several Quantitative Structure Property Relationship (QSPR) studies have analyzed the viscous behavior of ILs in terms of the electrostatic interactions between the cation and anion, interionic hydrogen bonding, and van der Waals interactions.<sup>97, 110</sup> Overall, viscous behavior of ILs, which is governed by their respective chemical structures, is a common problem during biomass dissolution. Therefore, it is speculated that altering the chemical structure of ILs will affect viscosity, i.e., polarity of molecules change when cations and/or anions are varied, hence affecting physical properties of an IL as well as biomass solubility.

Over the last few years, scientists have been extensively studying the properties of IL structures in an attempt to shed light on the poorly understood effect of ionic combination of ILs towards solvation.<sup>102-103</sup> In biomass processing, it has been long recognized that the anion of an ionic liquid plays a significant role in dissolving cellulose and lignin.<sup>89, 107, 111</sup> The anions e.g., chloride, acetate, and formate, which are conjugate bases, have high hydrogen bond basicity and favor non-covalent interactions with hydrogen atoms on the hydroxyl groups of cellulose and lignin. However, while the anionic mechanisms of ionic liquids have been explained experimentally and theoretically, the cationic mechanisms are still debated. Most ILs used in biomass processing have an organic, aromatic cation

due to their thermal stability. In particular, imidazolium and pyridinium cations are often deemed effective when coupled with highly basic anions.<sup>112</sup> Recent studies showed that it is especially important for IL cations to have an unsaturated heterocyclic structure in order to have large interaction energies and  $\pi$ -electron delocalization with cellulose.<sup>113</sup> Although these findings provide a rough basis for selection, the quantitative determination of the effects of IL physicochemical properties on biomass solubility is still an existing question.

In this paper, four ionic liquids are investigated by switching the cation-anion combinations to study their respective interactions leading to differences in biomass solubility. In a series of findings, we relate biomass solubility to the viscosity and other physicochemical properties of each IL. Our experimental results are further affirmed through molecular dynamics simulations, which provide estimates of virial coefficients that quantify the interaction strength between IL ions and plant polymers. These studies provide insights that may be used to further fine-tune IL composition for optimal biomass processing for production of fuels and chemicals.

## **Materials and methods**

### ***Biomass and ionic liquids***

The biomass, hybrid poplar (*Populus spp.*), was obtained from The Center for Renewable Carbon, The University of Tennessee. After being air-dried, the material was milled with a Wiley mill (Thomas Scientific™, Model # 3383-L10, Swedesboro, NJ) through a 40-mesh screen (0.425 mm).

The ionic liquids, 1-ethyl-3-methylimidazolium acetate ([EMIM]Acetate, purum  $\geq 95\%$ ), 1-ethyl-3-methylimidazolium formate ([EMIM]Formate, purum  $\geq 95\%$ ), 1-allyl-3-methylimidazolium formate ([AMIM]Formate, purum  $\geq 95\%$ ), and 1-allyl-3-methylimidazolium acetate ([AMIM]Acetate, purum  $\geq 95\%$ ) used in this

study were purchased from Iolitec Inc. (Tuscaloosa, AL) and were used as received. Deionized water was used in between steps.

## ***Biomass characterization***

### **1. Extractives removal**

The 40-mesh hybrid poplar powder was extracted in an Accelerated Solvent Extractor (ASE 350, Dionex, Sunnyvale, CA) to remove non-structural components known as extractives. The employed methodology was adapted from the National Renewable Energy Laboratory (NREL) Analytical Procedure: “Determination of Extractives in Biomass”. Approximately 7 g of biomass powder were mixed with 40 g of glass beads (3 mm) and added to a 66 mL extraction cell. The biomass underwent sequential extraction with water and ethanol under 1500 psi at 100 °C with a 7-minute static time per cycle (3 cycles). The wet, extractives-free hybrid poplar was then oven-dried at 40 °C until constant moisture content was achieved (less than 7% by weight).

### **2. Chemical composition analysis**

The chemical composition of the extractives-free hybrid poplar was analyzed using the National Renewable Energy Laboratory (NREL) Analytical Procedure: “Determination of Structural Carbohydrates and Lignin in Biomass”. The overall chemical composition is presented in Table 3.

**Table 3.** Chemical composition of hybrid poplar.

<b>Component</b>	Glucan	Xylan	Galactan	Arabinan	Mannan
<b>Amount (% on dry basis)</b>	44.27 ± 0.24	16.43 ± 0.14	1.20 ± 0.04	0.54 ± 0.07	2.41 ± 0.02

Standard deviations were obtained from triplicates

### ***Solubility of hybrid poplar in ionic liquids***

The solubility of the extractives-free hybrid poplar in four different ILs was assessed by measuring the maximum weight of biomass that can be dissolved in each IL at 80 °C after 7 days, following recommended methods that have been published.<sup>114</sup> The fraction of dissolved biomass was calculated based on the following Eq. (10):

$$\text{Biomass dissolved (\%)} = \frac{w_{\text{biomass}}}{w_{\text{biomass}} + w_{\text{IL}}} * 100\% \quad (10)$$

where  $w_{\text{biomass}}$  represents the 105 °C oven-dried biomass weight and  $w_{\text{IL}}$  represents the weight of ionic liquid.

In each solubility measurement, all four ILs were first heated to 100 °C to remove moisture before carrying out any measurements. After 15 minutes, the temperature was decreased to 80°C and biomass powder (0.05 g) was added daily to the ionic liquid (3.5 g) in a 20 mL vial. The vial was placed on a heating plate with a 100 RPM stirring. The solubility was monitored by placing an aliquot of the solution under a microscope at the end of Day 5. Additional biomass was added if no particles were observed. In the presence of undissolved particles, more ionic liquid was added to the solution until an equilibrium was achieved on Day 7. Triplicates were conducted for each experiment.

### ***Thermal analysis of ionic liquids***

A thermogravimetric analyzer (Pyris 1 TGA, Perkin Elmer, Shelton, CT) was used to conduct thermogravimetric analysis (TGA) of the neat ILs. About 8-10 mg of ionic liquid were heated in a platinum pan from 30 to 600 °C at a rate of 10 °C /min under 10 mL/min of nitrogen to collect the thermal decomposition curve. Thermograms obtained from the TGA were differentiated into weight loss rates known as differential TG (DTG) peaks to obtain the decomposition temperature of each IL.

### ***Rheological property measurements of ionic liquids***

The viscosity of [EMIM]Acetate, [AMIM]Formate, and [AMIM]Acetate was monitored over a temperature range of 25-100 °C and the viscosity of [EMIM]Formate from 45-100 °C (due to its solid state below 45 °C). The ILs were loaded onto a Peltier temperature-controlled plate of a controlled stress rheometer (TA Instruments AR-G2). Silicon oil and metal plate covers were used to prevent the IL from absorbing moisture during the measurement. The viscosity of each sample was measured at a shear rate of 100 s<sup>-1</sup>, determined by finding the linear region in a variable rate experiment, using 40 mm diameter cylindrical plates with a gap of 56 µm. Duplicate experiments were performed for each IL. A graphical software (OriginPro) was used to fit an exponential regression to the viscosity-temperature data

### ***Kamlet-Taft measurements***

The Kamlet-Taft parameters are often used to describe polarity and compare solvation properties in ILs that have slight differences in substituents.<sup>115</sup> In general,  $\beta$  indicates the hydrogen bond basicity which is governed by the nature of the anion,  $\alpha$  shows the hydrogen bond acidity, governed by the cation, and  $\pi^*$  describes the polarizability of an IL.<sup>116</sup> These parameters ( $\alpha$ ,  $\beta$ , and  $\pi^*$ ) are determined from the UV-Vis absorbance peaks of the following three dye solutions: Reichardt's dye (RD), N, N-diethyl-4-nitroaniline (DENA), and 4-nitroaniline (NA). Additionally, a transition energy parameter,  $E_T(30)$  measures the polarity determined by the charge-transfer absorption band of Reichardt's dyes.

To measure KT parameters, stock solutions of the dyes were first prepared in methanol (0.0005 mol/L of RD and 0.001 mol/L of DENA and NA). A mixture of 1.8 mL ionic liquid and each of the dye solutions was transferred into a vial, homogeneously mixed, and dried *in vacuo* at 40 °C for 24 h. After drying, 600 µL of each IL-dye mixture was pipetted into a Quartz cell (1.0 cm pathlength). The visible spectrum of the solutions was measured and recorded using a Thermo



Scientific™ GENESYS™ 10S UV-Vis Spectrophotometer. By obtaining the wavelength of dyes at maximum absorption ( $\lambda_{\max}$ ), the KT parameters were calculated using the published equations<sup>117</sup>:

$$v = 1/(\lambda_{\max}(\text{dye}) \times 10^{-4}) \quad (11)$$

$$\alpha = 0.0649 E_{\tau}(30) - 2.03 - 0.72\pi^* \quad (12)$$

$$E_{\tau}(30) = 28592 / \lambda_{\max}(\text{Reichardt's dye}) \quad (13)$$

$$\pi^* = 0.314(27.52 - v_{\text{N,N-diethyl-4-nitroaniline}}) \quad (14)$$

$$\beta = (1.035v_{\text{N,N-diethyl-4-nitroaniline}} + 2.64 - v_{\text{4-nitroaniline}}) / 2.80 \quad (15)$$

Measurements were carried out at 25 °C, following observations by Zhang et al. that the parameters do not differ when measured between 25-80 °C.<sup>118</sup>

### ***Simulation details***

All-atom molecular dynamics simulations of the four ionic liquids in the presence of representative poplar hemicellulose and lignin polymers were performed to obtain detailed descriptions of the effective interaction strengths of the anions and cations with the biopolymers, and structural properties (radial distribution functions) of the ILs. Parameters for the ionic liquids were obtained from the CHARMM-GUI interface with the CHARMM general force-field,<sup>119</sup> and the CHARMM parameters for hemicellulose<sup>120</sup> and lignin<sup>121</sup> were employed.

Simulation boxes of the ionic liquids were prepared using VMD and converted to GROMACS format for relaxation and production simulations with the GROMACS simulation suite.<sup>122</sup> For each IL, five independent sets of simulations were performed in two steps: an ~5.6 ns NPT relaxation followed by an ~60 ns NVT production simulation. During the relaxation simulations, the pressure was fixed to 1 bar using the Berendsen barostat, while the temperature was fixed to 353 K using the V-Rescale thermostat.<sup>123</sup> For both, the relaxation and production stages, the integration timestep was set to 2 fs and bonds were constrained using the LINCS algorithm.<sup>124</sup>

Radial distribution functions (RDFs) were obtained from the last 1.95  $\mu$ s of the production simulations. The RDFs were used to calculate the second virial coefficients (interaction virials) using the well-known liquid theory relation<sup>125</sup> :

$$B_2 = -2\pi \int_0^\infty (g(r) - 1)r^2 dr \quad (16)$$

where  $g(r)$  is the radial distribution function and  $r$  is the distance between pairs of interest.

## Results and discussion

In addition to 1-ethyl-3-methylimidazolium ([EMIM])Acetate, three different ILs were studied by varying the cation-anion combinations. The general structure of these ILs is shown in Figure 5 and their images are shown on Figure 6.

[EMIM]Acetate:	$R^1 = \text{CH}_2\text{CH}_3$	$R^2 = \text{CH}_3$
[EMIM]Formate:	$R^1 = \text{CH}_2\text{CH}_3$	$R^2 = \text{H}$
[AMIM]Formate:	$R^1 = \text{CH}_2\text{CHCH}_2$	$R^2 = \text{H}$
[AMIM]Acetate:	$R^1 = \text{CH}_2\text{CHCH}_2$	$R^2 = \text{CH}_3$

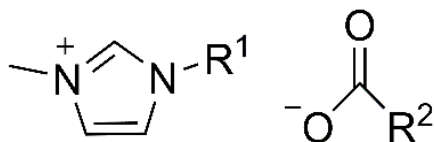


**Figure 5.** Chemical structure of the ionic liquid cation (left) and anion (right).



**Figure 6.** Ionic liquids used in this experiment. Top: [EMIM]Acetate (left), [EMIM]Formate (right). Bottom: [AMIM]Acetate (left), [AMIM]Formate (right).

**Table 4.** Hybrid poplar solubility in ionic liquids measured at 80 °C.

Ionic liquid	Solubility of Hybrid poplar @ 80°C (wt. %)
[EMIM]Acetate	5.27 <sup>a</sup>
[EMIM]Formate	5.28 <sup>a</sup>
[AMIM]Formate	7.39 <sup>b</sup>
[AMIM]Acetate	6.96 <sup>c</sup>

Biomass solubility was measured based on Eq.1. Means followed by the same letter are not significantly different at an alpha level of 0.05.

The role of the ion pairs, i.e., cation and anion of ILs in dissolving biopolymers was studied using two cations and two anions in four different combinations, with [EMIM]Acetate as the reference. The data in Table 4 show that ILs with [AMIM] cations have significantly higher biomass solubility than their [EMIM] counterparts. In particular, [AMIM]Formate and [AMIM]Acetate show increased dissolution by 40 and 32%, respectively compared to the commonly used IL [EMIM]Acetate. In the following paragraphs explaining MD simulations, we attribute the large difference in solubility to the ability of each IL to dissolve all of the major components of biomass, i.e., cellulose, hemicellulose, and lignin. To our knowledge, the role of hemicellulose in whole biomass dissolution in ILs still remains unclear.

Numerous studies have determined that [EMIM]Acetate is a highly efficient solvent when dissolving cellulose, achieving up to 15 wt.% at 25 °C.<sup>126</sup> Similarly, lignin solubility in [EMIM]Acetate was reported to be high enough to provide good extractability without solubilizing the whole wood feedstock.<sup>127</sup> However, [EMIM]Acetate has been reported to dissolve only ~5 wt.% of xylan at a temperature of 25 °C, which is one-third the amount of cellulose.<sup>128</sup> These results suggest that xylan, a component of hemicellulose, is the limiting factor for biomass solubilization with [EMIM]Acetate. Similar to the dissolution mechanism of glucan or cellulose in ILs, xylan requires the disruption of hydroxyl groups through hydrogen bond formation.<sup>88a</sup> Xylan has two hydroxyl groups per sugar monomer whereas glucan has three hydroxyl groups per D-glucose unit.<sup>129</sup> The low density of hydroxyl groups in xylan may explain its relatively low solubility in ILs and inability to compete with cellulose. In spite of that, Fukaya et al. showed that [AMIM]Formate can dissolve a significant quantity of xylan at temperatures above 60 °C, reaching up to 20 wt.% at 90 °C,<sup>117</sup> while [EMIM]Acetate can only dissolve half of that (~10 wt. %) at the same temperature.<sup>117, 128, 130</sup> The ILs [AMIM]Formate and [AMIM]Acetate also recorded high cellulose solubility, measuring up to 18.5 wt.% and 22.0 wt.% respectively, within an hour of mixing at 80 °C.<sup>118</sup> Although

these findings are consistent with our results for solubility, the authors were unable to infer whether the anion or cation of an IL dominates this behavior and contributes to the properties of an IL when dissolving components of biomass. Additionally, to our knowledge, there are no available temperature-dependent xylan or biomass solubility data for [EMIM]Formate and [AMIM]Acetate.

Several physical properties (thermal stability and viscosity) were of particular interest to our study to achieve an understanding of the interionic properties of ILs during biomass solubilization. The thermal stability of the ILs was determined by thermogravimetric analysis (TGA) at room temperature (day 0), and after heating at 80 °C for 7 days (Figures 7, 8 and 9) to mimic our solubility test. The ILs appeared to be stable throughout the course of the experiment and had decomposition temperatures,  $T_d$ , in the range of 205-242 °C, with [AMIM]Formate and [AMIM]Acetate being on the lower end (Table 5).

Decomposition studies of ILs have shown that the decomposition pathway is initiated by an  $S_N2$  nucleophilic attack of the anion on the cation.<sup>131</sup> The IL pool in this study suggests that the nucleophilic substitution mechanism highly depends on the alkyl substituent on the cation, as evidenced by the observed difference in  $T_d$  between ILs of the same anion, i.e., [AMIM]Formate and [EMIM]Formate or [AMIM]Acetate and [EMIM]Acetate (Table 5). Both ILs with an [EMIM] cation have higher  $T_d$  than their [AMIM] counterparts. These findings are consistent with the literature, showing that changes in electronic structure and size of ions, such as methylation on C2 site of cation, and alkyl substituent groups on the cation and the anion, can all significantly affect the IL decomposition profile.<sup>132</sup> Our dissolution data show that, similar to  $T_d$ , a slight change of substituent on the cation (ethyl or allyl) as well as anion can affect biomass solubility.

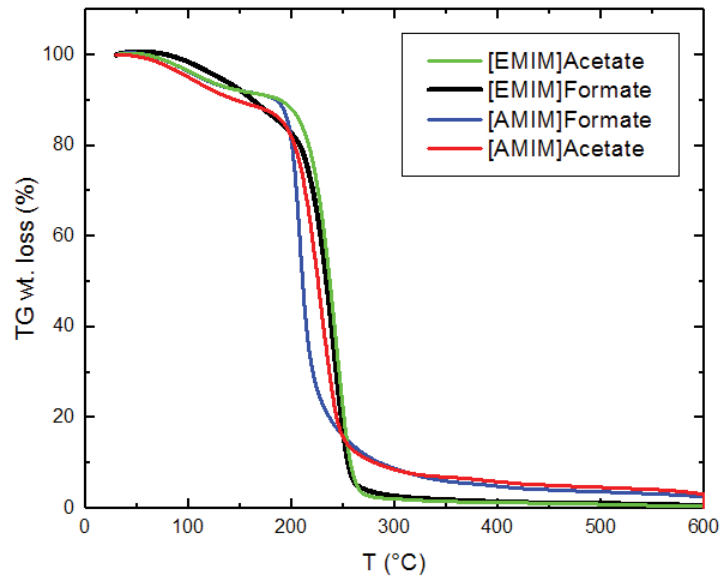


**Figure 7.** TGA thermographs for ionic liquids measured at a heating rate of 10 °C/min.

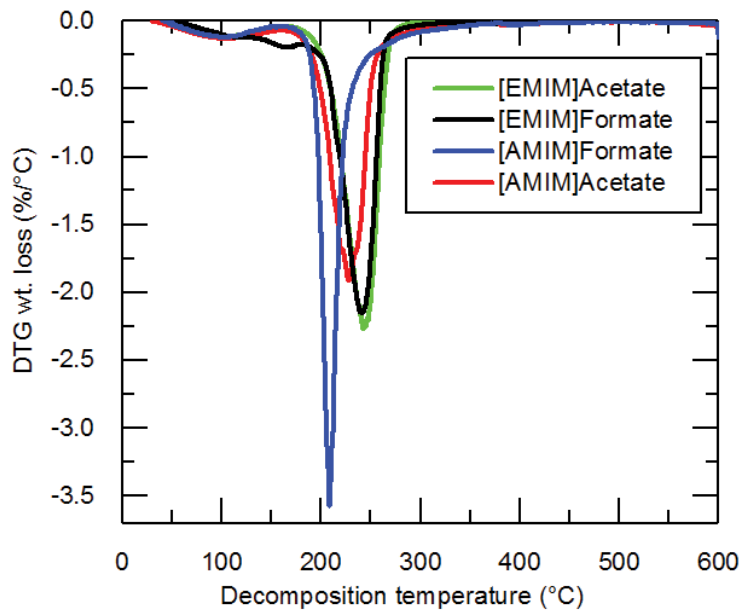


**Figure 8.** DTG curves for all four ionic liquids. The global maxima of each curve shows  $T_d$ .

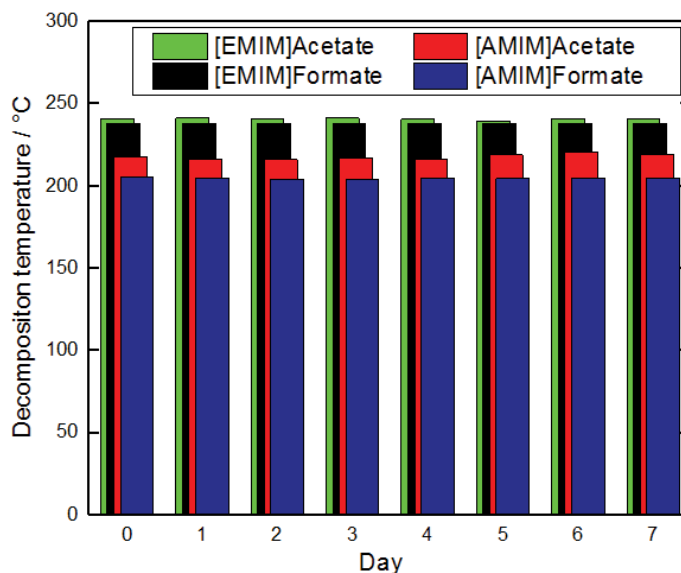


**Figure 9.** Thermal stability of ionic liquids over a 7-day period. Standard deviations were measured but not shown in the graph.

The viscosity of the ILs, measured at 80 °C (Table 5), showed a similar trend to that of  $T_d$ . The ILs with an [EMIM] cation are observed to have a higher viscosity than those with [AMIM] cations. Interestingly, there is virtually no difference between [EMIM]Formate and [AMIM]Acetate (which have a viscosity of 12.3 and 11.2 mPa-s respectively), despite being composed of different cations and anions. Imidazolium cations in general have low viscosities compared to other five-member ring cations. However, the side chain on the imidazolium ions can affect the conformational degrees of freedom of the cation, and when coupled with a highly basic anion, the cationic-anionic combination forms a dipole moment that results in a polarity-induced viscosity.<sup>133</sup> Therefore, the observed  $T_d$  and viscosity differences and similarities for the ILs in Table 5 are inferred to be a result of different interaction energies in the IL structure combination.

**Table 5.** Decomposition temperatures (Td) and viscosity of ILs (at 80 °C).

Ionic liquid	Td on Day 0 (°C)	Viscosity @ 80°C (mPa-s)
[EMIM]Acetate	241.1 ± 0.9	25.1
[EMIM]Formate	238.2 ± 0.7	12.3
[AMIM]Formate	205.6 ± 0.9	9.7
[AMIM]Acetate	217.7 ± 1.5	11.2

Standard deviations were obtained from triplicates

Further analyses of the IL structure-property relationships were determined through measurements of the Kamlet-Taft parameters ( $\alpha$ ,  $\beta$ , and  $\pi^*$ ) (Table 6). These parameters are widely used to explain the solvation behavior of ionic liquids. Previous studies have shown that hydrogen bond basicity of ILs is required for the weakening of cellulose inter and intramolecular hydrogen bonds.<sup>87</sup> The anionic function in solubilizing cellulose was further confirmed using COSMO-RS prediction, which screens *in silico* the dissolving power of ILs by calculating approximate chemical potentials.<sup>134</sup> The mechanism for lignin dissolution is still under debate. It has been suggested that IL anions form hydrogen bonds with the terminal hydroxyl groups of lignin similar to that of cellulose.<sup>135</sup> However, other data showing weaker correlation between  $\beta$  and lignin solubility suggest that the basicity is not as crucial as it is for cellulose dissolution.<sup>89, 136</sup>

Both anions (conjugate bases) used in our study, namely formate ( $\text{HCOO}^-$ ) and acetate ( $\text{CH}_3\text{COO}^-$ ), are good electron donating groups (EDGs) as denoted by their pKas or acidity values of their acids (3.75 and 4.75, respectively). As strong EDGs, these anions act as H-bond acceptors when interacting with hydroxyl groups in biomass, forming an electron donor-electron acceptor complex (EDA complex).<sup>137</sup> The ability of an IL to form EDA complexes depends on both ions, but the role of anions as the hydrogen bond acceptors is often credited for biomass



disruption. Anion basicity, denoted by the  $\beta$  values, are often estimated through Kamlet-Taft measurements to explain differences in dissolution ability of anions in ILs. However, when holding the anion constant, Table 6 shows no statistical difference between ILs containing formate or acetate with different cations. Additionally, there are no differences between the  $\beta$  values of [EMIM]Acetate and the other three ILs even though there are clear differences in biomass solubility in Table 4. Therefore, as stated by Kilpelainen et al., it is clear that the anionic mechanism is not the only factor that comes into play during IL dissolution of biomass.<sup>151</sup>

**Table 6.** Kamlet-Taft parameters for each ionic liquid.

Ionic liquid	Kamlet-Taft parameters		
	$\alpha$	$\beta$	$\pi^*$
[EMIM]Acetate	0.50 $\pm$ 0.03	1.07 $\pm$ 0.04 <sup>[a,b]</sup>	1.03 $\pm$ 0.02
[EMIM]Formate	0.49 $\pm$ 0.02	1.00 $\pm$ 0.02 <sup>[a]</sup>	1.03 $\pm$ 0.08
[AMIM]Formate	0.46 $\pm$ 0.01	1.01 $\pm$ 0.04 <sup>[a]</sup>	1.09 $\pm$ 0.02
[AMIM]Acetate	0.43 $\pm$ 0.03	1.11 $\pm$ 0.01 <sup>[b]</sup>	1.13 $\pm$ 0.08

For  $\beta$  parameters, means followed by the same letter are not significantly different at  $\alpha=0.05$ . No significant differences were observed between all  $\alpha$  and  $\pi^*$  values for each IL

In contrast, to analyze the behavior of cations in ILs, the cation was held constant as it has been suggested that the cationic property contributing to the hydrogen bond acidity of solvents,  $\alpha$ , is largely driven by the presence of an acidic C-H bond on the imidazolium ring.<sup>138</sup> However, despite the varying length of the side chain (ethyl or allyl) on both cations used in this study, the Kamlet-Taft

parameters once again showed no differences that are strong enough to explain the solubility data presented in Table 4. These individual parameters, although commonly used in explaining IL solvation properties, are deemed inconclusive for the purpose of explaining dissolution of the whole biomass in our study.

As an alternative, interactions between the cation and anion are considered, as opposed to examining them on their own. While cations and anions are usually analyzed separately for solvation properties using Kamlet-Taft, literature suggests that the product of  $\alpha$  and  $\beta$  of two ions indicates the strength of acid–base interactions between them.<sup>139</sup> The direct interaction between the cation and anion of an IL results in a strong association between the hydrogen bond accepting (hydrogen bond basicity) and hydrogen bond donating (hydrogen bond acidity) properties.<sup>140</sup> Lungwitz et al. have showed that the product of  $\alpha$  and  $\beta$  has a strong correlation with  $\pi^*$ , indicating that a strong interaction between anion and cation has an increasing effect on dipolarity.<sup>140b</sup> However, since our data show no significant differences between dipolarity ( $\pi^*$ ), a more rational screening process is required to find the missing link between overall interaction of ILs with each lignocellulosic components of biomass.

To gain a deeper understanding of how the local structure of ions and interactions between them affect biomass solubility, MD simulations were conducted for all four ILs in the presence of either hemicellulose or lignin. Hemicellulose and lignin were chosen for analysis as these components are not studied as well as cellulose in literature.<sup>141</sup> Therefore, unlike cellulose, temperature-dependent solubility data of lignin and hemicellulose in the four ILs presented in this paper are not readily available. Radial distribution functions and second virial coefficients were simulated for these ILs. Radial distribution functions (RDF), defined as the probability of finding an ion at a distance  $r$  from a plant polymer (lignin or hemicellulose), quantify local order in the ILs. The results are shown in Figure 10. The first peak indicates the average position of the ions in the solvation shell and the first minimum is commonly used to define the size of the

shell. The hemicellulose-IL RDFs are structured, with sharp maxima at  $\sim 4.5$  Å and 6 Å for the anions and cations, respectively. The larger height of the peaks for the anions indicate more anions reside in the solvation shell than cations do.

Interestingly, for the hemicellulose-anion interactions, when keeping the anion fixed, the height of the peak follows the same trend as the biomass solubility in Table 4, e.g. [AMIM]Formate has both higher solubility and higher RDF peak than [EMIM]Formate does. This suggests that cations influence the local ordering of anions on plant polymer surfaces. In contrast to hemicellulose, the lignin-IL RDFs are significantly less structured, indicating reduced local solvation layering, and show little variation between anions and cations.

Second virial coefficients ( $B_2$ ) quantify the IL-biomass polymer (lignin or hemicellulose) inter-molecular interaction strength and can be calculated by integrating the respective RDFs using Eq. 16 (Table 7). The smaller the  $B_2$ , the stronger the pairwise interaction. The interaction strength between lignin and all four ILs is found to be statistically similar. However, [AMIM]Formate, the IL that has the highest biomass solubility (Table 4), shows the most favourable interaction with hemicellulose. These results suggest that the interaction of the ILs with the hemicellulose influences the most biomass solubility.

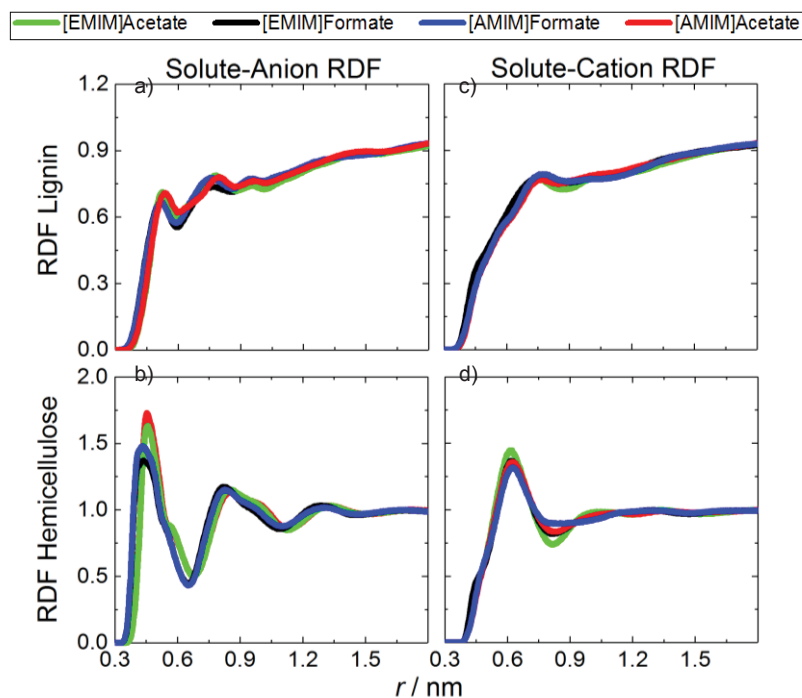


**Figure 10.** Radial distribution functions between the center of mass of ions and plant polymers. **(a)** solute-anion RDF for lignin and **(b)** hemicellulose. And the figures on the right-side show solute-cation RDF for **(c)** lignin and **(d)** hemicellulose.

**Table 7.** Calculated lignin-IL and hemicellulose-IL virial coefficients.

Ionic liquid	$B_2$ (Lignin-IL)	$B_2$ (Hemicellulose-IL)
[EMIM]Acetate	$2.02 \pm 0.02$	$0.50 \pm 0.02$
[EMIM]Formate	$1.95 \pm 0.06$	$0.47 \pm 0.03$
[AMIM]Formate	$1.99 \pm 0.03$	$0.40 \pm 0.04$
[AMIM]Acetate	$2.00 \pm 0.02$	$0.48 \pm 0.02$

## Conclusions

The relationship between the physicochemical properties of ILs and their ability to solubilize lignocellulosic biomass is of considerable importance in the production of biofuels and bioproducts. When comparing different ILs, the variation in viscosity or stability can in principle arise from their varying chemical structure leading to differences in dispersive interactions, hydrogen bonding strength, and molecular dipole moment. Present work shows that the overall structure of ILs is more important than individual ion contributions; solubility data coupled with measurements of Kamlet-Taft parameters and molecular dynamics simulations suggest that both cationic and anionic properties of ILs are cooperatively important in explaining solvent-solute interactions.

Of the four ionic liquids investigated for their potential in dissolving lignocellulosic biomass, the IL 1-allyl-3-methylimidazolium ([AMIM])Formate proves to be the most effective. Due to its ionic combination, [AMIM]Formate dissolves a significantly higher amount of biomass (+40%) compared to the commonly used [EMIM]Acetate. This is attributed to more favorable interactions (calculated from MD simulations) with the hemicellulose, whereas the interaction with lignin is found to be similar between all ILs studied here. The simulations identify hemicellulose as the cell wall component whose interactions with the ILs and local solvent structure vary more significantly as the ions are changed.

Additional molecular-level experimental and simulation studies on these select ILs are in order to further explain biomass-solvent reactions.

## Acknowledgments

The authors are grateful to the National Science Foundation: Chemical, Bioengineering, Environmental, and Transport Systems (Grant Number: 151181) for their financial support. M.D. Smith, J.C. Smith, and L. Petridis were supported

by the U.S. Department of Energy Genomic Science Program, Office of Biological and Environmental Research, U. S. Department of Energy, under Contract FWP ERKP752. We also thank Dr. David Harper for assisting with the AR-G2 rheometer, and Dr. Omid Hosseinaei for operating the 400 MHz Varian Liquid-state NMR spectrometer. Computer time was provided by the Innovative and Novel Computational Impact on Theory and Experiment (INCITE) program. This research used resources of the Oak Ridge Leadership Computing Facility, which is a DOE Office of Science User Facility supported under Contract DE-AC05-00OR22725.

## Appendix

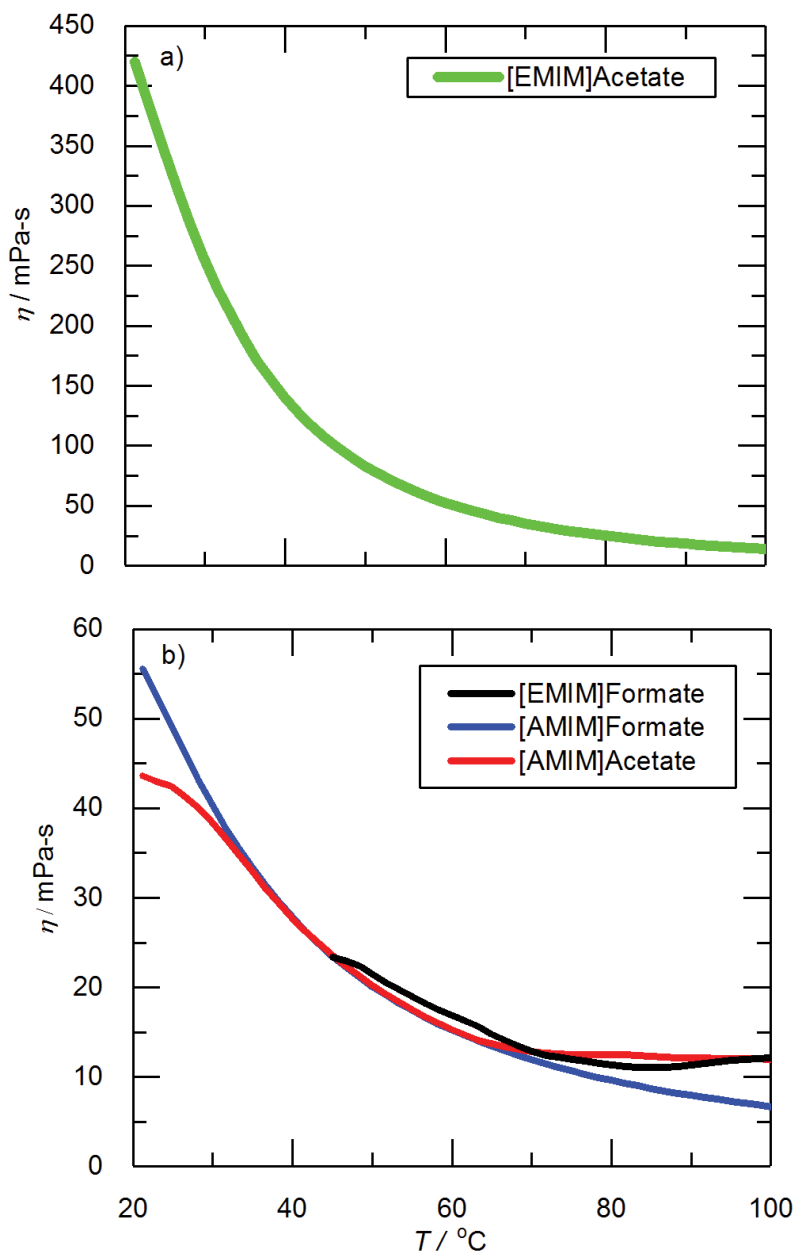


**Figure 11. (a)** Temperature-dependent viscosity of [EMIM]Acetate. **(b)** Temperature-dependent viscosity of [EMIM]Formate, [AMIM]Formate, and [AMIM]Acetate (Bottom).

## **CHAPTER III**

# **LIGNOCELLULOSIC BIOMASS ACTIVATION WITH IONIC LIQUIDS COMPRISING 3-METHYLIMIDAZOLIUM CATIONS AND CARBOXYLATE ANIONS**



*This chapter is a draft version of the following article:*

“Moyer, P., Kim, K., Abdoulmoumine, N., Chmely, S.C., Labbé, N. (2017).”  
Lignocellulosic biomass activation with ionic liquids comprising 3-methylimidazolium cations and carboxylate anions”.

Preenaa Moyer performed the experiments, conducted data analysis, and wrote the manuscript. Keonhee Kim assisted with FT-IR spectroscopy, chemical composition analysis, and enzymatic saccharification. Dr. Nourredine Abdoulmoumine edited the manuscript. Dr. Stephen C. Chmely assisted with data interpretation and edited the manuscript. Dr. Nicole Labbé oversaw the experimental design, assisted with data analysis, and edited the manuscript.

## **Abstract**

The production of chemicals and fuels from lignocellulosic biomass is an alternative to traditional, petroleum-based products. However, lignocellulosic biomass requires a form of pretreatment or fractionation to recover its individual components for further use as intermediate building blocks. Numerous ionic liquids have been used in biomass processing due to their ability to “activate” lignocellulosic biomass, by reducing its recalcitrance with minimal impact on the structural components. In this study, we compare 1-allyl-3-methylimidazolium ([AMIM])Formate to the commonly used 1-ethyl-3-methylimidazolium ([EMIM])Acetate for its potential to activate hybrid poplar and enable high cellulose and hemicellulose conversion. Although [EMIM]Acetate has been widely used for activation, [AMIM]Formate was recently identified to have a higher biomass solubility, with an increase of 40% over [EMIM]Acetate. Since IL activation captures the early stages of dissolution, the recalcitrance of [EMIM]Acetate and [AMIM]Formate-activated biomass was assessed through a suite of analytical tools. Data from FT-IR spectroscopy and X-Ray diffraction patterns show that activation using [AMIM]Formate does not deacetylate hybrid poplar as much as

[EMIM]Acetate, and preserves the crystallinity of the cellulose fraction. Enzymatic saccharification on activated biomass results in a higher cellulose and hemicellulose conversion for [EMIM]Acetate-activated biomass, about double the conversion for [AMIM]Formate. Scanning electron microscopy (SEM) further shows that the porosity that is seen in [EMIM]Acetate-activated biomass due to the aforementioned physical and chemical changes during activation. Therefore, [AMIM]Formate is much more suited for dissolution and direct product formation as opposed to the pathway for [EMIM]Acetate, which is activation and fractionation.

## Introduction

Current petroleum-based fuel production of 80 million barrels per day emits an alarming rate of carbon dioxide into a closed atmospheric system, contributing to a rise in average daily temperatures. In September 2017, NASA's Goddard Institute for Space Studies (GISS) stated that the surface temperatures in 2017 are consistent with the global average trends observing a gradually warmer climate since 1980. Anticipation of this phenomenon has motivated researchers to find alternatives for producing chemicals and fuels from lignocellulosic biomass, the only renewable sustainable carbon source.

Lignocellulosic biomass is mainly comprised of cellulose (30-45%), hemicellulose (20-40%), and lignin (5-35%).<sup>4</sup> The main component of the plant cell wall is cellulose, which is made of D-glucose monomer units linked by  $\beta$  (1 $\rightarrow$ 4) glycosidic bonds. Cellulose is a highly stable linear homopolymer, unlike hemicellulose and lignin, which have random and amorphous structures. Hemicellulose is made of a diverse class of polysaccharides, including xylan, glucuronoxylan, arabinoxylan, glucomannan, and xyloglucan. Lignin reinforces the cell wall of plants and forms a physical barrier against any form of chemical, biological, or physical attacks. Altogether, the heterogeneous structure and

complexity of cell wall constituents are the main contributors to biomass recalcitrance.<sup>142</sup> The recalcitrant structure of biomass hinders its potential for conversion into various intermediate chemicals and fuels. For biorefinery applications to be cost effective, an efficient biomass pretreatment or fractionation method is imperative for maximizing conversion yields.

Recently, the need for biomass valorization has compelled biorefineries to exhibit the ability to selectively recover each primary component of lignocellulosic biomass through maximum conversion of cellulose and hemicellulose into soluble sugars, yielding a lignin fraction of high purity.<sup>84, 143,144</sup> Numerous studies have demonstrated the ability to use various pretreatment methods such as dilute acid treatment, autohydrolysis, steam explosion, wet oxidation, and ammonia fiber expansion (AFEX), to recover only certain fractions of biomass but not all three (cellulose, hemicellulose, and lignin).<sup>63, 145</sup> Over the years, several fractionation processes using organic solvents i.e., ethanol, acetone, gamma valerolactone (GVL), tetrahydrofuran (THF), and ionic liquids have become prevalent in recovering all the components of lignocellulosic biomass.<sup>98a, 146</sup> While the organosolv process is known to produce fractions with high purity, the recovered lignin is depolymerized and does not re-form C-C bonds. Additionally, the use of toxic solvents and high temperatures makes this process hazardous, requiring reactors made with special alloys. The processes involving GVL and THF are fairly new and still being studied for their use as a pathway for biomass fractionation.<sup>70,</sup>

147

Ionic liquids have been around for decades and are salts with low melting points and high vapor pressure. They are non-toxic and suitable for biomass pretreatment (at temperatures over 100 °C and/or long residence times) or fractionation. During IL pretreatment, only a cellulose-rich fraction is generated through the degradation and removal of lignin and hemicellulose.<sup>148</sup> Conversely, biomass fractionation employs an IL activation step, which uses low severity, i.e., low temperatures to gently loosen the lignocellulosic components. One has to note

that the term “activation” and pretreatment are used interchangeably although activation is more accurate for processes that use temperatures of 50-80 °C, and targets the recovery of all the biomass constituents.<sup>92b</sup> After activation, biomass can either be regenerated through a solute displacement mechanism (using an anti-solvent) or subjected to *in situ* saccharification in an enzyme environment (discussed in Future Work).<sup>149</sup> The IL activation step allows the saccharide fraction (hemicellulose and cellulose) to become less intertwined with lignin and undergo maximum hydrolysis to glucose during an enzymatic saccharification.<sup>90, 92a</sup> Lignin can then be recovered in the solid fraction.

One of the main advantages of IL activation is that significant changes in biomass and cellulose crystallinity have been observed, in addition to the cleavage of acetyl groups in hemicellulose and lignin. Since cellulose has a crystalline structure unlike hemicellulose and lignin, reducing cellulose crystallinity is of considerable importance to provide access for hydrolytic enzymes.<sup>150</sup> Due to the mild process conditions used in IL activation, these structural changes occur within the biomass without compromising the overall chemical composition, like it would during a pretreatment step. In other words, the carbon content and the main three biomass constituents content are preserved. An IL that has been particularly well-known for pretreatment and activation is 1-ethyl-3-methylimidazolium acetate or [EMIM]Acetate.<sup>98a, 151</sup> While other ILs such as 1-allyl-3-methylimidazolium ([AMIM])Chloride and 1-butyl-3-methylimidazolium ([BMIM])Chloride have been used for biomass pretreatment or activation, [EMIM]Acetate is known to be an effective cellulose solvent, inducing changes in crystallinity even during IL activation.

As a pretreatment solvent, Singh and collaborators stated that [EMIM]Acetate is highly effective at 140 °C and 3 hr for production of sugars from switchgrass. Likewise, they have also tested several other temperatures (ranging from 110-140 °C) and residence times to pretreat biomass.<sup>90</sup> As an example of the different ways that IL pretreatment is carried out, a work by Shill et al. show that

[EMIM]Acetate can produce higher cellulose conversion using a biphasic and triphasic system after pretreating biomass for up to 44 hours at high temperatures.<sup>13a</sup> For a process employing IL activation alone, not much work has been shown significant results for cellulose conversion and recovery of lignin due to the difficulty of identifying the correct ratio of time and temperature that is effective for a select IL. Previously, Labbe et al. showed that biomass activation and regeneration with [EMIM]Acetate at a 4 wt.% biomass loading (BL) generated a low recalcitrant biomass. With a 72-hour activation time at 60 °C, the cellulose fraction of yellow poplar was converted into 100% glucose.<sup>92a</sup> Singh's research group recently made an attempt to activate switchgrass with an IL tetrabutylammonium hydroxide at 50 °C for 3 hours, at a 20 wt.% biomass loading.<sup>92b</sup> In addition to using ideal conditions for "activation", a higher loading is used to enhance energy efficiency and cost-effectiveness of a biorefinery process.

In order to optimize IL activation, shorter reaction times and lower temperatures have been examined as mentioned in the examples above. However, hemicellulose has low solubility in the commonly used [EMIM]Acetate at low temperatures, dissolving only 5 wt.% at 25 °C. Therefore, the hemicellulose coating on cellulosic fibrils will not be disrupted under mild conditions if it is first not dissolved. Recent work showed that partial removal of hemicellulose allows for shorter activation time using a coupled autohydrolysis-activation step.<sup>94</sup> Similarly, Wang et al. carried out autohydrolysis at 160 °C for 60 minutes, resulting in a 55% removal of hemicellulose. Following autohydrolysis, activation was carried out for only 3 hours at 10 wt.% BL, while still achieving a 100% conversion of cellulose into glucose.<sup>95</sup> These results provide some insight on the barrier imposed by hemicellulose onto the potential complete cellulose conversion. The partial removal of hemicellulose cleaves lignin carbohydrate complexes (LCC) and disrupts the linkages between lignin and hemicellulose.<sup>113, 152</sup>

In a very recent paper (reproduced in Chapter II), we show that 1-allyl-3-methylimidazolium formate or [AMIM]Formate efficiently dissolves 40% more

hybrid poplar compared to the commonly used [EMIM]Acetate. Through a series of experiments and molecular dynamics simulations, the large difference in dissolution was attributed to stronger interactions between hemicellulose and [AMIM]Formate. This results in increased dissolution of hybrid poplar in [AMIM]Formate, augmenting the contact between IL and each lignocellulosic component.

Since the dissolution of biomass in [AMIM]Formate is 40% higher than that in [EMIM]Acetate, these two ILs were compared in terms of activation. As the activation step is essentially an initial step of the dissolution process, the changes that take place would be similar. The effectiveness of each activation was evaluated by investigating several physical and chemical features of the biomass, i.e., deacetylation, cellulose crystallinity, chemical composition, and anatomical characteristics. Statistical analysis was performed to analyze the Fourier transform infrared (FT-IR) chemical signature of the activated/regenerated biomass and study the changes that occur in the biomass structure based on the IL activation parameters.

## **Materials and methods**

### ***Biomass and ionic liquids***

The biomass used in this study, hybrid poplar (*Populus spp.*) was obtained from The Center for Renewable Carbon, The University of Tennessee. Upon air-drying, the material was milled with a Wiley mill (Thomas Scientific™, Model # 3383-L10, Swedesboro, NJ) through a 40-mesh screen (0.425 mm).

The ionic liquids, 1-ethyl-3-methylimidazolium acetate ([EMIM]Acetate, purum ≥ 95%) and 1-allyl-3-methylimidazolium formate ([AMIM]Formate, purum ≥ 95) were purchased from Iolitec Inc. (Tuscaloosa, AL) and used as received. Deionized water was used in between steps.

### ***Activation and regeneration of hybrid poplar in ionic liquids***

The extractives-free hybrid poplar was “activated” in [EMIM]Acetate and [AMIM]Formate at a 10 wt.% loading. First, the ILs were weighed in a flask and heated at 100 °C to remove moisture. After 15 minutes, the temperature was set to 60 °C and the hybrid poplar (HP) was slowly added to the solvent. The biomass-IL mixture was agitated by a mechanical stirrer at 100 RPM for various time scales (3, 24, 48 and 72 hours). After the respective periods, the biomass was regenerated by adding the same weight of deionized water as an anti-solvent, and mixed for five additional minutes. The regenerated sample was further precipitated through washing and vacuum filtration steps, and then dried in a 40 °C oven for 5 days.

At least two replications were performed for each experiment and the recovered weight of biomass was recorded. The complete removal of ILs from the biomass was confirmed through Fourier Transform Infrared (FT-IR) spectroscopy and Pyrolysis-Gas Chromatography (Py-GC/MS).

### ***Chemical composition analysis***

The chemical composition of the raw and activated/regenerated hybrid poplar was determined using the National Renewable Energy Laboratory (NREL) Analytical Procedure: “Determination of Structural Carbohydrates and Lignin in Biomass”. The acid soluble lignin (ASL) content was measured at a wavelength of 240 nm, using a Thermo Scientific™ GENESYS™ 10S UV-Vis Spectrophotometer.

### ***Fourier Transform Infrared (FT-IR) spectroscopy***

The chemical signature of the HP samples was measured using a Perkin–Elmer Spectrum One FT-IR spectrometer (Waltham, MA). A small amount of biomass (~0.005 g) was placed on an attenuated total reflectance (ATR) accessory of the spectrometer. FT-IR spectra were collected over a range of 4000-600  $\text{cm}^{-1}$  in the absorbance mode, with a 4  $\text{cm}^{-1}$  resolution and 8 scans per sample. Five spectra were collected for each sample. The spectra were pre-treated with an ATR

correction, normalized and corrected by Multiplicative Scatter Correction (MSC) in The *Unscrambler*® X software version 9 (CAMO software).

### ***Statistical analysis: Principal component analysis of FT-IR spectra***

Principal Component Analysis (PCA), a multivariate analysis, was used to analyze the FT-IR spectral data. PCA allows for visualization of composite data by identifying the main sources of variation, and removing noise variability from the data. The spectral data are compressed and transformed into a data set that shows its most relevant factors, known as principal components or PC. The first principal component has the largest possible variance and accounts for most of the variability in the spectral data. Scatter plots of principal component scores show the pattern of the data and is called a scores plot. The relationship between wavenumber of the FT-IR spectrum and the PCs is shown on another plot called a loadings plot. The pattern on the loadings plot then shows how much each variable contributed to each PC.<sup>153</sup>

### ***X-Ray diffraction (XRD) of activated biomass***

Following the rapid screening through FT-IR, the raw and activated/regenerated HP samples were analyzed using powder X-ray diffraction for accurately determining the crystallinity of cellulose. The samples were individually mounted on a low-background quartz holder and measured using a PANalytical Empyrean X-Ray diffractometer (PANalytical Inc., Westborough, MA), with a Cu- $\alpha$  tube operated at 45 kV and 40 mA;  $\lambda = 1.5418 \text{ \AA}$ . The scatter angle,  $2\theta$  was measured at a range of  $9-41^\circ$ , with a step size of  $0.01^\circ$ , using a  $1/8^\circ$  fixed divergence, a  $1/4^\circ$  anti-scatter slit, as well as a 0.04 rad soller slit. The index of crystallinity (CrI) was determined using Segal's peak height method, shown in Eq.17 below:

$$\text{CrI} = \frac{I_{002} - I_{AM}}{I_{002}} \quad (17)$$

where  $I_{002}$  is the total intensity of the peak at  $2\theta = 22.5^\circ$  and  $I_{AM}$  is the intensity of the background scatter at  $2\theta = 18.7^\circ$ .<sup>154</sup>



The CrI for cellulose was normalized against untreated, commercial Avicel, which has a CrI of 100%. The XRD data were plotted and analyzed using Origin 2017 SR 1 software (OriginLab Corporation).

### ***Anatomical characterization***

Untreated and IL-activated/regenerated biomass samples were characterized using Scanning Electron Microscopy (SEM). A PhenomPro X desktop Scanning Electron Microscope was used to take micrograph images of the samples at 50kV using 400x and 1500x magnification.

### ***Enzymatic saccharification***

Following activation and regeneration, the HP samples were hydrolyzed with commercial enzymes based on the NREL Laboratory Analytical Procedure (Enzymatic saccharification of lignocellulosic biomass NREL/TP-510-42629). A biomass loading (BL) of 5 w/w% was used for saccharification with CTec 3 cellulases and HTec 3 hemicellulases (Novozymes). The saccharification was performed at 50 °C in a 50 mM citrate buffer (pH 5.0), using capped Erlenmeyer flasks. The shaker was set to 100 RPM. Aliquots of the saccharified samples were taken at predetermined times of 0, 1, 3, 6, 12, 24, 48 and 72 hr, boiled for 5-10 minutes to denature the enzymes, and centrifuged at 10,000 rpm for 5 minutes. The aliquots were then filtered through 0.45 µm nylon membrane filters from Millipore (Billerica, MA) and analyzed through High Performance Liquid Chromatography (HPLC). A Bio-Rad Aminex HPX-87P carbohydrate analysis column (Richmond, CA) and a de-ashing guard column (Biorad, Hercules, CA) were used at 85 °C, with a mobile phase (H<sub>2</sub>O) flow rate of 0.25 mL/min. To measure acetyl content, a Bio-Rad Aminex HPX-87H column was used with a mobile phase (H<sub>2</sub>SO<sub>4</sub>) flow rate of 0.6 mL/min.

## Results and discussion

An activation step is equivalent to the first few hours of a dissolution process, in which biomass is continuously mixed with an IL under controlled mixing and temperature conditions. However, unlike dissolution, biomass is only partially dissolved in the IL during activation, and changes that take place during this phase can be studied by regenerating or precipitating the biomass after a short period through rapid addition of an anti-solvent. To assess these changes, several physical characteristics are studied including chemical composition, cellulose crystallinity, anatomical features, and ability to enzymatically release sugars. The mass of regenerated biomass after IL activation is often a first indicator if any loss of lignocellulosic components took place during activation. The data in Table 8 show the mass recovery for all the regenerated HP samples that were activated with [EMIM]Acetate and [AMIM]Formate at 10 wt.% biomass loading for different periods.

**Table 8.** Mass recovery of hybrid poplar (%) by ionic liquid type.

Activation time (h)	Hybrid poplar mass recovery (%)	
	[EMIM]Acetate	[AMIM]Formate
3	96.1 ± 0.2	98.2 ± 0.0
24	96.1 ± 0.2	96.8 ± 0.4
48	96.1 ± 0.5	93.2 ± 1.0
72	94.1 ± 1.0	92.1 ± 0.8

The mass of recovered IL-activated HP decreased with increasing activation time, with a maximum loss of 6-8% during the 72-hour activation for both ILs. The loss is not attributed to the removal of water, extractives, or inorganics

from biomass, as these were accounted for during the experiment and previously extracted before activation, respectively. For [EMIM]Activated-biomass, this mass loss has been attributed to the deacetylation of hemicellulose and lignin during the activation step.<sup>92</sup> Additionally, the biomass undergoes crystallinity changes when the IL solvent penetrates into the hydrogen bonded sheets of cellulose I, resulting in an expansion of the lattice structure.<sup>155</sup> Hence, it is essential to know if a similar deacetylation or change in cellulose takes place during [AMIM]Formate activation.

An initial screening of the chemical signature of the IL-activated HP was performed by FT-IR spectroscopy coupled with a multivariate analysis, i.e principal component analysis (PCA). PCA's scores and loadings plots highlight the significant differences caused by the different activation times for [EMIM]Acetate (Figure 12a and b, corresponding to scores and loadings plot respectively) and [AMIM]Formate (Figure 13a and b) when compared to the control (untreated HP) in the FT-IR fingerprint region. For [EMIM]Acetate The scores plot shows that samples activated for 3, 24, and 48-hour clustered along PC1 with the 72-hour activated samples being farthest away from the untreated biomass. The loadings plot identify the significant spectral changes occurred at 1737 and 1233  $\text{cm}^{-1}$ ; both bands assigned to acetyl group vibrations, C=O and C-O stretch, respectively.<sup>156</sup> Since the acetyl group bands are positive (Fig 12b), and the 72-hour [EMIM]Acetate-activated samples are located in the negative quadrant of PC 1 (Fig. 12a), this confirms that there are fewer acetyl groups in these samples compared to the control and lower activation times.<sup>92a</sup>

Similarly, the scores plot for [AMIM]Formate-activated HP at different times is shown in Figure 13a with the 72-hour activated samples being furthest from the control. However, unlike with [EMIM]Acetate, the loadings plot for [AMIM]Formate-activated samples (Figure 13b) does not show a significant difference in the acetyl region when projected onto PC 1. Nevertheless, there is an intense negative band at 1033  $\text{cm}^{-1}$ , indicating that biomass activated with [AMIM]Formate for 72 hours contains a higher amount of the C-O functional group stretching compared to the

other samples. This observation is speculated to explain the recovery data in Table 8 being attributed to C-O stretching in cellulose, and hemicellulose, and subsequent loss.<sup>157</sup> Overall, the sample clustering with both ILs shows that longer activation time has a greater impact on the chemical feature of the hybrid poplar. However, unlike [EMIM]Acetate, very little changes are observed when hybrid poplar is activated with [AMIM]Formate.

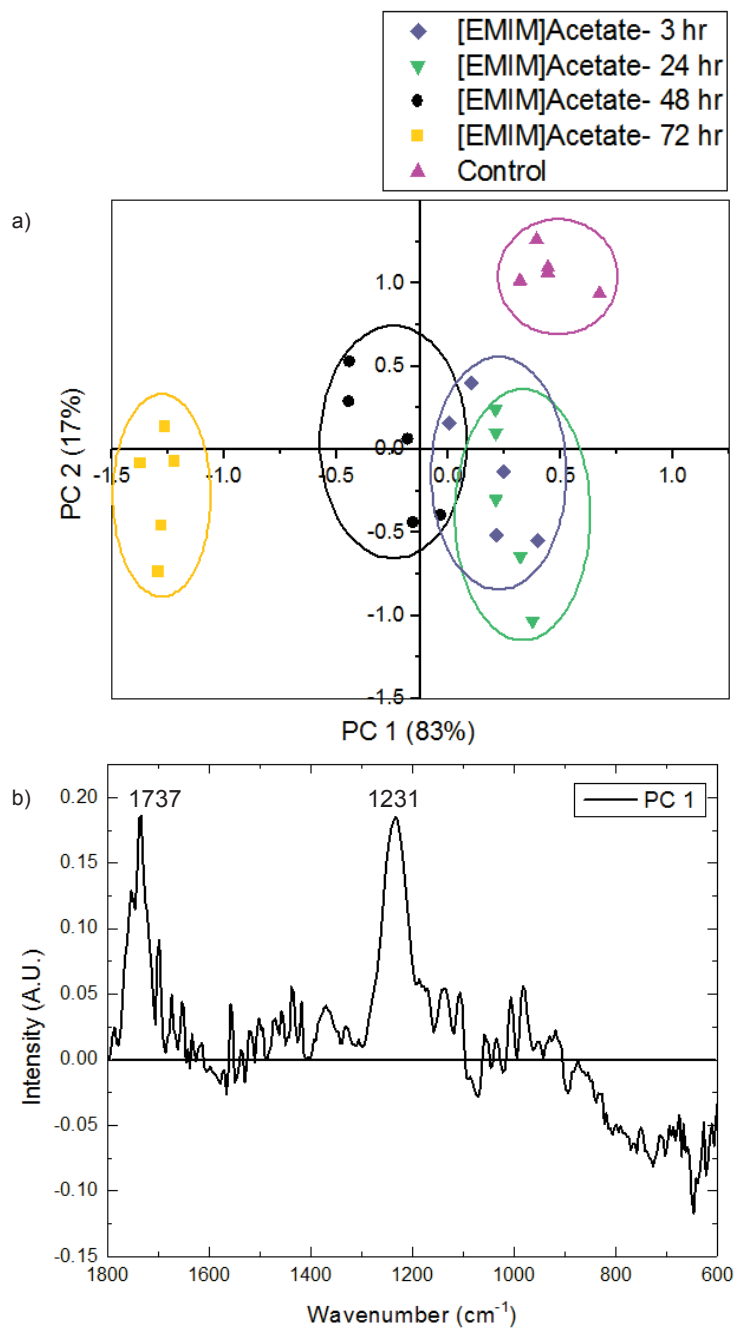


**Figure 12.** Principal component analysis (PCA) on [EMIM]Acetate-activated samples for 3, 24, 48, and 72-hour activation times. The scores plot is shown on the left (a), and the loadings plot for PC 1 on the right (b).

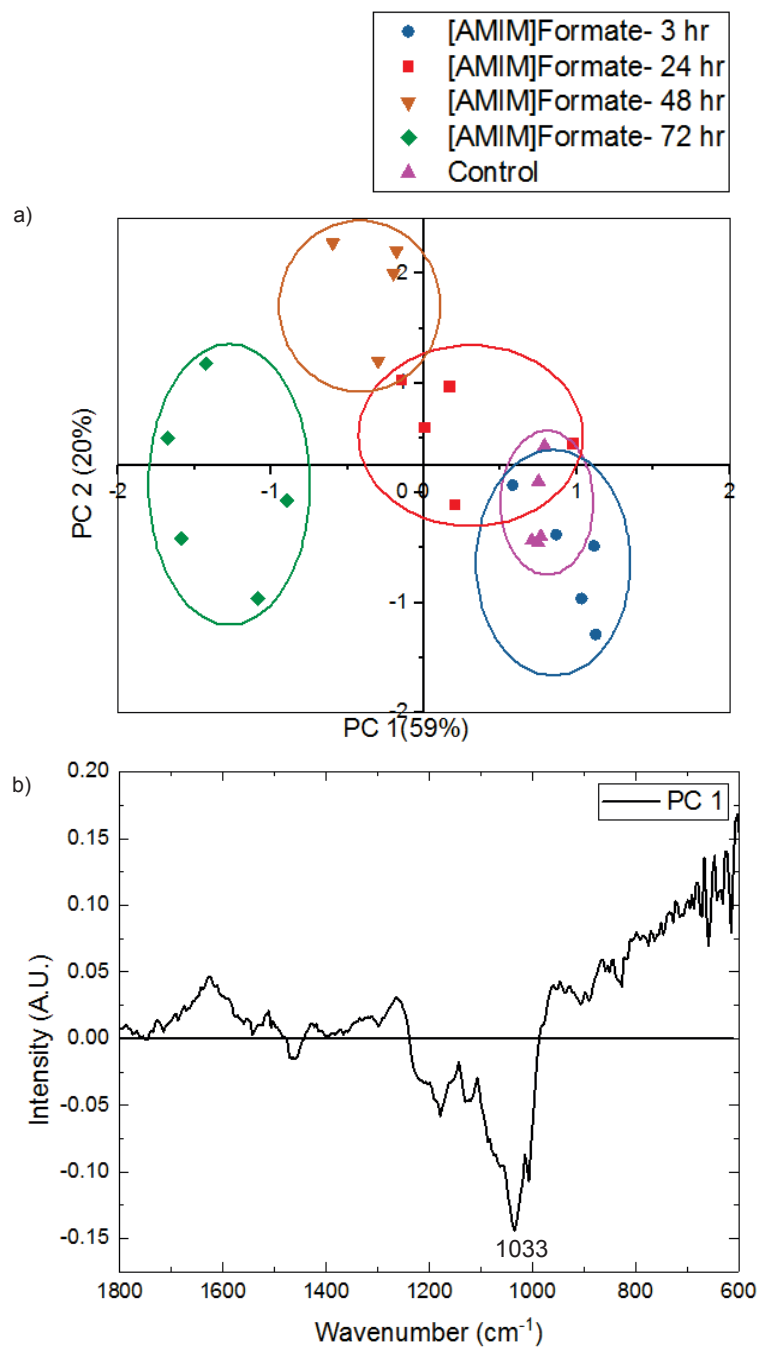


**Figure 13.** Principal component analysis (PCA) on [AMIM]Formate-activated samples for 3, 24, 48, and 72-hour activation times. The scores plot is shown on the left (a), and the loadings plot for PC 1 on the right (b).

To narrow down on activation times and focus on the extremes, only the 3 and 72-hour activation times were studied further for each IL. Additionally, these activation times were selected for comparison with previous work.<sup>24, 90, 158</sup> A 72-hour activation time is known to produce the same amount of glucose conversion as a 3-hour activation coupled with autohydrolysis.<sup>95</sup> A PCA of the FTIR spectra collected on the 3 and 72-hour activated samples for both ILs was performed to investigate the chemical features of these samples by IL type and activation time (Figure 14a and b). According to the loadings plot (Fig 14b), the most significant spectral changes occurred at 1735, 1371, 1220, 1039, and 1011  $\text{cm}^{-1}$ . The two intense bands at 1735 and 1233  $\text{cm}^{-1}$  (identified on the plot) are assigned to acetyl group vibrations, whereas the remaining bands are assigned to the stretching and bending of the carbohydrates backbone, i.e., C-H stretching and deformation.<sup>156</sup> Similar to the observation for Figure 12, these acetyl group bands are positive, and both 72-hour IL-activated samples are located on the negative quadrant of PC 1, suggesting that there are fewer acetyl groups in these samples compared to the control. Overall, the variations in the FT-IR spectra confirm that [EMIM]Acetate changes the chemical features of biomass significantly, while [AMIM]Formate does not as much.

To confirm the FTIR findings and ensure that there was no significant loss in any biomass component, the chemical composition of activated/regenerated HP was determined. Table 9 shows that all the regenerated HP samples for [EMIM]Acetate and [AMIM]Formate maintain a similar chemical composition for cellulose, hemicellulose, and lignin as the control (untreated HP).

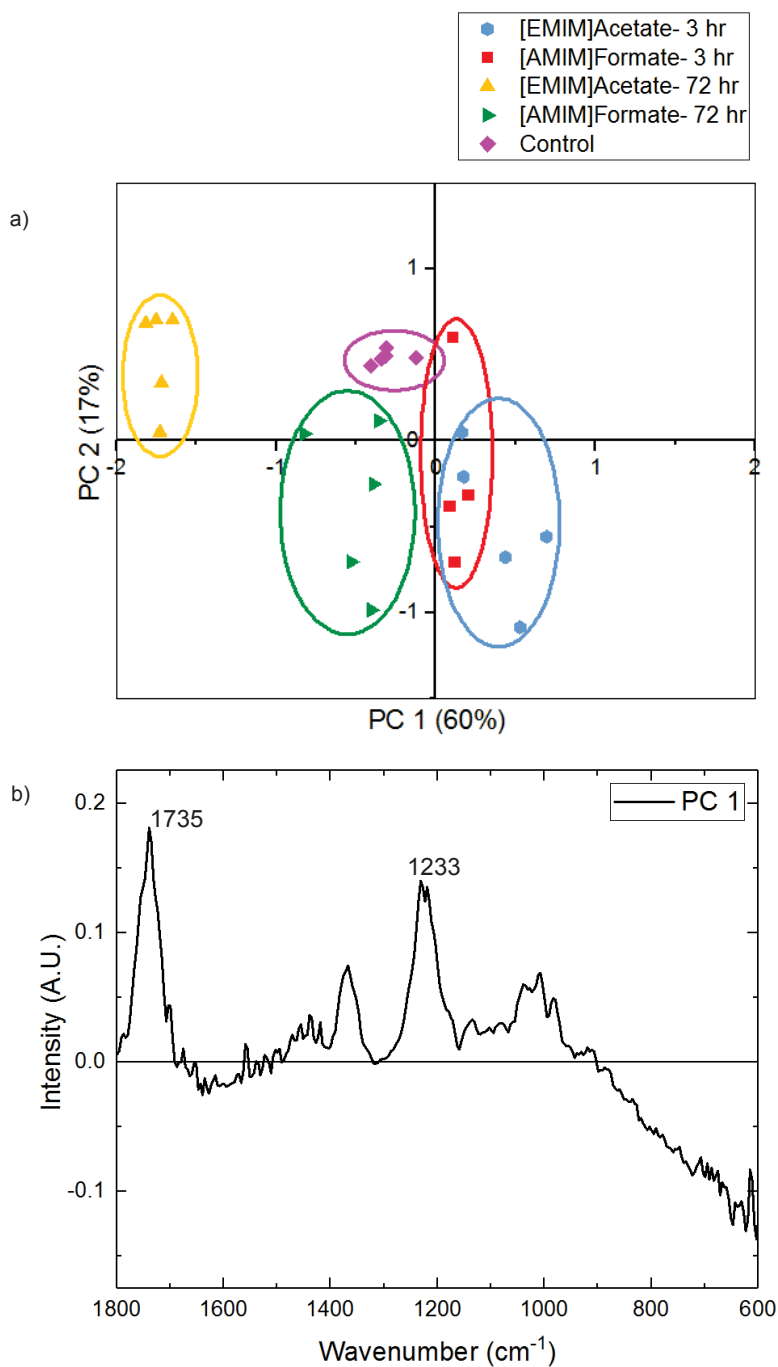


**Figure 14. (a)** Principal component analysis (PCA) scores plot of IL-activated hybrid poplar compared to untreated HP (control). **(b)** PCA loadings plot for PC 1.



**Table 9.** Chemical composition of regenerated HP after IL activation at 10 wt.% loading.

	Control	[EMIM]Acetate		[AMIM]Formate	
		3 hr	72 hr	3 hr	72 hr
Cellulose (%)	44.3 ± 0.2	43.4 ± 0.1	43.5 ± 0.3	42.8 ± 0.2	42.6 ± 0.1
Hemicellulose (%)	20.6 ± 0.1	20.2 ± 0.0	19.9 ± 0.0	18.8 ± 0.0	18.5 ± 0.1
Lignin (%)	27.8 ± 0.5	28.8 ± 0.2	27.8 ± 0.3	27.9 ± 0.1	27.2 ± 0.2
Acetyl content (%)	5.9 ± 0.1	5.3 ± 0.1	3.3 ± 0.0	4.93 ± 0.1	4.7 ± 0.1

Standard deviations are based on triplicate measurements

As for the acetyl group, the composition analysis shows that after a 3-hour activation acetyl content decreases to 5.3% and 4.9% in [EMIM]Acetate and [AMIM]Formate, respectively. After 72-hour activation with [EMIM]Acetate acetyl content drops to 3.3%; a reduction of 44% compared to the control. The acetyl content for [AMIM]Formate with the same activation time did not decrease as much (from 5.9 to 4.7%). Contrary to [EMIM]Acetate, these results indicate that only a small fraction of the acetyl group in hybrid poplar is cleaved during activation with [AMIM]Formate

In addition to chemical changes, the crystallinity of the activated/regenerated biomass was investigated by X-Ray diffraction (Figure 15).

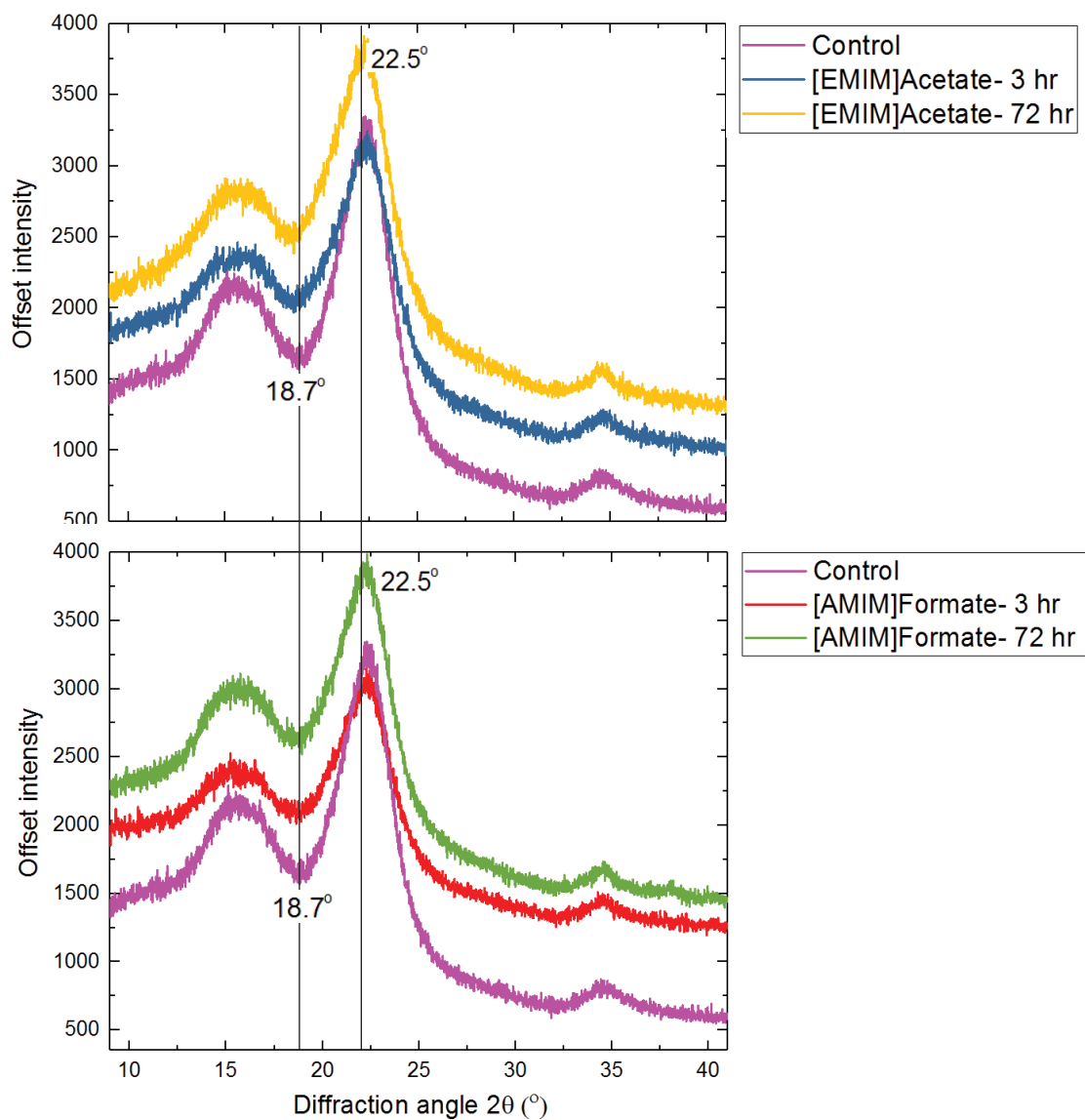


**Figure 15.** X-Ray diffraction (XRD) patterns for IL-activated sample at 10 wt.% biomass loading. Index of crystallinity for cellulose was calculated using Eq.17.

**Table 10.** Comparison of index of crystallinity (Crl) measured through XRD for [EMIM]Acetate and [AMIM]Formate-activated samples.

	Control	[EMIM]Acetate		[AMIM]Formate	
		3 hr	72 hr	3 hr	72 hr
XRD (%)	61.4	50.6	43.5	54.2	49.6

Activation of HP with IL slightly modifies the crystalline structure of the biomass, in which a slight broadening of the main peak at  $2\theta = 22.5^\circ$  compared to the control is observed. Although no peak shifts are observed, usually an indicator that cellulose I transitions into cellulose II, there seems to be a slight decrease in peak intensity at  $35^\circ$  for the 72-hour activated samples, due to a possible disruption of the microfibril alignment of the cellulose chains.<sup>159</sup> The Crl calculated from the XRD patterns is provided in Table 10. Similar to acetyl content in Table 9, a small decrease in the Crl for the 3-hour activated samples is observed, 10.8% and 7.2% decrease for [EMIM]Acetate and [AMIM]Formate respectively, compared to the control. However, for the 72-hour activated samples, [EMIM]Acetate reduces cellulose crystallinity of hybrid poplar from 61.4 to 43.5%. On the other hand, the cellulose crystallinity for [AMIM]Formate only decreased to 49.6 % and not as much as [EMIM]Acetate. Overall, when comparing the two ILs and activation times, the data confirm a higher structural disruption of the primary components of HP with [EMIM]Acetate at 72 hours.

To visualize the physical changes that took place during the 72-hour IL activation, scanning electron microscopy (SEM) images were taken and analyzed (Figure 16). In the control (untreated HP), the structure of hardwood is clearly seen with visible vessels, pits, and broad ray cells along the tangential plan.<sup>160</sup> The morphology and structural ordering of [EMIM]Acetate and [AMIM]Formate activated biomass appear to have many differences compared to each other and

to the control. One similarity for both ILs is the lack of lignin droplet accumulation on the cellulose fibers indicating that the linkages between lignin and cellulose were not completely disrupted. This observation is important because previous studies using dilute acid pretreatment have reported the coalescence of lignin droplets on the surface of wood, presenting a barrier for enzymatic hydrolysis.<sup>161</sup>

The [EMIM]Acetate-activated biomass (Figure 16b) appears to have many ring-like porous structures around the microfibrils of cellulose. Although the broad rays are still seen, the activation seemed to change the structure of the wood making it more porous, increasing vessel size, and making it accessible for further degradation using enzymes. On the other hand, the SEM image for [AMIM]Formate-activated biomass (Figure 16c) shows re-folding of the fibers with little to none porosity. It appears as if the activation only disrupted the broad ray cells of the sample, without affecting its porosity. These images are consistent with the FT-IR spectroscopy and X-Ray diffraction data demonstrating that among the two tested ILs, [AMIM]Formate has the least impact on the chemical and physical properties of biomass.

To explain the chemical (deacetylation) and physical (cellulose crystallinity) changes (or lack thereof) that takes place during IL activation, the mechanism for deacetylation in both ILs as well as enzymatic saccharification are investigated (Figure 17 and 18).<sup>92a</sup> The mechanism shown in Figure 17 begins with the anion of the IL deprotonating the 3-methylimidazolium cation, forming an N-heterocyclic carbene (NHC).<sup>131</sup> This leads to an attack of the carbonyl (2) of the acetyl groups present in the biomass. Then, the imidazolium cation is deprotonated through a nucleophilic substitution. Comparing the mechanism of [EMIM]Acetate and [AMIM]Formate requires looking at their respective pKa values of their acids, which is 4.76 for the former and 3.75 for the latter. Since the pKa of formic acid (formate being the conjugate base) is relatively higher than that of acetic acid, we can conclude that the anion on [AMIM]Formate has a relatively lower ability to deprotonate the cation compared to [EMIM]Acetate, making step 1 a rate-limiting

step.<sup>162</sup> This phenomenon can explain why deacetylation is much more pronounced in [EMIM]Acetate-activated biomass.

The chemical changes of the biomass have a strong linear relationship with the rate of enzymatic conversion, therefore the observation is validated through enzymatic saccharification using commercial enzymes. The conversion rates of cellulose and hemicellulose for the 72-hours [EMIM]Acetate and [AMIM]Formate-activated samples were monitored and presented in Figure 18a and b. The observed conversion trends for the sample showed similarities to the CrI trend in Table 10. The highest cellulose conversion of 44% was obtained for the [EMIM]Acetate-activated sample after a 72-hour activation, while only 20% of the cellulose in the [AMIM]Formate-activated sample are converted. Similarly, the highest hemicellulose conversion is obtained for [EMIM]Acetate-activation of the hybrid poplar.

The observations from FT-IR spectroscopy, X-ray diffraction, SEM, and enzymatic saccharification confirm that [EMIM]Acetate and [AMIM]Formate do not activate hybrid poplar in a similar manner. While [EMIM]Acetate is able to open the structure of the biomass, deacetylate hemicellulose and lignin, and significantly decrease cellulose crystallinity, deacetylation does not occur during activation with [AMIM]Formate despite a larger amount of biomass being able to dissolve in this IL. Instead, the [AMIM]Formate-activated HP shows folding of fibers on its surface, and potential hornification of the biomass. Hornification, a term used in the pulp and paper industry, refers to an increase in the degree of cross-linking between microfibrils due to additional hydrogen bonds formed (during activation) and not broken during the regeneration step in which water is added.<sup>163</sup>

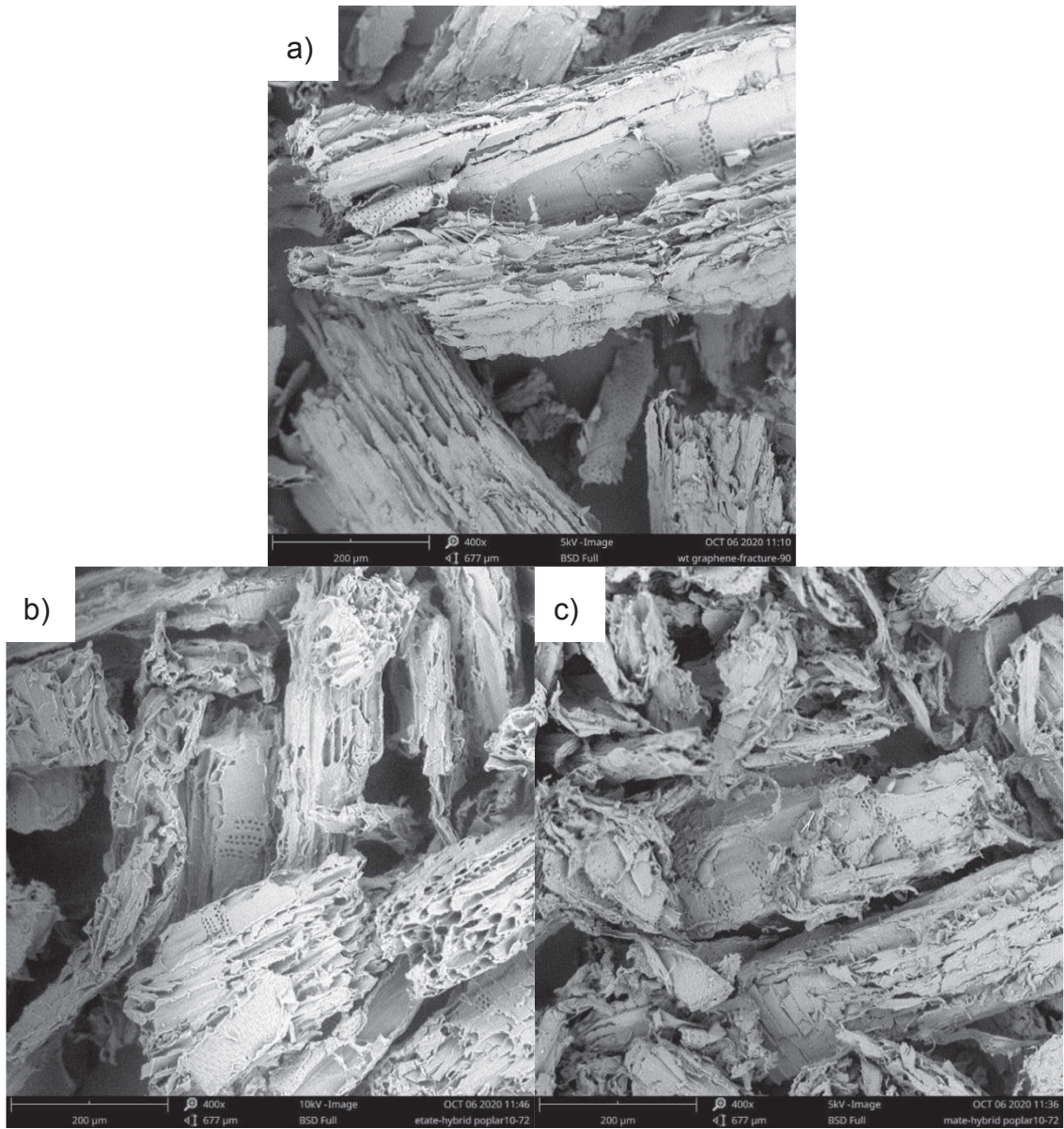


**Figure 16.** (a) SEM micrographs of control (untreated HP), (b) [EMIM]Acetate-activated HP, and (c) [AMIM]Formate-activated HP. Images were taken at 400x magnification.

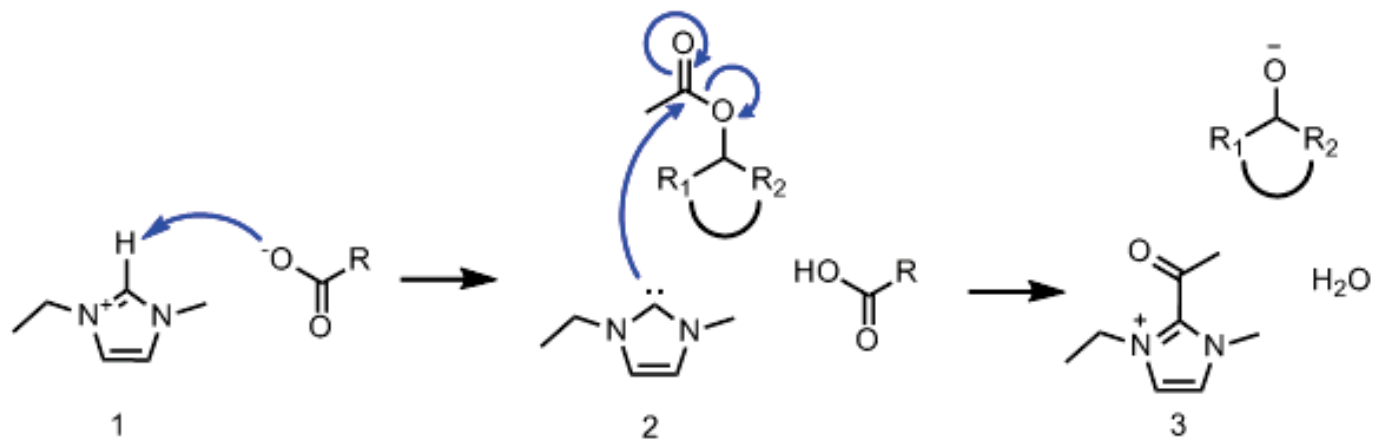


**Figure 17.** Mechanism for deacetylation of biomass using ionic liquids. R represents the H or CH<sub>3</sub> attached to the formate or acetate anion. R<sub>1</sub> and R<sub>2</sub> represent the carbon chain on the biomass structure.

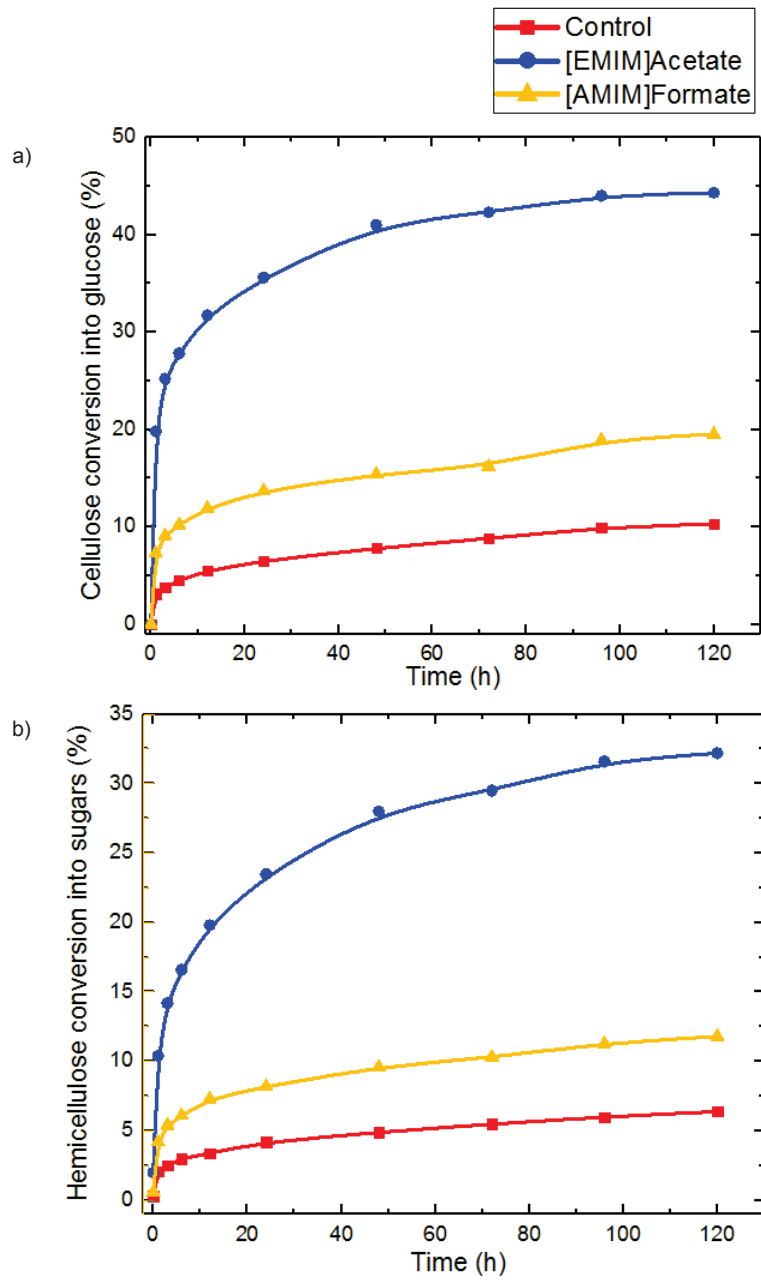


**Figure 18.** Kinetics of enzymatic saccharification on cellulose (a) and hemicellulose (b) of 72-hour activated biomass at a 10 wt.% biomass loading. The conversion was calculated based on the chemical composition of raw hybrid poplar.



Nevertheless, the behavior of [AMIM]Formate during activation is a highly valued characteristic of ILs for the production of films and fibers from whole biomass-IL system.<sup>164</sup> Since [AMIM]Formate is known to have better dissolution properties compared to [EMIM]Acetate, such as low viscosity, there is potential for [AMIM]Formate to become a solvent for textile and membrane sensor production. Also, [AMIM]Formate preserves the crystalline nature of the biomass which could translate in the production of fibers with higher mechanical properties. While [EMIM]Acetate has been used for fiber spinning in recent studies, our work shows that [EMIM]Acetate performs better at activating and thereby producing sugars and lignin through a fractionation approach while [AMIM]Formate performs better at dissolving whole biomass for the direct processing of products such as fibers and films.

## **Conclusion**

Our overall observations show that hybrid poplar activated using [EMIM]Acetate for 72 hours underwent deacetylation, has reduced cellulose crystallinity (43.5%), and resulted in 44% cellulose conversion during enzymatic saccharification. The uncommon IL [AMIM]Formate did not produce similar results, indicating that the acetyl groups in biomass and crystallinity of cellulose were retained even after 72-hour mixing under 60 °C. These findings open doors to new research for using [AMIM]Formate to dissolve biomass and extrude fibers with high crystallinity and mechanical strength.

## **Acknowledgments**

The authors are grateful to the National Science Foundation: Chemical, Bioengineering, Environmental, and Transport Systems (Grant Number: 151181) for their financial support. We thank Novozymes for providing the CTec 3 cellulases and HTec 3 hemicellulases. Additionally, we would like to thank Mr. Chris Wetteland and Mr. Jordan T. Sutton of the University of Tennessee for assisting with the scanning electron microscopy (SEM) images.

## **CHAPTER IV**

### **CONCLUSIONS AND FUTURE WORK**

## Overall conclusions

Due to the complex architecture of plant cell wall, lignocellulosic biomass requires some form of chemical, biological, or thermal treatment to disrupt its structure and allow for further conversion. As presented in the introduction, there exists many biomass pretreatment methods that use high severity to cause physical or chemical deconstruction and degradation of cell wall constituents. However, biomass valorization has encouraged biomass researchers to use mild process conditions to utilize all the fractions of lignocellulosic biomass.

This study explored the advantages of ionic liquids to (1) completely dissolve lignocellulosic biomass, (2) allow for an “activation” step that loosens the components of biomass, i.e., cellulose, hemicellulose, and lignin, and (3) fractionate them into high yield and high purity compounds. Ionic liquids are proven to be good solvents for biomass fractionation, in which they isolate lignocellulosic fractions with low severity. Since the possibility of ion combinations are endless, four ionic liquids were selected in this study by identifying cations and anions that are known to be efficient for biomass processing. Through a series of experiments in this project, an IL with high dissolution capacity was identified and used to activate biomass, as a comparison to [EMIM]Acetate. The activated biomass was then subjected to enzymatic saccharification to obtain a liquid fraction of sugars and a solid fraction of lignin. The overall scheme is shown in Figure 19.

In Chapter I, four ionic liquids with varying cations and anions were investigated, to identify the role of individual ions as well as its combination. The series of tests used to screen for an IL with “ideal” dissolution properties were thermal stability, viscosity, Kamlet-Taft parameter measurements, and molecular dynamics simulations. Among four tested ILs ([EMIM]Acetate, [EMIM]Formate, [AMIM]Formate, and [AMIM]Acetate), [AMIM]Formate was identified as a much better solvent to dissolve biomass when compared to [EMIM]Acetate, with a 40% increase in solubility. Due to several of its physicochemical properties,

[AMIM]Formate has strong interactions with hemicellulose, and therefore, high biomass solubility.

Chapter II then goes on to analyze the potential for [AMIM]Formate to “activate” biomass as well as the commonly used [EMIM]Acetate. The two ILs were subjected to IL “activation” for a series of times, and subsequent enzymatic saccharification to measure the conversion of cellulose and hemicellulose into soluble sugars. Measurements of cellulose crystallinity, conversion rates, and SEM images show that [EMIM]Acetate is a better IL for reducing the recalcitrance of biomass compared to [AMIM]Formate. The IL [AMIM]Formate retains most of the acetyl group after activation and shows little reduction in cellulose crystallinity. Therefore, since [AMIM]Formate dissolves more biomass due to reasons found in Chapter I and goes on to retain the chemical signature of biomass during activation (Chapter II), this IL can be widely used for fiber production in textile industries.

The table below (Table 11) compares some of the physical and chemical properties of the IL with best solubility ([AMIM]Formate) and the reference IL ([EMIM]Acetate). Through our findings in Chapter I and II, it can be concluded that ionic liquids have varying properties despite similar ionic combinations. Based on Table 11, we see that some of the IL properties are very similar, while there are a few very different properties, especially viscosity. Therefore, ILs have to be screened for specific uses in biomass processing, i.e., pretreatment, dissolution, activation, and fractionation.

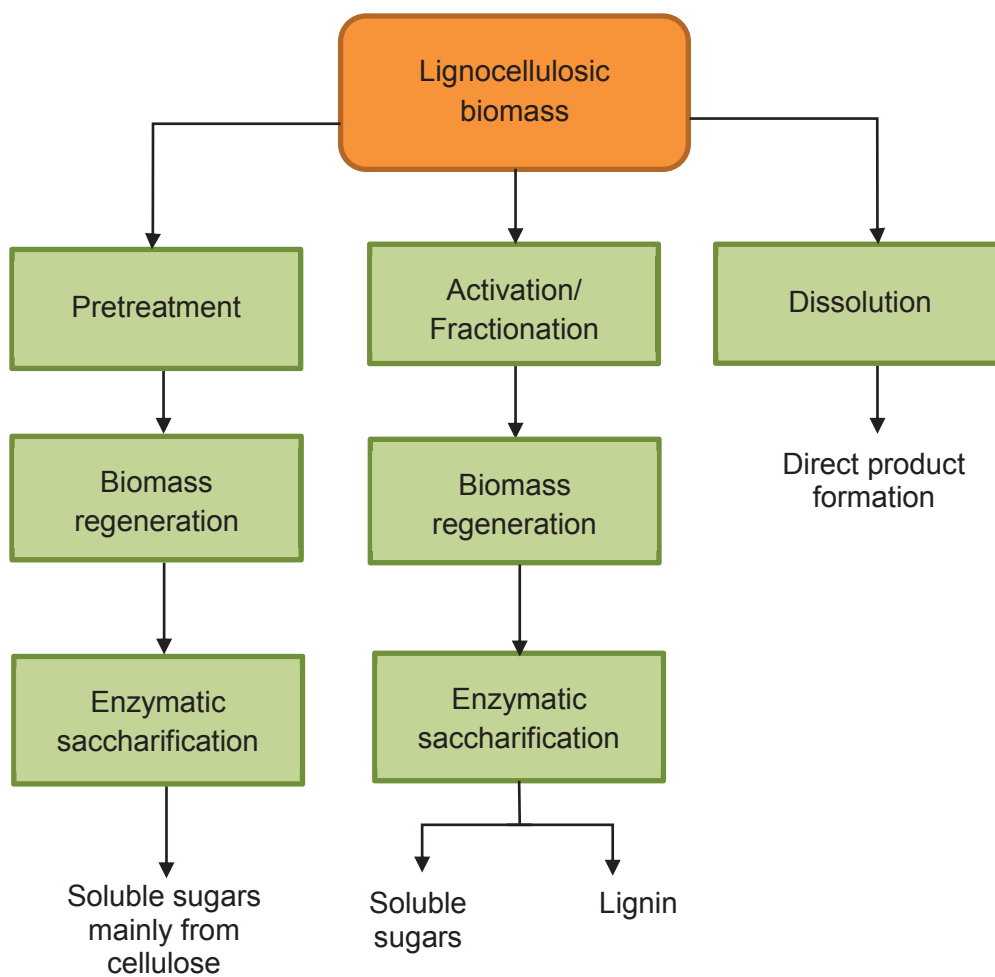


**Figure 19.** Overall process scheme for lignocellulosic biomass processing.

**Table 11.** Comparison of physical and chemical properties for [EMIM]Acetate and [AMIM]Formate.

	<b>[EMIM]Acetate</b>	<b>[AMIM]Formate</b>
Density (g/cm <sup>3</sup> )	1.03	1.11
Viscosity at 80 °C (mPa-s)	25.1	9.7
Decomposition temperature (°C)	241.1	205.6
Hydrogen bond basicity	1.07	1.01
Hydrogen bond acidity	0.50	0.46
Polarizability	1.03	1.09
Biomass solubility at 80 °C (wt.%)	5.27	7.39
Virial coefficients with hemicellulose	0.50	0.40
Virial coefficients with lignin	2.02	1.99

## Future work

The research topics in this thesis present opportunities for future work using ionic liquids as a solvent to fractionate biomass. Some of which include:

### ***In situ saccharification of activated biomass***

Due to the high viscosity of ionic liquids, it is difficult to remove them after IL-activation and biomass regeneration. Additionally, complete removal of ILs using water-rinse is a tedious process and requires large volume of water, as the ratio of ILs to water is 1: 200. Therefore, developing an *in situ* saccharification process following IL-activation will allow for a cost-effective process.

Kamiya et al.<sup>165</sup> reported the feasibility of an *in situ* system, in which enzymatic saccharification of Avicel occurred in the presence of an ionic liquid.<sup>166</sup> However, cellulases are known to show inactivity even in low concentrations of some ionic liquids. Turner et al. studied enzymatic saccharification of cellulose using *Trichoderma reesei* cellulases in solutions of 1-butyl-3-methylimidazolium-based ILs, [BMIM]Chloride and [BMIM]Tetrafluoroborate, and found that the cellulases were deactivated in the presence of an IL concentration as low as 22mM.<sup>167</sup> In 2011, Wang et al. found that commercial cellulases are able to retain at least 60% of their activity even in a 30% IL ([EMIM]Acetate) environment.<sup>168</sup> However, hemicellulases were not studied. Therefore, it is essential to find a compatible IL-enzymes system to effectively activate biomass and simultaneously carry out enzymatic hydrolysis to ensure high conversions of both cellulose and hemicellulose.

Recently, Hu et al. studied enzymatic saccharification in a system containing ILs 1-ethyl-3-methylimidazolium dimethylphosphate, 1-ethyl-3-methylimidazolium diethyl phosphate, and 1-ethyl-3-methylimidazolium acetate.<sup>169</sup> However, low concentrations of ILs were used and only cellulose conversion into glucose was taken into account. Our preliminary study for activation and *in situ* saccharification with [EMIM]Acetate using both cellulases and hemicellulases



(CTec 3 and HTec 3, Novozymes) have shown promising results for further study. Figure 20 shows the cellulose (a) and hemicellulose (b) conversions for an IL-enzyme system pre-incubated at 4 °C for 24 hours, and saccharification was carried out using a pH 4.5 sodium citrate buffer at 52 °C.

Both the cellulases and hemicellulases retained 60 and 35% of their activity respectively, even in the presence of 20% IL. These findings show that an *in situ* saccharification is feasible, given that the IL is effective enough to activate the biomass prior to enzymatic hydrolysis.

### ***Designing an apparatus setup to enable higher biomass loading***

To achieve high biomass solubility and effective activation, adequate mixing is required with an optimum experimental design to ensure maximum contact between the ILs and biomass. With a better apparatus setup, the surface contact area of biomass with ionic liquids will increase and allow for an effective dissolution and activation (as investigated in Chapter I and II, respectively).

Currently, round bottom flasks and vials are used in the laboratory for small scale activation and dissolution. The mixture is agitated using either an overhead stirrer or magnetic stir bars set at 100-200 RPM. However, several limitations arise from these methods as they lack in uniformity of stirring and are inconsistent in heat transfer. Therefore, some preliminary work has been done on designing a better apparatus setup for more effective mixing of biomass in ILs. Some of the components that have been implemented in the preliminary design are: a custom-built glass vessel that fits an overhead stainless-steel propeller, a side inlet for ionic liquid and thermocouples, a coarse frit filter and valves to remove ionic liquid after the process.

This new setup has proven thus far that it is better than the traditional round bottom flask setup, but still needs further improvements and testing.

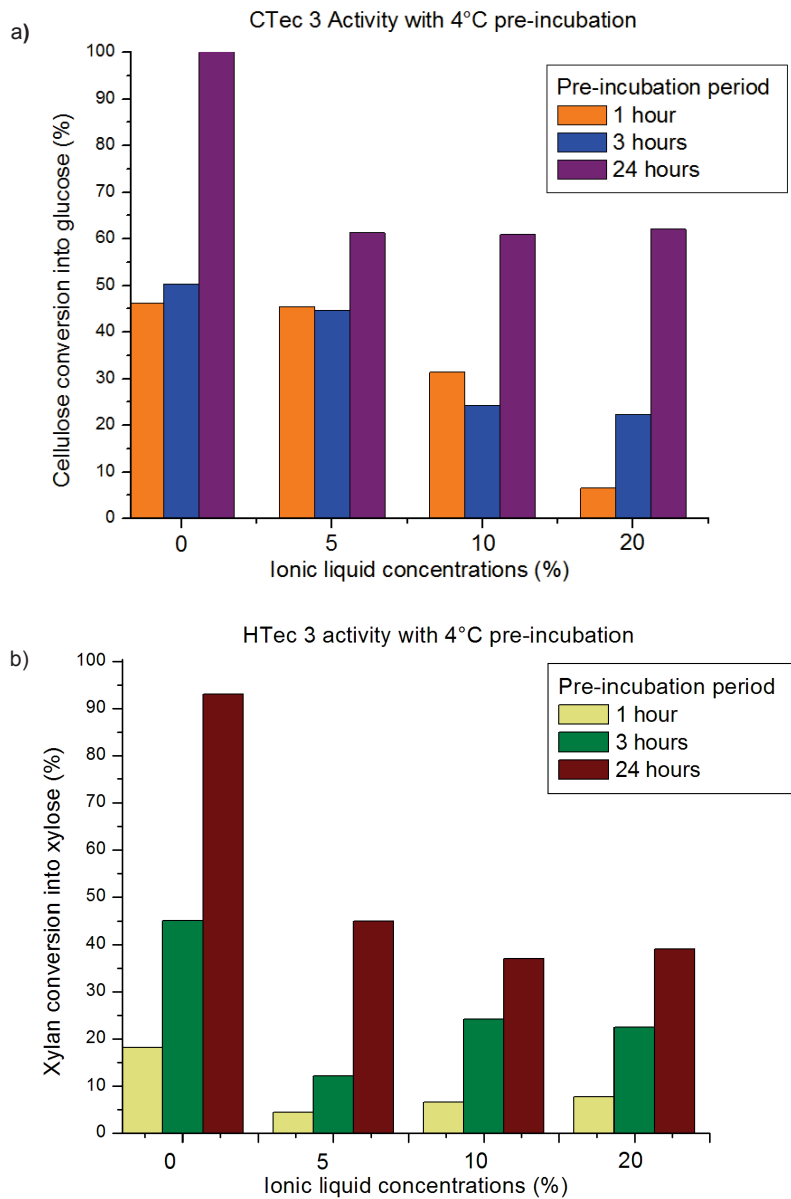


**Figure 20.** Activity of CTEC 3 cellulases (a) and HTEC 3 hemicellulases (b) in the presence of 0, 5, 10, and 20% IL.

### ***Understanding the role of acetate anion as during activation***

Based on Objective 2, the biomass deacetylation mechanism using ILs show that the presence of an acetate anion promotes deacetylation compared to a formate anion. Therefore, there exists a possibility for the acetate anion to act as a catalyst in a given IL.

Current experiments are underway to investigate several ratio combinations of [EMIM]Formate and [EMIM]Acetate as well as [AMIM]Formate and [AMIM]Acetate to understand the effects of combining the anions: acetate and formate, with a constant cation.

### ***Analyzing the structure and interactions of ILs using small-angle neutron scattering (SANS)***

As more and more ILs are being discovered for their specific uses, much of their properties are still not fully investigated. In the topic of biomass pretreatment and fractionation, many ILs with different ionic combinations have claimed their fame to deacetylating biomass and reducing cellulose crystallinity. However, much like the topic presented in Chapter I, it is essential to understand the interactions and reactions that take place between the biomass and IL at a smaller scale, i.e. nanoscopic. Research is already underway to use Small Angle Neutron Scattering (SANS) to test the hypothesis that [EMIM]Acetate increases porosity radius of activated biomass compared to [AMIM]Formate and the other ILs in this study.<sup>170</sup>

### ***Understanding the potential for [AMIM]Formate to spin fibers***

Over the past years, biobased fibers and films have been produced through direct processing of biomass-IL solutions using several imidazolium-based ILs such as [BMIM]Chloride and [EMIM]Acetate.<sup>98b</sup> Recent work by Wang et al. shows that biomass dissolution in [EMIM]Acetate retains the polymeric features of lignocellulosic components, therefore allowing for defect-free and wrinkle-free films.<sup>164</sup> However, based on our conclusions in Chapter I and II, it is highly likely

that the IL 1-allyl-3-methylimidazolium ([AMIM])Formate is better suited for extrusion of films and fibers than [EMIM]Acetate. Since [AMIM]Formate has high solubility for biomass and is less effective during activation, it can not only dissolve more biomass but also retain the biomass constituents without activating or loosening the structure. Therefore, further understanding is required of [AMIM]Formate's properties after completely dissolving biomass to study its potential for direct transformation. The IL-biomass mixture requires further chemical characterization.

### ***Analyzing [EMIM]Formate and [AMIM]Acetate for biomass activation***

In objective 1, four ILs were investigated for their respective biomass solubilities. The study showed that [AMIM]Formate dissolved the highest amount of biomass (7.39 wt.%) while [EMIM]Acetate dissolved the lowest (5.27 wt.%). Therefore, in Objective 2, only these two ILs were further investigated. The remaining two ILs ([EMIM]Formate and [AMIM]Acetate) have yet to be investigated.

Literature shows that [EMIM]Formate, when coupled with a glycerol co-solvent, performs better than [EMIM]Acetate during pretreatment of rice hulls. The hemicellulose conversion of [EMIM]Formate-treated biomass was slightly higher (~75% hemicellulose converted into xylose) than that of [EMIM]Acetate-treated biomass.<sup>171</sup> However, the IL [AMIM]Acetate has not been investigated for biomass processing by anyone, according to our knowledge. Therefore, more work needs to be done to identify the potential for [EMIM]Formate and [AMIM]Acetate to either pretreat or activate biomass for the production of soluble sugars and/or pure lignin.

## REFERENCES

1. Mosier, N.; Wyman, C.; Dale, B.; Elander, R.; Lee, Y. Y.; Holtzapple, M.; Ladisch, M., Features of promising technologies for pretreatment of lignocellulosic biomass. *Bioresource Technology* **2005**, *96* (6), 673-686.
2. Samayam, I. P.; Schall, C. A., Saccharification of ionic liquid pretreated biomass with commercial enzyme mixtures. *Bioresource Technology* **2010**, *101* (10), 3561-3566.
3. (a) Qin, Z.; Zhuang, Q.; Zhu, X., Carbon and nitrogen dynamics in bioenergy ecosystems: 2. Potential greenhouse gas emissions and global warming intensity in the conterminous United States. *GCB Bioenergy* **2015**, *7* (1), 25-39; (b) Wang, M.; Wu, M.; Huo, H., Life-cycle energy and greenhouse gas emission impacts of different corn ethanol plant types. *Environmental Research Letters* **2007**, *2* (2), 024001.
4. (a) Soudham, V. P.; Grasvik, J.; Alriksson, B.; Mikkola, J. P.; Jonsson, L. J., Enzymatic hydrolysis of Norway spruce and sugarcane bagasse after treatment with 1-allyl-3-methylimidazolium formate. *Journal of Chemical Technology and Biotechnology* **2013**, *88* (12), 2209-2215; (b) Rabideau, B. D.; Ismail, A. E., Mechanisms of hydrogen bond formation between ionic liquids and cellulose and the influence of water content. *Physical chemistry chemical physics : PCCP* **2015**, *17* (8), 5767-75; (c) Lynd, L. R.; Cushman, J. H.; Nichols, R. J.; Wyman, C. E., Fuel ethanol from cellulosic biomass. *Science* **1991**, *251* (4999), 1318-23.
5. Santiago, R.; Barros-Rios, J.; Malvar, R. A., Impact of cell wall composition on maize resistance to pests and diseases. *International Journal of Molecular Sciences* **2013**, *14* (4), 6960-6980.
6. da Costa Lopes, A. M.; João, K. G.; Morais, A. R. C.; Bogel-Lukasik, E.; Bogel-Lukasik, R., Ionic liquids as a tool for lignocellulosic biomass fractionation. *Sustainable Chemical Processes* **2013**, *1* (1), 3.
7. Hendriks, A.; Zeeman, G., Pretreatments to enhance the digestibility of lignocellulosic biomass. *Bioresource Technology* **2009**, *100* (1), 10-18.
8. Jørgensen, H.; Kristensen, J. B.; Felby, C., Enzymatic conversion of lignocellulose into fermentable sugars: challenges and opportunities. *Biofuels, Bioproducts and Biorefining* **2007**, *1* (2), 119-134.
9. Astner, A. F., Lignin yield maximization of lignocellulosic biomass by Taguchi robust product design using organosolv fractionation. **2012**.
10. Schwab, A. *Bioenergy Technologies Office Multi-Year Program Plan. March 2016*; Bioenergy Technologies Office, Washington, DC (United States): 2016.
11. Ghosh, D.; Dasgupta, D.; Agrawal, D.; Kaul, S.; Adhikari, D. K.; Kurmi, A. K.; Arya, P. K.; Bangwal, D.; Negi, M. S., Fuels and chemicals from lignocellulosic biomass: an integrated biorefinery approach. *Energy & Fuels* **2015**, *29* (5), 3149-3157.

12. (a) Zhu, Y., Overview Of Biomass Pretreatment Technologies. *Retrieved on December 2011*, 26, 2012; (b) Lynd, L. R., Overview and evaluation of fuel ethanol from cellulosic biomass: technology, economics, the environment, and policy. *Annual review of energy and the environment* **1996**, 21 (1), 403-465; (c) Yang, B.; Wyman, C. E., Pretreatment: the key to unlocking low-cost cellulosic ethanol. *Biofuels, Bioproducts and Biorefining* **2008**, 2 (1), 26-40.
13. (a) Shill, K.; Padmanabhan, S.; Xin, Q.; Prausnitz, J. M.; Clark, D. S.; Blanch, H. W., Ionic liquid pretreatment of cellulosic biomass: enzymatic hydrolysis and ionic liquid recycle. *Biotechnology and Bioengineering* **2011**, 108 (3), 511-520; (b) Yuan, X.; Liu, S.; Feng, G.; Liu, Y.; Li, Y.; Lu, H.; Liang, B., Effects of ball milling on structural changes and hydrolysis of lignocellulosic biomass in liquid hot-water compressed carbon dioxide. *Korean Journal of Chemical Engineering* **2015**, 1-8; (c) Tassinari, T. H.; Macy, C. F.; Spano, L. A., Technology advances for continuous compression milling pretreatment of lignocellulosics for enzymatic hydrolysis. *Biotechnology and Bioengineering* **1982**, 24 (7), 1495-1505.
14. Zhu, J.; Wang, G.; Pan, X.; Gleisner, R., Specific surface for evaluating wood size-reduction and pretreatment efficiencies. *Chemical Engineering Science* **2009**, 64, 474-485.
15. Zhu, J.; Pan, X., Woody biomass pretreatment for cellulosic ethanol production: technology and energy consumption evaluation. *Bioresource Technology* **2010**, 101 (13), 4992-5002.
16. Ikeda, T.; Holtman, K.; Kadla, J. F.; Chang, H.-m.; Jameel, H., Studies on the effect of ball milling on lignin structure using a modified DFRC method. *Journal of Agricultural and Food Chemistry* **2002**, 50 (1), 129-135.
17. Lin, Z.; Huang, H.; Zhang, H.; Zhang, L.; Yan, L.; Chen, J., Ball milling pretreatment of corn stover for enhancing the efficiency of enzymatic hydrolysis. *Applied Biochemistry and Biotechnology* **2010**, 162 (7), 1872-1880.
18. (a) Wooley, R.; Ruth, M.; Sheehan, J.; Ibsen, K.; Majdeski, H.; Galvez, A. *Lignocellulosic biomass to ethanol process design and economics utilizing co-current dilute acid prehydrolysis and enzymatic hydrolysis current and futuristic scenarios*; DTIC Document: 1999; (b) Grohmann, K.; Torget, R.; Himmel, M.; Scott, C. In *Dilute acid pretreatment of biomass at high acid concentrations*, Biotechnol. Bioeng. Symp.;(United States), Solar Energy Research Institute, Golden, CO 80401, USA. Solar Fuels Research Div.: 1986.
19. (a) Knappert, D.; Grethlein, H.; Converse, A., Partial acid hydrolysis of cellulosic materials as a pretreatment for enzymatic hydrolysis. *Biotechnology and Bioengineering* **1980**, 22 (7), 1449-1463; (b) Yang, B.; Wyman, C. E., Effect of xylan and lignin removal by batch and flowthrough pretreatment on the enzymatic digestibility of corn stover cellulose. *Biotechnology and Bioengineering* **2004**, 86 (1), 88-98.

20. Wyman, C. E.; Dale, B. E.; Elander, R. T.; Holtzapple, M.; Ladisch, M. R.; Lee, Y.; Mitchinson, C.; Saddler, J. N., Comparative sugar recovery and fermentation data following pretreatment of poplar wood by leading technologies. *Biotechnology Progress* **2009**, *25* (2), 333-339.
21. Du, X.; Lucia, L. A.; Ghiladi, R. A., Development of a highly efficient pretreatment sequence for the enzymatic saccharification of loblolly pine wood. *ACS Sustainable Chemistry & Engineering* **2016**.
22. (a) Zhao, X.; Peng, F.; Cheng, K.; Liu, D., Enhancement of the enzymatic digestibility of sugarcane bagasse by alkali-peracetic acid pretreatment. *Enzyme and Microbial Technology* **2009**, *44* (1), 17-23; (b) Kim, S.; Park, J. M.; Seo, J.-W.; Kim, C. H., Sequential acid-/alkali-pretreatment of empty palm fruit bunch fiber. *Bioresource Technology* **2012**, *109*, 229-233.
23. Chen, W.-H.; Tu, Y.-J.; Sheen, H.-K., Disruption of sugarcane bagasse lignocellulosic structure by means of dilute sulfuric acid pretreatment with microwave-assisted heating. *Applied Energy* **2011**, *88* (8), 2726-2734.
24. Cheng, G.; Varanasi, P.; Li, C.; Liu, H.; Melnichenko, Y. B.; Simmons, B. A.; Kent, M. S.; Singh, S., Transition of cellulose crystalline structure and surface morphology of biomass as a function of ionic liquid pretreatment and its relation to enzymatic hydrolysis. *Biomacromolecules* **2011**, *12* (4), 933-941.
25. Liu, C.; Wyman, C. E., Partial flow of compressed-hot water through corn stover to enhance hemicellulose sugar recovery and enzymatic digestibility of cellulose. *Bioresource Technology* **2005**, *96* (18), 1978-1985.
26. (a) Alvira, P.; Tomás-Pejó, E.; Ballesteros, M.; Negro, M., Pretreatment technologies for an efficient bioethanol production process based on enzymatic hydrolysis: a review. *Bioresource Technology* **2010**, *101* (13), 4851-4861; (b) Kim, Y.; Mosier, N. S.; Ladisch, M. R., Enzymatic digestion of liquid hot water pretreated hybrid poplar. *Biotechnology Progress* **2009**, *25* (2), 340-348.
27. (a) Sun, S.; Wen, J.; Sun, S.; Sun, R.-C., Systematic evaluation of the degraded products evolved from the hydrothermal pretreatment of sweet sorghum stems. *Biotechnology for Biofuels* **2015**, *8* (1), 1; (b) Garrote, G.; Dominguez, H.; Parajo, J., Hydrothermal processing of lignocellulosic materials. *European Journal of Wood and Wood Products* **1999**, *57* (3), 191-202; (c) Liu, S., Woody biomass: Niche position as a source of sustainable renewable chemicals and energy and kinetics of hot-water extraction/hydrolysis. *Biotechnology Advances* **2010**, *28* (5), 563-582.
28. Michelin, M.; Teixeira, J. A., Liquid hot water pretreatment of multi feedstocks and enzymatic hydrolysis of solids obtained thereof. *Bioresource Technology* **2016**.



29. Xiao, X.; Bian, J.; Peng, X.-P.; Xu, H.; Xiao, B.; Sun, R.-C., Autohydrolysis of bamboo (*Dendrocalamus giganteus* Munro) culm for the production of xylo-oligosaccharides. *Bioresource Technology* **2013**, *138*, 63-70.
30. (a) Pu, Y.; Cao, S.; Studer, M.; Ragauskas, A.; Wyman, C. In *Chemical characterization of poplar after hot water pretreatment*, 32th Symposium on Biotechnology for Fuels and Chemicals, April, 2010; pp 19-22; (b) Samuel, R.; Cao, S.; Das, B. K.; Hu, F.; Pu, Y.; Ragauskas, A. J., Investigation of the fate of poplar lignin during autohydrolysis pretreatment to understand the biomass recalcitrance. *RSC Advances* **2013**, *3* (16), 5305-5309.
31. (a) Mosier, N.; Kim, Y.; Zeng, M.; Hendrickson, R.; Dien, B.; Welsh, G.; Ladisch, M. In *Optimization of controlled pH liquid hot water pretreatment of corn fiber and stover*, American Institute of Chemical Engineers Annual Meeting, 2003; (b) Heitz, M.; Capek-Menard, E.; Koeberle, P.; Gagne, J.; Chornet, E.; Overend, R.; Taylor, J.; Yu, E., Fractionation of *Populus tremuloides* at the pilot plant scale: Optimization of steam pretreatment conditions using the STAKE II technology. *Bioresource Technology* **1991**, *35* (1), 23-32.
32. Overend, R. P.; Chornet, E.; Gascoigne, J., Fractionation of lignocellulosics by steam-aqueous pretreatments [and discussion]. *Philosophical Transactions of the Royal Society of London A: Mathematical, Physical and Engineering Sciences* **1987**, *321* (1561), 523-536.
33. Weil, J.; Brewer, M.; Hendrickson, R.; Sarikaya, A.; Ladisch, M. R., Continuous pH monitoring during pretreatment of yellow poplar wood sawdust by pressure cooking in water. *Applied Biochemistry and Biotechnology* **1998**, *70* (1), 99-111
34. Vishtal, A. G.; Kraslawski, A., Challenges in industrial applications of technical lignins. *BioResources* **2011**, *6* (3), 3547-3568.
35. Sjöström, E., *Wood chemistry: fundamentals and applications*. Gulf Professional Publishing: 1993.
36. Sluiter, A.; Hames, B.; Ruiz, R.; Scarlata, C.; Sluiter, J.; Templeton, D.; Crocker, D., Determination of structural carbohydrates and lignin in biomass. *NREL Laboratory Analytical Procedure* **2008**, 1617.
37. Ko, J. K.; Kim, Y.; Ximenes, E.; Ladisch, M. R., Effect of liquid hot water pretreatment severity on properties of hardwood lignin and enzymatic hydrolysis of cellulose. *Biotechnology and Bioengineering* **2015**, *112* (2), 252-262.
38. Borrega, M.; Sixta, H., Water prehydrolysis of birch wood chips and meal in batch and flow-through systems: a comparative evaluation. *Industrial & Engineering Chemistry Research* **2015**, *54* (23), 6075-6084.
39. Process and apparatus for disintegration of wood and the like. Google Patents: 1926.

40. Heitz, M.; Capek-Ménard, E.; Koeberle, P. G.; Gagné, J.; Chornet, E.; Overend, R. P.; Taylor, J. D.; Yu, E., Fractionation of *Populus tremuloides* at the pilot plant scale: Optimization of steam pretreatment conditions using the STAKE II technology. *Bioresource Technology* **1991**, *35* (1), 23-32.
41. Cantarella, M.; Cantarella, L.; Gallifuoco, A.; Spera, A.; Alfani, F., Effect of inhibitors released during steam-explosion treatment of Poplar wood on subsequent enzymatic hydrolysis and SSF. *Biotechnology Progress* **2004**, *20* (1), 200-206.
42. Varga, E.; Schmidt, A. S.; Réczey, K.; Thomsen, A. B., Pretreatment of corn stover using wet oxidation to enhance enzymatic digestibility. *Applied Biochemistry and Biotechnology* **2003**, *104* (1), 37-50.
43. Bjerre, A. B.; Olesen, A. B.; Fernqvist, T.; Plöger, A.; Schmidt, A. S., Pretreatment of wheat straw using combined wet oxidation and alkaline hydrolysis resulting in convertible cellulose and hemicellulose. *Biotechnology and Bioengineering* **1996**, *49* (5), 568-577.
44. (a) Fox, M.; Noike, T., Wet oxidation pretreatment for the increase in anaerobic biodegradability of newspaper waste. *Bioresource Technology* **2004**, *91* (3), 273-281; (b) Lissens, G.; Klinke, H.; Verstraete, W.; Ahring, B.; Thomsen, A. B., Wet oxidation treatment of organic household waste enriched with wheat straw for simultaneous saccharification and fermentation into ethanol. *Environmental Technology* **2004**, *25* (6), 647-655.
45. Banerjee, S.; Sen, R.; Pandey, R. A.; Chakrabarti, T.; Satpute, D.; Giri, B. S.; Mudliar, S., Evaluation of wet air oxidation as a pretreatment strategy for bioethanol production from rice husk and process optimization. *Biomass and Bioenergy* **2009**, *33* (12), 1680-1686.
46. Szijártó, N.; Kádár, Z.; Varga, E.; Thomsen, A. B.; Costa-Ferreira, M.; Réczey, K., Pretreatment of reed by wet oxidation and subsequent utilization of the pretreated fibers for ethanol production. *Applied Biochemistry and Biotechnology* **2009**, *155* (1-3), 83-93.
47. Banerjee, S.; Sen, R.; Mudliar, S.; Pandey, R.; Chakrabarti, T.; Satpute, D., Alkaline peroxide assisted wet air oxidation pretreatment approach to enhance enzymatic convertibility of rice husk. *Biotechnology Progress* **2011**, *27* (3), 691-697.
48. Martín, C.; Thomsen, A. B., Wet oxidation pretreatment of lignocellulosic residues of sugarcane, rice, cassava and peanuts for ethanol production. *Journal of Chemical Technology and Biotechnology* **2007**, *82* (2), 174-181.
49. (a) Soto, M.; Dominguez, H.; Nunez, M.; Lema, J., Enzymatic saccharification of alkali-treated sunflower hulls. *Bioresource Technology* **1994**, *49* (1), 53-59; (b) MacDonald, D. G.; Bakhshi, N. N.; Mathews, J. F.; Roychowdhury, A.; Bajpai, P.; Moo-Young, M., Alkali treatment of corn stover to improve sugar

production by enzymatic hydrolysis. *Biotechnology and Bioengineering* **1983**, 25 (8), 2067-2076.

50. Kong, F.; Engler, C. R.; Soltes, E. J., Effects of cell-wall acetate, xylan backbone, and lignin on enzymatic hydrolysis of aspen wood. *Applied Biochemistry and Biotechnology* **1992**, 34 (1), 23-35.

51. Kim, S.; Holtzapfle, M. T., Effect of structural features on enzyme digestibility of corn stover. *Bioresource Technology* **2006**, 97 (4), 583-591.

52. Fan, L.; Gharpuray, M. M.; Lee, Y.-H., *Cellulose hydrolysis*. Springer Science & Business Media: 2012; Vol. 3.

53. (a) Hu, Z.; Wang, Y.; Wen, Z., Alkali (NaOH) pretreatment of switchgrass by radio frequency-based dielectric heating. *Applied Biochemistry and Biotechnology* **2008**, 148 (1-3), 71-81; (b) Hu, Z.; Wen, Z., Enhancing enzymatic digestibility of switchgrass by microwave-assisted alkali pretreatment. *Biochemical Engineering Journal* **2008**, 38 (3), 369-378.

54. Holtzapfle, M. T.; Lundeen, J. E.; Sturgis, R.; Lewis, J. E.; Dale, B. E., Pretreatment of lignocellulosic municipal solid waste by ammonia fiber explosion (AFEX). *Applied Biochemistry and Biotechnology* **1992**, 34 (1), 5-21.

55. Chaturvedi, V.; Verma, P., An overview of key pretreatment processes employed for bioconversion of lignocellulosic biomass into biofuels and value added products. *3 Biotech* **2013**, 3 (5), 415-431.

56. (a) Yoon, H.; Wu, Z.; Lee, Y., Ammonia-recycled percolation process for pretreatment of biomass feedstock. *Applied Biochemistry and Biotechnology* **1995**, 51 (1), 5-19; (b) Iyer, P. V.; Wu, Z.-W.; Kim, S. B.; Lee, Y. Y. In *Ammonia recycled percolation process for pretreatment of herbaceous biomass*, Seventeenth Symposium on Biotechnology for Fuels and Chemicals, Springer: 1996; pp 121-132.

57. Bradshaw, T. C.; Alizadeh, H.; Teymouri, F.; Balan, V.; Dale, B. E., Ammonia Fiber Expansion Pretreatment and Enzymatic Hydrolysis on Two Different Growth Stages of Reed Canarygrass. In *Applied Biochemistry and Biotechnology: The Twenty-Eighth Symposium Proceedings of the Twenty-Eight Symposium on Biotechnology for Fuels and Chemicals Held April 30–May 3, 2006, in Nashville, Tennessee*, Mielenz, J. R.; Klasson, K. T.; Adney, W. S.; McMillan, J. D., Eds. Humana Press: Totowa, NJ, 2007; pp 395-405.

58. (a) Kim, T. H.; Lee, Y. Y., Pretreatment and fractionation of corn stover by ammonia recycle percolation process. *Bioresource Technology* **2005**, 96 (18), 2007-2013; (b) Kumar, R.; Mago, G.; Balan, V.; Wyman, C. E., Physical and chemical characterizations of corn stover and poplar solids resulting from leading pretreatment technologies. *Bioresource Technology* **2009**, 100 (17), 3948-3962.

59. Ichwan, M.; Son, T. In *Study on organosolv pulping methods of oil palm biomass*, Proceedings of the International Seminar on Chemistry, 2011; pp 364-370.
60. Ghose, T.; Pannir Selvam, P.; Ghosh, P., Catalytic solvent delignification of agricultural residues: organic catalysts. *Biotechnology and Bioengineering* **1983**, *25* (11), 2577-2590.
61. Chum, H.; Douglas, L.; Feinberg, D.; Schroeder, H., Evaluation of pretreatments for enzymatic hydrolysis of cellulose. 1985.
62. Zhao, X.; Cheng, K.; Liu, D., Organosolv pretreatment of lignocellulosic biomass for enzymatic hydrolysis. *Applied Microbiology and Biotechnology* **2009**, *82* (5), 815-827.
63. Bozell, J. J.; Black, S. K.; Myers, M.; Cahill, D.; Miller, W. P.; Park, S., Solvent fractionation of renewable woody feedstocks: Organosolv generation of biorefinery process streams for the production of biobased chemicals. *Biomass and Bioenergy* **2011**, *35* (10), 4197-4208.
64. Sun, Y.; Cheng, J., Hydrolysis of lignocellulosic materials for ethanol production: a review. *Bioresource Technology* **2002**, *83* (1), 1-11.
65. Agbor, V. B.; Cicek, N.; Sparling, R.; Berlin, A.; Levin, D. B., Biomass pretreatment: fundamentals toward application. *Biotechnology Advances* **2011**, *29* (6), 675-685.
66. Horváth, I. T., Solvents from nature. *Green Chemistry* **2008**, *10* (10), 1024-1028.
67. Wettstein, S. G.; Alonso, D. M.; Chong, Y.; Dumesic, J. A., Production of levulinic acid and gamma-valerolactone (GVL) from cellulose using GVL as a solvent in biphasic systems. *Energy & Environmental Science* **2012**, *5* (8), 8199-8203.
68. (a) Serrano-Ruiz, J. C.; Luque, R.; Sepulveda-Escribano, A., Transformations of biomass-derived platform molecules: from high added-value chemicals to fuels via aqueous-phase processing. *Chemical Society Reviews* **2011**, *40* (11), 5266-5281; (b) Alonso, D. M.; Bond, J. Q.; Dumesic, J. A., Catalytic conversion of biomass to biofuels. *Green Chemistry* **2010**, *12* (9), 1493-1513.
69. Bozell, J. J.; Petersen, G. R., Technology development for the production of biobased products from biorefinery carbohydrates—the US Department of Energy’s “top 10” revisited. *Green Chemistry* **2010**, *12* (4), 539-554.
70. Alonso, D. M.; Wettstein, S. G.; Dumesic, J. A., Gamma-valerolactone, a sustainable platform molecule derived from lignocellulosic biomass. *Green Chemistry* **2013**, *15* (3), 584-595.
71. Wu, M.; Liu, J.-K.; Yan, Z.-Y.; Wang, B.; Zhang, X.-M.; Xu, F.; Sun, R.-C., Efficient recovery and structural characterization of lignin from cotton stalk based

on a biorefinery process using a  $\gamma$ -valerolactone/water system. *RSC Advances* **2016**, 6 (8), 6196-6204.

72. Tabasso, S.; Grillo, G.; Carnaroglio, D.; Calcio Gaudino, E.; Cravotto, G., Microwave-assisted  $\gamma$ -valerolactone production for biomass lignin extraction: A cascade protocol. *Molecules* **2016**, 21 (4), 413.

73. Luterbacher, J. S.; Rand, J. M.; Alonso, D. M.; Han, J.; Youngquist, J. T.; Maravelias, C. T.; Pfleger, B. F.; Dumesic, J. A., Nonenzymatic sugar production from biomass using biomass-derived  $\gamma$ -valerolactone. *Science* **2014**, 343 (6168), 277-280.

74. Luterbacher, J. S.; Azarpira, A.; Motagamwala, A. H.; Lu, F.; Ralph, J.; Dumesic, J. A., Lignin monomer production integrated into the  $\gamma$ -valerolactone sugar platform. *Energy & Environmental Science* **2015**, 8 (9), 2657-2663.

75. Grande, P. M.; Viell, J.; Theyssen, N.; Marquardt, W.; de María, P. D.; Leitner, W., Fractionation of lignocellulosic biomass using the OrganoCat process. *Green Chemistry* **2015**, 17 (6), 3533-3539.

76. vom Stein, T.; Grande, P. M.; Kayser, H.; Sibilla, F.; Leitner, W.; de María, P. D., From biomass to feedstock: one-step fractionation of lignocellulose components by the selective organic acid-catalyzed depolymerization of hemicellulose in a biphasic system. *Green Chemistry* **2011**, 13 (7), 1772-1777.

77. He, T.; Jiang, Z.; Wu, P.; Yi, J.; Li, J.; Hu, C., Fractionation for further conversion: from raw corn stover to lactic acid. *Scientific Reports* **2016**, 6.

78. Crocker, M., *Thermochemical conversion of biomass to liquid fuels and chemicals*. Royal Society of Chemistry: 2010.

79. Li, C.; Knierim, B.; Manisseri, C.; Arora, R.; Scheller, H. V.; Auer, M.; Vogel, K. P.; Simmons, B. A.; Singh, S., Comparison of dilute acid and ionic liquid pretreatment of switchgrass: biomass recalcitrance, delignification and enzymatic saccharification. *Bioresource Technology* **2010**, 101 (13), 4900-4906.

80. (a) Dupont, J., On the solid, liquid and solution structural organization of imidazolium ionic liquids. *Journal of the Brazilian Chemical Society* **2004**, 15 (3), 341-350; (b) Hurley, F. H.; Wier, T. P., Electrodeposition of metals from fused quaternary ammonium salts. *Journal of The Electrochemical Society* **1951**, 98 (5), 203-206.

81. (a) Dupont, J.; de Souza, R. F.; Suarez, P. A., Ionic liquid (molten salt) phase organometallic catalysis. *Chemical Reviews* **2002**, 102 (10), 3667-3692; (b) Postleb, F.; Stefanik, D.; Seifert, H.; Giernoth, R., Bionic liquids: Imidazolium-based ionic liquids with antimicrobial activity. *Zeitschrift für Naturforschung B* **2013**, 68 (10), 1123-1128; (c) Giridhar, P.; Venkatesan, K.; Srinivasan, T.; Rao, P. V., Electrochemical behavior of uranium (VI) in 1-butyl-3-methylimidazolium chloride and thermal characterization of uranium oxide deposit. *Electrochimica Acta* **2007**, 52 (9), 3006-3012.

82. Olivier-Bourbigou, H.; Magna, L.; Morvan, D., Ionic liquids and catalysis: Recent progress from knowledge to applications. *Applied Catalysis A: General* **2010**, *373* (1), 1-56.
83. Dadi, A. P.; Schall, C. A.; Varanasi, S., Mitigation of cellulose recalcitrance to enzymatic hydrolysis by ionic liquid pretreatment. In *Applied Biochemistry and Biotechnology*, Springer: 2007; pp 407-421.
84. Tadesse, H.; Luque, R., Advances on biomass pretreatment using ionic liquids: an overview. *Energy & Environmental Science* **2011**, *4* (10), 3913-3929.
85. Villanueva, M.; Coronas, A.; García, J.; Salgado, J., Thermal stability of ionic liquids for their application as new absorbents. *Industrial & Engineering Chemistry Research* **2013**, *52* (45), 15718-15727.
86. Sun, N.; Rodríguez, H.; Rahman, M.; Rogers, R. D., Where are ionic liquid strategies most suited in the pursuit of chemicals and energy from lignocellulosic biomass? *Chemical Communications* **2011**, *47* (5), 1405-1421.
87. Swatloski, R. P.; Spear, S. K.; Holbrey, J. D.; Rogers, R. D., Dissolution of cellulose with ionic liquids. *Journal of the American Chemical Society* **2002**, *124* (18), 4974-4975.
88. (a) Zhang, H.; Wu, J.; Zhang, J.; He, J., 1-Allyl-3-methylimidazolium chloride room temperature ionic liquid: a new and powerful nonderivatizing solvent for cellulose. *Macromolecules* **2005**, *38* (20), 8272-8277; (b) Zavrel, M.; Bross, D.; Funke, M.; Büchs, J.; Spiess, A. C., High-throughput screening for ionic liquids dissolving (ligno-) cellulose. *Bioresource Technology* **2009**, *100* (9), 2580-2587.
89. Pu, Y.; Jiang, N.; Ragauskas, A. J., Ionic liquid as a green solvent for lignin. *Journal of Wood Chemistry and Technology* **2007**, *27* (1), 23-33.
90. Singh, S.; Simmons, B. A.; Vogel, K. P., Visualization of biomass solubilization and cellulose regeneration during ionic liquid pretreatment of switchgrass. *Biotechnology and Bioengineering* **2009**, *104* (1), 68-75.
91. Brandt, A.; Ray, M. J.; To, T. Q.; Leak, D. J.; Murphy, R. J.; Welton, T., Ionic liquid pretreatment of lignocellulosic biomass with ionic liquid–water mixtures. *Green Chemistry* **2011**, *13* (9), 2489-2499.
92. (a) Labbé, N.; Kline, L. M.; Moens, L.; Kim, K.; Kim, P. C.; Hayes, D. G., Activation of lignocellulosic biomass by ionic liquid for biorefinery fractionation. *Bioresource Technology* **2012**, *104*, 701-707; (b) Parthasarathi, R.; Sun, J.; Dutta, T.; Sun, N.; Pattathil, S.; Konda, N. M.; Peralta, A. G.; Simmons, B. A.; Singh, S., Activation of lignocellulosic biomass for higher sugar yields using aqueous ionic liquid at low severity process conditions. *Biotechnology for Biofuels* **2016**, *9* (1), 160.

93. Jiang, L.-Q.; Fang, Z.; Li, X.-K.; Luo, J.; Fan, S.-P., Combination of dilute acid and ionic liquid pretreatments of sugarcane bagasse for glucose by enzymatic hydrolysis. *Process Biochemistry* **2013**, *48* (12), 1942-1946.
94. Deb, S.; Labafzadeh, S. R.; Liimatainen, U.; Parviainen, A.; Hauru, L. K.; Azhar, S.; Lawoko, M.; Kulomaa, T.; Kakko, T.; Fiskari, J., Application of mild autohydrolysis to facilitate the dissolution of wood chips in direct-dissolution solvents. *Green Chemistry* **2016**, *18* (11), 3286-3294.
95. Wang, J., The impacts of biopolymer-ionic liquid interactions on the utilization of lignocellulosic biomass. **2016**.
96. Wang, J.; Boy, R.; Nguyen, N. A.; Keum, J.; Cullen, D. A.; Chen, J.; Soliman, M.; Littrell, K. C.; Harper, D. P.; Tetard, L., Controlled assembly of lignocellulosic biomass components and properties of reformed materials. *ACS Sustainable Chemistry & Engineering* **2017**.
97. Yu, G.; Zhao, D.; Wen, L.; Yang, S.; Chen, X., Viscosity of ionic liquids: Database, observation, and quantitative structure-property relationship analysis. *AIChE Journal* **2012**, *58* (9), 2885-2899.
98. (a) Sun, N.; Rahman, M.; Qin, Y.; Maxim, M. L.; Rodríguez, H.; Rogers, R. D., Complete dissolution and partial delignification of wood in the ionic liquid 1-ethyl-3-methylimidazolium acetate. *Green Chemistry* **2009**, *11* (5), 646-655; (b) Fort, D. A.; Remsing, R. C.; Swatloski, R. P.; Moyna, P.; Moyna, G.; Rogers, R. D., Can ionic liquids dissolve wood? Processing and analysis of lignocellulosic materials with 1-n-butyl-3-methylimidazolium chloride. *Green Chemistry* **2007**, *9* (1), 63-69.
99. (a) Abbott, A. P.; Capper, G.; Davies, D. L.; Rasheed, R. K.; Tambyrajah, V., Novel solvent properties of choline chloride/urea mixtures. *Chemical Communications* **2003**, (1), 70-71; (b) Fischer, S.; Leipner, H.; Thümmel, K.; Brendler, E.; Peters, J., Inorganic molten salts as solvents for cellulose. *Cellulose* **2003**, *10* (3), 227-236; (c) Alvarez-Vasco, C.; Ma, R.; Quintero, M.; Guo, M.; Geleynse, S.; Ramasamy, K. K.; Wolcott, M.; Zhang, X., Unique low-molecular-weight lignin with high purity extracted from wood by deep eutectic solvents (DES): a source of lignin for valorization. *Green Chemistry* **2016**, *18* (19), 5133-5141; (d) Pang, Z.; Dong, C.; Pan, X., Enhanced deconstruction and dissolution of lignocellulosic biomass in ionic liquid at high water content by lithium chloride. *Cellulose* **2016**, *23* (1), 323-338.
100. Wasserscheid, P.; Welton, T., *Ionic liquids in synthesis*. John Wiley & Sons: 2008.
101. Isik, M.; Sardon, H.; Mecerreyes, D., Ionic liquids and cellulose: dissolution, chemical modification and preparation of new cellulosic materials. *International Journal of Molecular Sciences* **2014**, *15* (7), 11922-11940.

102. Mood, S. H.; Golfeshan, A. H.; Tabatabaei, M.; Jouzani, G. S.; Najafi, G. H.; Gholami, M.; Ardjmand, M., Lignocellulosic biomass to bioethanol, a comprehensive review with a focus on pretreatment. *Renewable and Sustainable Energy Reviews* **2013**, *27*, 77-93.
103. (a) Brandt, A.; Hallett, J. P.; Leak, D. J.; Murphy, R. J.; Welton, T., The effect of the ionic liquid anion in the pretreatment of pine wood chips. *Green Chemistry* **2010**, *12* (4), 672-679; (b) Brandt, A.; Gräsvik, J.; Hallett, J. P.; Welton, T., Deconstruction of lignocellulosic biomass with ionic liquids. *Green Chemistry* **2013**, *15* (3), 550-583.
104. Dibble, D. C.; Li, C.; Sun, L.; George, A.; Cheng, A.; Çetinkol, Ö. P.; Benke, P.; Holmes, B. M.; Singh, S.; Simmons, B. A., A facile method for the recovery of ionic liquid and lignin from biomass pretreatment. *Green Chemistry* **2011**, *13* (11), 3255-3264.
105. George, A.; Brandt, A.; Tran, K.; Zahari, S. M. N. S.; Klein-Marcuschamer, D.; Sun, N.; Sathitsuksanoh, N.; Shi, J.; Stavila, V.; Parthasarathi, R., Design of low-cost ionic liquids for lignocellulosic biomass pretreatment. *Green Chemistry* **2015**, *17* (3), 1728-1734.
106. Kilpelainen, I.; Xie, H.; King, A.; Granstrom, M.; Heikkinen, S.; Argyropoulos, D. S., Dissolution of wood in ionic liquids. *Journal of Agricultural and Food Chemistry* **2007**, *55* (22), 9142-8.
107. Badgujar, K. C.; Bhanage, B. M., Factors governing dissolution process of lignocellulosic biomass in ionic liquid: Current status, overview and challenges. *Bioresource Technology* **2015**, *178*, 2-18.
108. (a) Fendt, S.; Padmanabhan, S.; Blanch, H. W.; Prausnitz, J. M., Viscosities of acetate or chloride-based ionic liquids and some of their mixtures with water or other common solvents. *Journal of Chemical & Engineering Data* **2010**, *56* (1), 31-34; (b) Vitz, J.; Erdmenger, T.; Haensch, C.; Schubert, U. S., Extended dissolution studies of cellulose in imidazolium based ionic liquids. *Green Chemistry* **2009**, *11* (3), 417-424.
109. Zhao, H.; Baker, G. A.; Song, Z.; Olubajo, O.; Crittle, T.; Peters, D., Designing enzyme-compatible ionic liquids that can dissolve carbohydrates. *Green Chemistry* **2008**, *10* (6), 696-705.
110. Seddon, K. R.; Stark, A.; Torres, M. J., Viscosity and density of 1-alkyl-3-methylimidazolium ionic liquids. ACS Publications: 2002.
111. Wang, H.; Gurau, G.; Rogers, R. D., Ionic liquid processing of cellulose. *Chemical Society Reviews* **2012**, *41* (4), 1519-1537.
112. Heinze, T.; Schwikal, K.; Barthel, S., Ionic liquids as reaction medium in cellulose functionalization. *Macromolecular Bioscience* **2005**, *5* (6), 520-525.



113. Li, Y.; Liu, X.; Zhang, Y.; Jiang, K.; Wang, J.; Zhang, S., Why only ionic liquids with unsaturated heterocyclic cations can dissolve cellulose: A simulation study. *ACS Sustainable Chemistry & Engineering* **2017**, *5* (4), 3417-3428.
114. (a) Balensiefer, T.; Schroeder, H.; Freyer, S.; D'Andola, G.; Massonne, K., US 2010/0081798 A1: 2010; (b) D'andola, G.; Szarvas, L.; Massonne, K.; Stegmann, V., US 8044120 B2: 2011.
115. Lee, J.-M.; Ruckes, S.; Prausnitz, J. M., Solvent polarities and Kamlet– Taft parameters for ionic liquids containing a pyridinium cation. *The Journal of Physical Chemistry B* **2008**, *112* (5), 1473-1476.
116. Kamlet, M. J.; Taft, R., The solvatochromic comparison method. I. The beta.-scale of solvent hydrogen-bond acceptor (HBA) basicities. *Journal of the American Chemical Society* **1976**, *98* (2), 377-383.
117. Fukaya, Y.; Sugimoto, A.; Ohno, H., Superior solubility of polysaccharides in low viscosity, polar, and halogen-free 1, 3-dialkylimidazolium formates. *Biomacromolecules* **2006**, *7* (12), 3295-3297.
118. Zhang, Y.; Xu, A.; Lu, B.; Li, Z.; Wang, J., Dissolution of cellulose in 1-allyl-3-methylimidazolium carboxylates at room temperature: a structure–property relationship study. *Carbohydrate Polymers* **2015**, *117*, 666-672.
119. (a) Vanommeslaeghe, K.; Hatcher, E.; Acharya, C.; Kundu, S.; Zhong, S.; Shim, J.; Darian, E.; Guvench, O.; Lopes, P.; Vorobyov, I., CHARMM general force field: A force field for drug-like molecules compatible with the CHARMM all-atom additive biological force fields. *Journal of Computational Chemistry* **2010**, *31* (4), 671-690; (b) Lee, J.; Cheng, X.; Jo, S.; Mackerell, A. D.; Klauda, J. B.; Im, W., CHARMM-GUI input generator for NAMD, Gromacs, Amber, Openmm, and CHARMM/OpenMM Simulations using the CHARMM36 Additive Force Field. *Biophysical Journal* **2016**, *110* (3), 641a-641a.
120. Guvench, O.; Greene, S. N.; Kamath, G.; Brady, J. W.; Venable, R. M.; Pastor, R. W.; Mackerell, A. D., Additive empirical force field for hexopyranose monosaccharides. *Journal of Computational Chemistry* **2008**, *29* (15), 2543-2564.
121. Petridis, L.; Smith, J. C., A molecular mechanics force field for lignin. *Journal of Computational Chemistry* **2009**, *30* (3), 457-467.
122. (a) Humphrey, W.; Dalke, A.; Schulten, K., VMD: visual molecular dynamics. *Journal of Molecular Graphics* **1996**, *14* (1), 33-38; (b) Pall, S.; Abraham, M. J.; Kutzner, C.; Hess, B.; Lindahl, E. In *Tackling exascale software challenges in molecular dynamics simulations with GROMACS*, International Conference on Exascale Applications and Software, Springer: 2014; pp 3-27.
123. (a) Bussi, G.; Donadio, D.; Parrinello, M., Canonical sampling through velocity rescaling. *The Journal of Chemical Physics* **2007**, *126* (1), 014101; (b) Berendsen, H. J. C.; Postma, J. P. M.; Vangunsteren, W. F.; Dinola, A.; Haak, J.

R., Molecular-Dynamics with Coupling to an External Bath. *Journal of Chemical Physics* **1984**, *81* (8), 3684-3690.

124. (a) Hess, B., P-LINCS: A parallel linear constraint solver for molecular simulation. *Journal of Chemical Theory and Computation* **2008**, *4* (1), 116-122; (b) Hess, B.; Bekker, H.; Berendsen, H. J.; Fraaije, J. G., LINCS: a linear constraint solver for molecular simulations. *Journal of computational chemistry* **1997**, *18* (12), 1463-1472.

125. (a) McMillan Jr, W. G.; Mayer, J. E., The statistical thermodynamics of multicomponent systems. *The Journal of Chemical Physics* **1945**, *13* (7), 276-305; (b) Hill, T. L., *Statistical Mechanics*. McGraw-Hill, New York: 1956.

126. Castro, M. C.; Rodríguez, H.; Arce, A.; Soto, A., Mixtures of ethanol and the ionic liquid 1-Ethyl-3-methylimidazolium Acetate for the fractionated solubility of biopolymers of lignocellulosic biomass. *Industrial & Engineering Chemistry Research* **2014**, *53* (29), 11850-11861.

127. Lee, S. H.; Doherty, T. V.; Linhardt, R. J.; Dordick, J. S., Ionic liquid-mediated selective extraction of lignin from wood leading to enhanced enzymatic cellulose hydrolysis. *Biotechnology and Bioengineering* **2009**, *102* (5), 1368-1376.

128. Zhang, S.; Wang, J.; Zhao, Q.; Zhou, Q., *Structures and interactions of ionic liquids*. Springer-Verlag, Berlin Heidelberg: 2014; Vol. 151.

129. Kulasinski, K.; Salmén, L.; Derome, D.; Carmeliet, J., Moisture adsorption of glucomannan and xylan hemicelluloses. *Cellulose* **2016**, *23* (3), 1629-1637.

130. Rahman, M.; Sun, N.; Qin, Y.; Maxim, M. L.; Rogers, R. D., US 2011/0251377 A1: 2009.

131. Clough, M. T.; Geyer, K.; Hunt, P. A.; Mertes, J.; Welton, T., Thermal decomposition of carboxylate ionic liquids: trends and mechanisms. *Physical Chemistry Chemical Physics* **2013**, *15* (47), 20480-20495.

132. Babucci, M.; Akçay, A.; Balci, V.; Uzun, A., Thermal stability limits of imidazolium ionic liquids immobilized on metal-oxides. *Langmuir* **2015**, *31* (33), 9163-9176.

133. An, X.; Du, X.; Duan, D.; Shi, L.; Hao, X.; Lu, H.; Guan, G.; Peng, C., An absorption mechanism and polarity-induced viscosity model for CO<sub>2</sub> capture using hydroxypyridine-based ionic liquids. *Physical Chemistry Chemical Physics* **2017**, *19* (2), 1134-1142.

134. Kahlen, J.; Masuch, K.; Leonhard, K., Modelling cellulose solubilities in ionic liquids using COSMO-RS. *Green Chemistry* **2010**, *12* (12), 2172-2181.

135. Lateef, H.; Grimes, S.; Kewcharoenwong, P.; Feinberg, B., Separation and recovery of cellulose and lignin using ionic liquids: a process for recovery from paper-based waste. *Journal of Chemical Technology and Biotechnology* **2009**, *84* (12), 1818-1827.

136. Ab Rani, M.; Brant, A.; Crowhurst, L.; Dolan, A.; Lui, M.; Hassan, N. H.; Hallett, J.; Hunt, P.; Niedermeyer, H.; Perez-Arlandis, J., Understanding the polarity of ionic liquids. *Physical Chemistry Chemical Physics* **2011**, *13* (37), 16831-16840.
137. Moulthrop, J. S.; Swatloski, R. P.; Moyna, G.; Rogers, R. D., High-resolution <sup>13</sup>C NMR studies of cellulose and cellulose oligomers in ionic liquid solutions. *Chemical Communications* **2005**, (12), 1557-1559.
138. Fredlake, C. P.; Muldoon, M. J.; Aki, S. N.; Welton, T.; Brennecke, J. F., Solvent strength of ionic liquid/CO<sub>2</sub> mixtures. *Physical Chemistry Chemical Physics* **2004**, *6* (13), 3280-3285.
139. Mittal, K. L.; Anderson, H. R., *Acid-base interactions: relevance to adhesion science and technology*. Vsp: 1991.
140. (a) Lungwitz, R.; Spange, S., Determination of Hydrogen-Bond-Accepting and-Donating Abilities of Ionic Liquids with Halogeno Complex Anions by Means of <sup>1</sup>H NMR Spectroscopy. *ChemPhysChem* **2012**, *13* (7), 1910-1916; (b) Lungwitz, R.; Strehmel, V.; Spange, S., The dipolarity/polarisability of 1-alkyl-3-methylimidazolium ionic liquids as function of anion structure and the alkyl chain length. *New Journal of Chemistry* **2010**, *34* (6), 1135-1140.
141. Liu, H.; Sale, K. L.; Holmes, B. M.; Simmons, B. A.; Singh, S., Understanding the interactions of cellulose with ionic liquids: a molecular dynamics study. *The Journal of Physical Chemistry B* **2010**, *114* (12), 4293-4301.
142. Himmel, M. E.; Ding, S.-Y.; Johnson, D. K.; Adney, W. S.; Nimlos, M. R.; Brady, J. W.; Foust, T. D., Biomass recalcitrance: engineering plants and enzymes for biofuels production. *Science* **2007**, *315* (5813), 804-807.
143. Appels, L.; Dewil, R., Biomass valorization to energy and value added chemicals: The future of chemical industry. *Resources, Conservation and Recycling* **2012**.
144. Bozell, J. J., An evolution from pretreatment to fractionation will enable successful development of the integrated biorefinery. *BioResources* **2010**, *5* (3), 1326-1327.
145. Kumar, P.; Barrett, D. M.; Delwiche, M. J.; Stroeve, P., Methods for pretreatment of lignocellulosic biomass for efficient hydrolysis and biofuel production. *Industrial & Engineering Chemistry Research* **2009**, *48* (8), 3713-3729.
146. (a) Plechkova, N. V.; Seddon, K. R., Applications of ionic liquids in the chemical industry. *Chemical Society Reviews* **2008**, *37* (1), 123-150; (b) Rogers, R. D.; Seddon, K. R., Ionic liquids--solvents of the future? *Science* **2003**, *302* (5646), 792-793.
147. Mostofian, B.; Cai, C. M.; Smith, M. D.; Petridis, L.; Cheng, X.; Wyman, C. E.; Smith, J. C., Local phase separation of co-solvents enhances pretreatment of

biomass for bioenergy applications. *Journal of the American Chemical Society* **2016**, *138* (34), 10869-10878.

148. Sathitsuksanoh, N.; Holtman, K. M.; Yelle, D. J.; Morgan, T.; Stavila, V.; Pelton, J.; Blanch, H.; Simmons, B. A.; George, A., Lignin fate and characterization during ionic liquid biomass pretreatment for renewable chemicals and fuels production. *Green Chemistry* **2014**, *16* (3), 1236-1247.

149. Zhu, S.; Wu, Y.; Chen, Q.; Yu, Z.; Wang, C.; Jin, S.; Ding, Y.; Wu, G., Dissolution of cellulose with ionic liquids and its application: a mini-review. *Green Chemistry* **2006**, *8* (4), 325-327.

150. Samayam, I. P.; Hanson, B. L.; Langan, P.; Schall, C. A., Ionic-liquid induced changes in cellulose structure associated with enhanced biomass hydrolysis. *Biomacromolecules* **2011**, *12* (8), 3091-3098.

151. (a) Kilpeläinen, I.; Xie, H.; King, A.; Granstrom, M.; Heikkinen, S.; Argyropoulos, D. S., Dissolution of wood in ionic liquids. *Journal of Agricultural and Food Chemistry* **2007**, *55* (22), 9142-9148; (b) Lucas, M.; Macdonald, B. A.; Wagner, G. L.; Joyce, S. A.; Rector, K. D., Ionic liquid pretreatment of poplar wood at room temperature: swelling and incorporation of nanoparticles. *ACS Applied Materials & Interfaces* **2010**, *2* (8), 2198-2205.

152. Socha, A. M.; Parthasarathi, R.; Shi, J.; Pattathil, S.; Whyte, D.; Bergeron, M.; George, A.; Tran, K.; Stavila, V.; Venkatachalam, S.; Hahn, M. G.; Simmons, B. A.; Singh, S., Efficient biomass pretreatment using ionic liquids derived from lignin and hemicellulose. *Proceedings of the National Academy of Sciences* **2014**, *111* (35), E3587-E3595.

153. Martens, H.; Naes, T., *Multivariate Calibration*. John Wiley & Sons: 1989.

154. Segal, L.; Creely, J.; Martin Jr, A.; Conrad, C., An empirical method for estimating the degree of crystallinity of native cellulose using the X-ray diffractometer. *Textile Research Journal* **1959**, *29* (10), 786-794.

155. Cheng, G.; Varanasi, P.; Arora, R.; Stavila, V.; Simmons, B. A.; Kent, M. S.; Singh, S., Impact of ionic liquid pretreatment conditions on cellulose crystalline structure using 1-ethyl-3-methylimidazolium acetate. *The Journal of Physical Chemistry B* **2012**, *116* (33), 10049-10054.

156. (a) Xu, F.; Yu, J.; Tesso, T.; Dowell, F.; Wang, D., Qualitative and quantitative analysis of lignocellulosic biomass using infrared techniques: a mini-review. *Applied Energy* **2013**, *104*, 801-809; (b) Mussatto, S. I., *Biomass fractionation technologies for a lignocellulosic feedstock based biorefinery*. Elsevier: 2016.

157. (a) Schwanninger, M.; Rodrigues, J.; Pereira, H.; Hinterstoisser, B., Effects of short-time vibratory ball milling on the shape of FT-IR spectra of wood and cellulose. *Vibrational Spectroscopy* **2004**, *36* (1), 23-40; (b) Kubo, S.; Kadla, J. F.,

Hydrogen bonding in lignin: a Fourier transform infrared model compound study. *Biomacromolecules* **2005**, 6 (5), 2815-2821.

158. Yuan, X.; He, L.; Singh, S.; Simmons, B. A.; Cheng, G., Effect of ionic liquid pretreatment on the porosity of pine wood: insights from small angle neutron scattering, nitrogen adsorption analysis and X-ray diffraction. *Energy & Fuels* **2017**.

159. Zhang, J.; Wang, Y.; Zhang, L.; Zhang, R.; Liu, G.; Cheng, G., Understanding changes in cellulose crystalline structure of lignocellulosic biomass during ionic liquid pretreatment by XRD. *Bioresource Technology* **2014**, 151, 402-405.

160. Wheeler, E. A.; Baas, P.; Gasson, P. E., IAWA list of microscopic features for hardwood identification. **1989**.

161. Pu, Y.; Hu, F.; Huang, F.; Davison, B. H.; Ragauskas, A. J., Assessing the molecular structure basis for biomass recalcitrance during dilute acid and hydrothermal pretreatments. *Biotechnology for Biofuels* **2013**, 6 (1), 15.

162. Ault, A., General acid and general base catalysis. *Journal of Chemical Education* **2007**, 84 (1), 38.

163. Minor, J. L., Hornification-its origin and meaning. *Progress in Paper Recycling* **1994**, 3 (2), 93-95.

164. Wang, J.; Boy, R.; Nguyen, N. A.; Keum, J. K.; Cullen, D. A.; Chen, J.; Soliman, M.; Littrell, K. C.; Harper, D.; Tetard, L., Controlled assembly of lignocellulosic biomass components and properties of reformed materials. *ACS Sustainable Chemistry & Engineering* **2017**, 5 (9), 8044-8052.

165. Kamiya, N.; Matsushita, Y.; Hanaki, M.; Nakashima, K.; Narita, M.; Goto, M.; Takahashi, H., Enzymatic in situ saccharification of cellulose in aqueous-ionic liquid media. *Biotechnology Letters* **2008**, 30 (6), 1037.

166. Hu, D.; Ju, X.; Li, L.; Hu, C.; Yan, L.; Wu, T.; Fu, J.; Qin, M., Improved in situ saccharification of cellulose pretreated by dimethyl sulfoxide/ionic liquid using cellulase from a newly isolated *Paenibacillus* sp. LLZ1. *Bioresource Technology* **2016**, 201, 8-14.

167. Turner, M. B.; Spear, S. K.; Huddleston, J. G.; Holbrey, J. D.; Rogers, R. D., Ionic liquid salt-induced inactivation and unfolding of cellulase from *Trichoderma reesei*. *Green Chemistry* **2003**, 5 (4), 443-447.

168. Wang, Y.; Radosevich, M.; Hayes, D.; Labbé, N., Compatible ionic liquid-cellulases system for hydrolysis of lignocellulosic biomass. *Biotechnology and Bioengineering* **2011**, 108 (5), 1042-1048.

169. Liu, Y.; Chen, W.; Xia, Q.; Guo, B.; Wang, Q.; Liu, S.; Liu, Y.; Li, J.; Yu, H., Efficient cleavage of lignin-carbohydrate complexes and ultrafast extraction of

lignin oligomers from wood biomass by microwave-assisted treatment with deep eutectic solvent. *ChemSusChem* **2017**, *10* (8), 1692-1700.

170. Yuan, X.; Duan, Y.; He, L.; Singh, S.; Simmons, B.; Cheng, G., Characterization of white poplar and eucalyptus after ionic liquid pretreatment as a function of biomass loading using X-ray diffraction and small angle neutron scattering. *Bioresource Technology* **2017**, *232*, 113-118.

171. Lynam, J. G.; Coronella, C. J., Glycerol as an ionic liquid co-solvent for pretreatment of rice hulls to enhance glucose and xylose yield. *Bioresource Technology* **2014**, *166*, 471-478.

## VITA

Preenaa (Venugopal) Moyer was born and raised in Malaysia with two sisters. After graduating from high school, Preenaa was accepted into Penn State University in 2011, where she met her husband, Seth Moyer. During college, Preenaa worked as an undergraduate research assistant for two years under the supervision of Dr. Paul M. Smith. In 2015, Preenaa obtained her Bachelor's degree in Chemical Engineering and later decided to accept an offer for a graduate research assistantship at the University of Tennessee, Knoxville. Her advisers were Dr. Nicole Labbé and Dr. Nourredine Abdoulmoumine, whose research interests involve lignocellulosic biomass fractionation methods for biorefinery applications. Preenaa graduated with a Master of Science degree in December 2017 and currently lives with her husband in State College, PA.